SIMULATING A HEAT AND MOISTURE TRANSFER PANEL (HAMP) FOR MAINTAINING SPACE HUMIDITY

A Thesis Submitted to the College of Graduate Studies and Research in

Partial Fulfillment of the Requirements for the Degree of Master of Science in the

Department of Mechanical Engineering

University of Saskatchewan

Saskatoon

By

Radia Eldeeb

PERMISSION TO USE

In presenting this thesis in partial fulfillment of the requirements for a Postgraduate degree from the University of Saskatchewan, I agree that the Libraries of this University may make it freely available for inspection. I further agree that permission for copying of this thesis in any manner, in whole or in part, for scholarly purposes may be granted by the professor or professors who supervised my thesis work or, in their absence, by the Head of the Department or the Dean of the College in which my thesis work was done. It is understood that any copying or publication or use of this thesis or parts thereof for financial gain shall not be allowed without my written permission. It is also understood that due recognition shall be given to me and to the University of Saskatchewan in any scholarly use which may be made of any material in my thesis.

Requests for permission to copy or to make other use of material in this thesis in whole or part should be addressed to:

Head of the Department of Mechanical Engineering

University of Saskatchewan

Saskatoon, Saskatchewan

S7N 0W0, Canada

ABSTRACT

The main objective of this thesis research is to test the applicability of a novel heat and moisture transfer panel (HAMP) in an office building to control the space humidity. A HAMP is a panel that uses a liquid desiccant to add or remove heat and moisture to or from a space. This thesis research uses the TRNSYS computer package to model an office building in four different cities representing four climatic conditions. The cities are Saskatoon, Saskatchewan; Chicago, Illinois; Phoenix, Arizona; and Miami, Florida; representing cold-dry, cool-humid, hot-dry, and hot-humid climates, respectively.

The HAMP is employed in the office building with a radiant ceiling panel (RCP) system. Three other HVAC systems are examined and compared to the system employing the HAMP. The systems are: a conventional all-air system, a RCP system with 100% outdoor air, a RCP system with a parallel dedicated outdoor air system (DOAS), and the RCP system with the HAMP and 100% outdoor air. In the latter, the HAMP covers 10% of the ceiling area and uses lithium chloride solution as the liquid desiccant at different temperatures and concentrations.

The results show that the HAMP is able to control the space humidity within the control limits in all climates. The HAMP also shows the ability to provide better humidity control than the other systems as it directly responds to the space latent loads. The HAMP is able to control the relative humidity between 26% RH and 62%, 24% RH and 57% RH, 27% RH and 60%, and 40% RH and 62% RH in Chicago, Saskatoon, Phoenix, and Miami, respectively. The HAMP is

able to achieve a relative humidity of 35% in Chicago, Saskatoon, and Phoenix for 14%, 13%, and 20% of the working hours of the year, respectively. It is also able to achieve a relative humidity of 60% in Chicago, and Miami 10% and 55% of the working hours of the year, respectively.

The results also show the potential of the RCP system with the HAMP to reduce the total energy consumed by a conventional all-air system in the hot climates by 40%, and 54% in Miami and Phoenix respectively, and in the cold climates by 14% and 23% in Saskatoon and Chicago, respectively.

ACKNOWLEDGEMENT

I would like to express my sincere thanks to my supervisor C.J. Simonson for his advice and guidance in this research and in the preparation of this thesis. I would also like to convey special thanks to my husband Mohamed Beshr for his support and encouragement during this research.

I would like to thank the College of Graduate Studies and Research for providing financial support in the form of the Dean's scholarship.

TABLE OF CONTENTS

PAGE

LIST OF TABLES

PAGE

LIST OF FIGURES

PAGE

NOMENCLATURE

ACRONYMS:

ACH	Air Change per Hour
ASHRAE	American Society of Heating, Refrigeration, and Air-Conditioning Engineers
C	Cooling unit
CBECS	Commercial Building Energy Consumption Survey
CT	Cooling Tower
DB	Dry Bulb
DOAS	Dedicated Outdoor Air System
E	Economizer
EA	Exhaust Air
EF	Exhaust Fan
H	Heating unit
HAMP	Heat And Moisture transfer Panel
HVAC	Heating, Ventilation, and Air Conditioning
ISO	International Organization of Standardization
LEED	Leadership in Energy and Environmental Design
LiCl	Lithium Chloride
MV	Mechanical Ventilation

OA	Outdoor Air
PNL	Pacific Northwest national Laboratory
RA	Return Air
RCP	Radiant Ceiling Panels
RH	Relative Humidity
RW	Return Water
SA	Supply Air
SF	Supply Fan
TESS	Thermal Energy Systems Specialists
TMY	Typical Meteorological Year
TRNBuild	TRNSYS Building program
TRNSYS	TRaNsient SYstem Simulation Program
US	United States
VAV	Variable Air Volume
WB	Wet Bulb
WP	Water Pump

SYMBOLS:

A	floor area [m^2]
A_s	HAMP cross-sectional area [m^2]
C	desiccant solution concentration [%]

D	occupants diversity
D_{AB}	diffusivity of moisture into air [m^2/s]
h	enthalpy of air [kJ/kg]
h_{c1}	convective heat transfer coefficient between HAMP external surface and space air [$W/m^2 \cdot K$]
h_{c2}	convective heat transfer coefficient between HAMP internal surface and desiccant solution [$W/m^2 \cdot K$]
h_r	radiative heat transfer coefficient [$W/m^2 \cdot K$]
h_{fg}	latent heat of vaporization of air [kJ/kg]
Inf	infiltration [ACH]
k_f	conductivity of air [$W/m \cdot K$]
k_{th}	thermal conductivity of HAMP membrane [$W/m \cdot K$]
K_1	constant infiltration coefficient [ACH]
K_2	temperature related infiltration coefficient [ACH/°C]
K_3	wind speed related infiltration coefficient [$ACH \cdot s/m$]
L	characteristic length [m]
$\dot{m}$	air mass flow rate [kg/s]
NTU	number of heat transfer units
NTU_m	number of mass transfer units
Nu	Nusselt number
P	number of persons
p	partial pressure [kPa]

P_{atm}	atmospheric pressure [kPa]
Pr	Prandtl number
Q	heating or cooling load [kW]
R	air gas constant [J/kg·K]
R_a	ventilation flow rate per area [L/s·m^2]
R_p	ventilation flow rate per persons [L/s·person]
RH	relative humidity [%]
Sc	Schmidt number
Sh	Sherwood number
T	temperature [°C]
U	overall heat transfer coefficient including convection and radiation [W/m^2·K]
U_c	overall convective heat transfer coefficient [W/m^2·K]
U_m	mass transfer coefficient [m/s]
V	ventilation air flow rate [L/s]
V_{wind}	wind speed [m/s]
W	humidity ratio
X	fraction of recirculation air used

Greek Symbols:

Δ	difference between two values
υ	Kinematic viscosity [kg/s·m]
ρ	density [kg/m^3]

Subscripts:

a	space air
amb	ambient air
bypass	economizer bypass temperature value above which the economizer is turned on
corr	corrected
design	design value
dryair	air without water vapour
in	into the space
lat	latent
m	mass
max	maximum value
n	exponent constant
out	out of the space
p	panel
s	surface
sa	supply air condition
SA	supply air
v	water vapour
z	zone

CHAPTER 1 INTRODUCTION

In Northern American cities, people spend most of their time in buildings and a large portion of primary energy is consumed in buildings. Thus, the design of effective and energy efficient heating, ventilating and air conditioning (HVAC) systems is necessary. In conventional all-air HVAC systems, air is heated or cooled by means of another system that can be water or refrigerants and then supplied to a building space. Although conventional HVAC systems are effective and provide adequate comfort, they are not the most energy efficient systems.

Radiant panels, on the other hand, are temperature controlled indoor surfaces placed on ceilings, floors or walls and have 50% or more of the design heat transfer taking place by thermal radiation. Room temperature is maintained by circulating water, air, or electric current. Radiant panels provide better comfort conditions and consume less energy than conventional HVAC systems (ASHRAE 2012). Radiant panels are already available commercially but they are not able to control moisture (or latent) loads. It is important to control indoor relative humidity in buildings between 30% and 70% as suggested by ISO Standard 7730 (ISO Standard 7730, 1994). Indoor humidity levels outside this range lead to discomfort and lower productivity (Bornehag et al. 2001, Kosonen & Tan 2004). In cold climates, relative humidity levels greater than 50% RH may cause condensation on windows and elsewhere which will lead to mold growth on cool interior surfaces. In warm climates this is reversed such that condensation and mold growth can take place on exterior surfaces.

A novel heat and moisture transfer panel (HAMP) has been developed and studied at the University of Saskatchewan to achieve humidity control (Fauchoux et al. 2008, 2009, 2010). A HAMP is a panel constructed from a porous membrane that uses a salt solution as the transfer medium so that it can control both temperature and relative humidity in a space. A HAMP can be used simultaneously with radiant panels to optimize both heat and moisture transfer to/from a building space. Figure 1.1 shows a HAMP prototype with the liquid flowing in from a tube to five channels while the air is flowing over the surface of the HAMP. The surface of the HAMP consists of a porous membrane that allows heat and moisture transfer while it contains the liquid desiccant. The membrane will be discussed in more detail in Section 1.3.

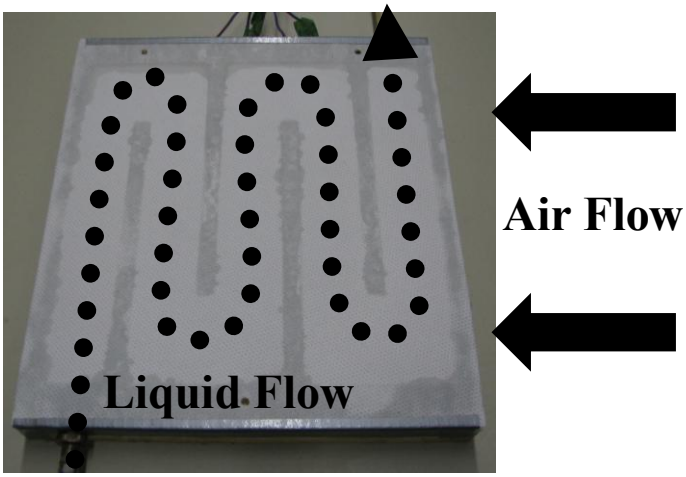

Figure 1.1: The HAMP showing the liquid flow and the air flow.

1.1 RADIANT PANELS

Radiant panel systems have been used in Europe for over 25 years in facilities such as hospitals, museums, office buildings, and stores (Mumma 2001a, Simmonds 1997). Figure 1.2 shows the processes taking place in a space with radiant cooling panels placed on the ceiling. The figure shows the ventilation openings between the panels. As described earlier, radiation heat transfer takes place between the space surfaces and objects and is the dominant mode of heat transfer. Natural convection also takes place due to the air buoyancy. The ventilation air can be used at high velocities to create forced convection which enhances the convective heat transfer coefficient between the radiant panels and the space air.

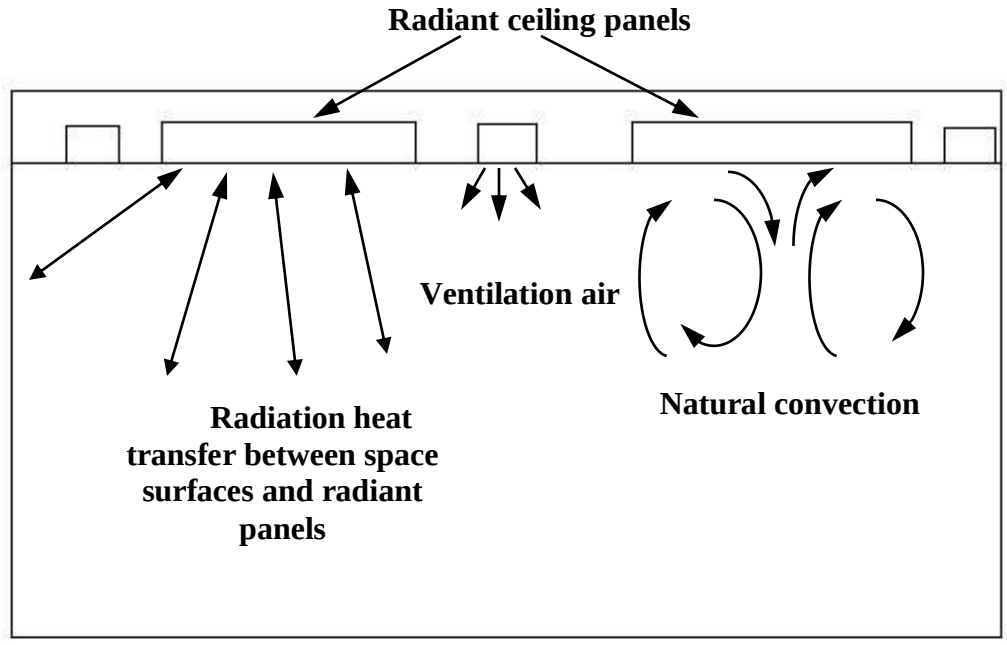

Figure 1.2: Schematic of the radiant panels placed on the ceiling of a space.

A lot of research has been carried out on radiant panels showing that radiant panels have the potential to save energy and provide better thermal comfort. Radiant panels were studied in ceiling and floor positions performing heating, cooling, or both, and compared to traditional variable air volume (VAV) HVAC systems. Simmonds (1997) found the following advantages for radiant panels:

- The first cost is 15% less with experienced contractors.
- The long term savings due to using smaller chillers and reduced fan power is 20-30%.
- There are much less moving parts showing potential reduced operational and maintenance costs.
- Testing and balancing at commissioning is simpler and less expensive.

Simmonds (1997) also studied the advantages of radiant systems over traditional VAV systems concerning comfort, architectural and design, and climatic considerations and concluded the following.

- Radiant systems minimize drafts leading to more uniform thermal comfort because radiant systems do not depend on forced air flow or convection to condition a space and thus radiant systems create a uniform vertical temperature distribution in a space.
- Ceiling cooling panels operate at relatively high surface temperatures of 15°C which prevents overcooling and water vapour condensation from room air.
- Radiant panels are aesthetically superior compared to all-air systems.

- Radiant panels downsize the space needed for equipment (the plenum size can be reduced by 20%) so the HVAC system operates silently.

Simmonds (1997) presented a comparison between floor and ceiling systems. This comparison included that floor systems are favorable for buoyancy ventilation where the heated air in contact with the floor panels becomes less dense and replaces the colder air which is denser and thus allows air movement in the space. On the other hand, ceiling systems free up the floor space for electrical cabling. Simmonds (1997) also mentioned that ceiling systems respond faster to load changes than floor systems. However, whether floor systems or ceiling systems are used, the choice of the radiant panels' position depends on the specific case, location, and architectural concerns of the building. There are several examples of modern buildings that employ radiant systems. One of these examples that employs a floor heating and cooling system is the Museum of Water and Life in southern California. Another example that employs both radiant heating and cooling integrated with a solar chimney is Manitoba Hydro Place, which is the headquarters building of Manitoba Hydro, the provincially owned electric and natural gas utility in Winnipeg.

Many papers discuss and document the theory and performance of radiant cooling regarding its comfort, efficiency, and cost effectiveness. Kulpmann (1993) studied a space with a cooled ceiling and found that the system achieved good thermal comfort. Sodec (1999), Miriel et al. (2002), and Vangtook & Chirarattananon (2006, 2007) all showed that radiant panels consume less energy than all-air systems. Sodec (1999) used a numerical simulation, using the TRNSYS simulation program, and the weather data of Essen, Germany, to compare an all-air VAV system

with a radiant ceiling system regarding the energy costs, first costs, and the space requirements. It was concluded that, as the energy removed per unit area increases, the energy costs, first costs and space requirements decrease. It was also concluded that at the cooling energy of 45-55 W/m^2, the energy savings using free cooling can be up to 10-20% in cooling, the first costs can be reduced by up to 20%, and the space requirements can be reduced by 40-55%.

Imanari et al. (1999) conducted computer simulations to compare a radiant ceiling panel system and a conventional all-air system. The radiant ceiling panel (RCP) system is used in one floor only of a six-floor office building in Tokyo, Japan. The RCP reduced the energy consumption by 10% due to the reduced required heating and cooling and buoyancy effect of the space air. The required conditioning (heating or cooling) was reduced due to the direct heating or cooling of the space air by the water flowing in the panels rather than heating or cooling the supply air and then pump it to the space. Miriel et al. (2002) performed an experimental study to verify the results obtained using a computer simulation using the TRNSYS simulation program to study the energy performance of radiant heating and cooling panels. Experimental results were obtained from two winters and one summer in a test room in an experimental house built in Rennes in western France. The study showed the ability of the panels to perform heating and cooling provided that the loads are low and the minimum cooling panel ceiling temperature is 17°C to avoid condensation and mold formation. Mold growth depends on temperature, humidity and time. Mold growth requires temperatures above 0°C and humidities above 80% RH (Hukka and Viitanen 1999, Viitanen 1996).

Vangtook & Chirarattananon (2006, 2007) tested radiant cooling in a hot and humid climate using a test room equipped with radiant cooling panels for experimentation (Vangtook & Chirarattananon 2006) and a numerical simulation program using TRNSYS (Vangtook & Chirarattananon 2007) and using weather data of Southeast Asia. The experimental and numerical results both agreed and proved that radiant cooling can achieve thermal comfort in hot humid climates. Also radiant cooling produces less or no noise at all when compared to all-air systems. The experiments showed that to avoid condensation on the surface of the panels, the supply water temperature should be kept above 24-25°C which limits the cooling capacity to 40 W/m^2 for the panel.

The ASHRAE, Systems and Equipment Handbook, (2012) lists 25 advantages of radiant panel systems from which seven are related to this research; they are:

- Reduced sensible heating or cooling loads as the operative temperature for required human thermal comfort is controlled by the mean radiant temperature. This radiant heat transfer between the occupants and the radiant panel allows a lower air dry-bulb temperature in the heating season and a higher air dry-bulb temperature in the cooling season.
- Better comfort levels for occupants than conventional systems because radiant loads are treated directly and the air motion in the space is due to ventilation air flow only.

- Supply air quantities are lower because air is supplied only for ventilation and dehumidification.
- The coupling of waste and low-enthalpy energy sources and heat pumps with panel systems can be directly done with little extra costs of equipment sizing and operation.
- Highest energy savings potential compared to all other all-air systems.
- In a new construction money can be saved in construction by decreasing the overall height of the building or adding about one floor for every five floors when compared to conventional construction and all-air systems. This is because smaller ducts mean smaller plenums.
- Noise associated with fan-coil or induction units is eliminated.

There are three disadvantages listed from which two are related to this research, and they are:

- Response time can be slow if the system design and controls are not selected or installed correctly.
- Panels can satisfy only sensible heating and cooling loads. If room air moisture content decreases near the panels, condensation will take place on the panel and the panel temperature drops below the dew point temperature of the space. This should be avoided as it will cause moisture damage, mold growth, occupant health problems and comfort negative effects.

With proper selection and installation of the ceiling panels, the only problem faced by this system is condensation. To overcome this problem, many researchers introduced the idea of using radiant ceiling panels integrated with other all-air systems. Conroy & Mumma (2001) reported the use of radiant ceiling panels to control sensible load only, while a dedicated outdoor air system (DOAS) controlled 100% of the space latent load so that the dew point temperature of the space could be controlled. This thesis research will study a heat and moisture transfer panel (HAMP) to remove moisture from building spaces and the risk of condensation with radiant panel systems.

In cold climates such as Saskatoon, it is common to use baseboard heaters especially to heat the exterior zones. Baseboard heaters are hydronic heaters that heat mainly by convection with some radiation and are somewhat similar to the radiant floor heating systems. They are compact heaters that are placed near the floor such that the heated air rises due to buoyancy forces. However, the radiant heating panel system has some advantages over the baseboard heaters as follows:

- Better design for interior architecture.
- The radiant heating system can be installed using the same water system as the building HVAC system with no extra cost.
- No extra space is required to place the heaters.
- Less maintenance is needed as the floor panels are not equipped with fins.

1.2 CONTROLLING INDOOR RELATIVE HUMIDITY

Controlling the indoor relative humidity is important for occupant health and productivity. As previously mentioned, ISO Standard 7730 (1994) suggests that the indoor relative humidity be controlled between 30% and 70%. Bornehag et al. (2001) and Kosonen and Tan (2004) reported that indoor humidity levels outside this range leads to occupant discomfort, and lower productivity.

Although research has not strictly proven that there are direct health problems resulting from high humidity, humidity control is important and requires further study especially since a lot of health problems have been shown to increase in damp buildings. However, research has shown that air home virus and bacteria person-to-person transmission is enhanced with high humidity levels and very low humidity levels in rooms (Bornehag et al. 2001).

Sources of moisture and dampness in buildings are summarized by Bornehag et al. (2001) into four main sources which are: outdoor sources such as rain or snow, indoor sources such as moisture from occupants and indoor sources such as the use of equipment for washing, cooking, and humidifiers, building sources such as moisture stored in building and construction materials, and accidents such as water leakage from pipes. Bornehag et al. (2001) reviewed 61 articles that include experiments carried on more than 100,000 occupants, about dampness in buildings. This review showed that dampness appears to increase health effects including respiratory problems such as asthma, coughing, and wheezing, and other problems such as headaches, tiredness, and mite allergies. Also when the humidity level is high in the surroundings, the human body's

ability to transpire will decrease which will increase the feeling of stickiness and discomfort of the occupants.

Kosonen and Tan (2004) did a theoretical study that showed that task related performances are affected by the occupants' perception of perceived air quality. They showed that high humidity levels in buildings affect thermal comfort and perceived air quality. They also showed that the productivity loss due to discomfort is more severe for occupant thinking processes or problem solving than the productivity loss for routine typing. They concluded that ventilation level is crucial to improve perceived air quality and thermal comfort which improve the levels of work productivity. This improvement is translated into profits that could be gained due to higher levels of workers' productivity. They referred to US studies that estimated that US$ 6-14 billion per year can be gained by the reduction of respiratory infection while US$ 15-38 billion per year can be gained by the reduction of sick building syndrome.

On the other hand, low humidity levels cause dry nose and throat, headaches, and loss of concentration. In extreme cases, it causes nose bleeding to some types of occupants. Wyon et al. (2006) conducted experiments on 17 females and 12 males for five hours at a temperature of 22°C and a relative humidity of 5%, 15%, 25%, and 35%. Experiments at low humidity levels showed that occupants blink more rapidly due to eye dryness and there is a corresponding decrease in office work productivity in three office tasks by 3-7%. However, they concluded that more experiments need to be done to prove the lower productivity levels resulting from low humidity and justify a minimum humidity level. In either case, low or high humidity levels, an

intervention should be done to make sure the humidity in buildings is within its recommended range with desirable energy consumption without causing excessive costs for building owners.

Busweiler (1993) introduced the first system that used desiccant cooling with a cooled ceiling system. It is also the first such system installed in Germany. Due to limited space in the plenum above the suspended ceilings in a hotel in Bremen, a conventional all-air HVAC system could not be installed. This led to the selection and installation of a cooled ceiling system with ventilation air supplied in from diffusers near the floor. A desiccant wheel was used to dehumidify a 100% outdoor air stream, and an evaporative cooler was used to humidify it according to the air conditions. The system ran successfully for a year and saved energy and reduced the peak electric consumption. In general, according to Mumma (2001a) ceiling panels with their different applications are more widely used in Europe than in North America.

Desiccant systems have also been used as hybrid systems in different applications. Burns et al. (1985) used a hybrid desiccant system in supermarket applications, which consume 4% of the U.S. electrical energy, and showed that 63% savings of the air conditioning electrical energy cost can be achieved when the system is running at the design condition.

1.3 HEAT AND MOISTURE TRANSFER PANEL (HAMP)

It is important to control the indoor relative humidity, as discussed in Section 1.2, and thus, a HAMP is designed to transfer heat and moisture to/from a space simultaneously. The HAMP can be placed in the ceiling position, as shown in Figure 1.3, or the floor position.

The HAMP is constructed from a porous membrane, shown in Figure 1.4, which uses a desiccant solution as the transfer media so that it can control both temperature and relative humidity. The desiccant solution is held by retaining walls on the top and sides. Research is carried out and ongoing at the University of Saskatchewan on a prototype of the HAMP in the lab. This research was started by the Ph.D. student Melanie T. Fauchoux (Fauchoux 2012).

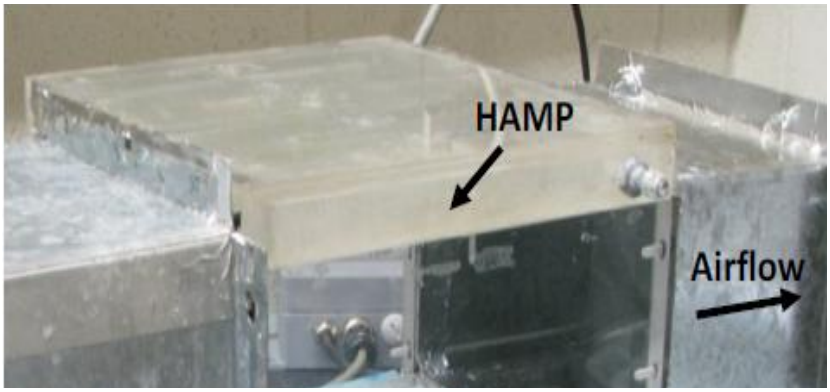

Figure 1.3: The HAMP in the lab placed in ceiling configuration (Fauchoux et al. 2010).

The porous membrane is permeable to water vapor but impermeable to liquid water or desiccant solution. This allows the desiccant solution to be in direct contact with the porous membrane without any leakage to the space even if the panel is used in the ceiling position.

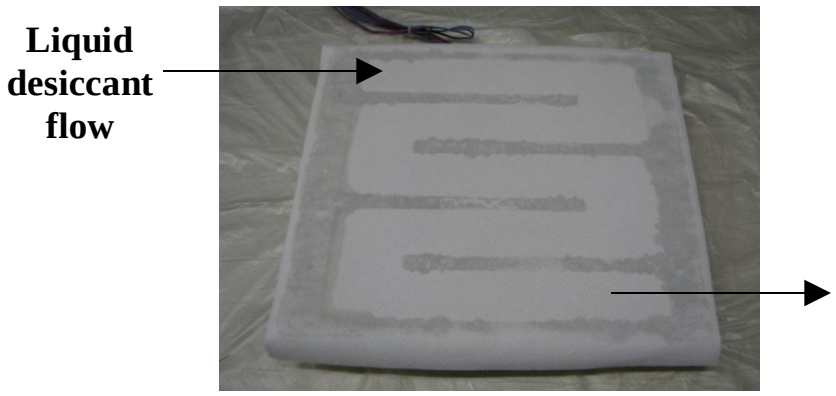

Figure 1.4: The porous membrane used in HAMP testing.

Figure 1.5 shows a sketch of the top and side views of the HAMP as used in testing. The salt used in the desiccant solution is lithium chloride (LiCl). All solution properties used for calculations are based on LiCl properties.

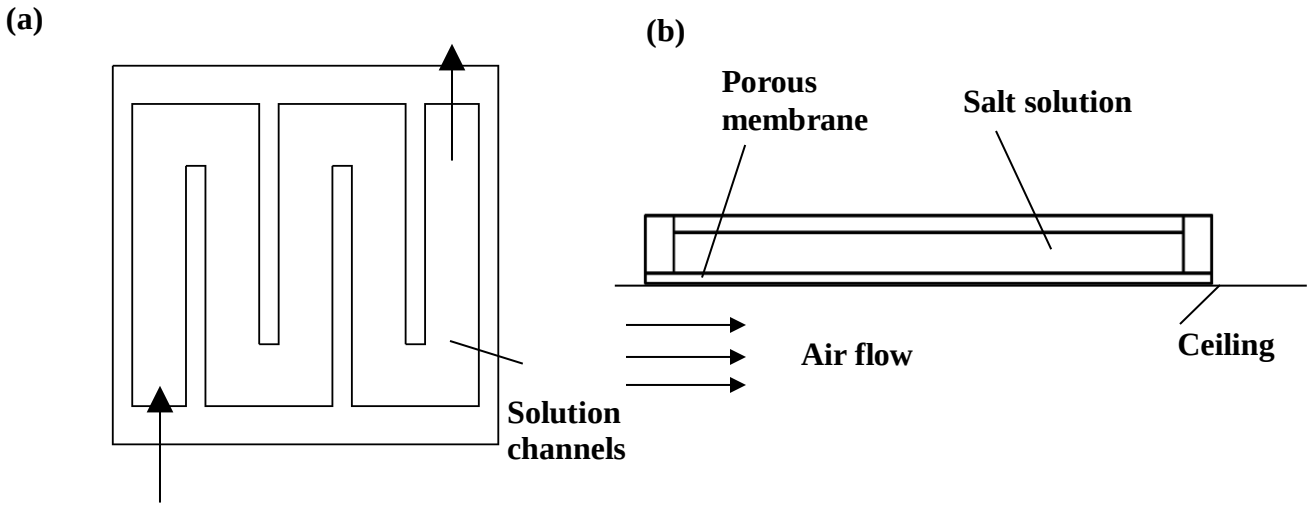

Figure 1.5: The (a) top view, and (b) side view of the HAMP used in testing.

The HAMP in the lab is placed in a test section in a small tunnel. All the research for the design, selection, and commissioning of the experiments was done by Fauchoux et al. (2010). Figure 1.6 shows the HAMP in the lab placed in the ceiling position. The HAMP is also tested in other positions such as the floor position.

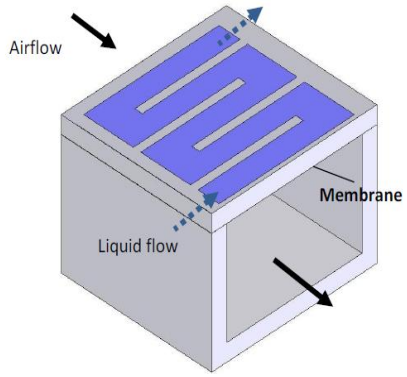

Figure 1.6: Test section with HAMP in the ceiling position (Fauchoux et al. 2010).

The first experiments done by Fauchoux et al. (2009) showed the ability of the HAMP to transfer heat and moisture to/from a space. The finding and conclusions of these experiments can be summarized as follows:

a) The HAMP is able to heat, cool, humidify, and dehumidify or any combination of these. This means that the HAMP can be used for heating and humidification, heating and dehumidification, cooling and humidification, cooling and dehumidification, humidification only, or dehumidification only.
b) The typical latent effectiveness of the HAMP is in the range of 25-45% and the typical sensible effectiveness is in the range of 5-30%.

c) The heat transfer rate of the HAMP depends on the HAMP surface temperature while the mass transfer rate depends on the HAMP surface humidity ratio. For a temperature difference between the HAMP surface and the space of 10°C and 15°C, the heat transfer rate is 4 W/m^2 and 6 W/m^2, respectively, excluding radiation heat transfer. The typical mass transfer rate is approximately 0.01 $g/s \cdot m^2$. A seated human with light work produces 45 W of latent load which is equal to 0.02 g/s. Therefore, a 2 m^2 area of HAMP would be needed to remove the latent load produced by one person.

d) The effectiveness of the HAMP is affected by the following parameters:
   - Buoyancy: large buoyancy forces increase the effectiveness if favourable.
   - The humidity ratio difference and the temperature difference between the HAMP surface and the air.
   - The number of heat transfer units (NTU) and the number of mass transfer units (NTU_m) of the HAMP. The sensible effectiveness increases with increasing NTU and latent effectiveness increases with increasing NTU_m.
   - Reynolds number of the air.
   - Cr*.
   - Radiation flux.

To achieve heat and moisture transfer there should be a temperature and concentration gradient, respectively, between the HAMP and the space air. The temperature gradient is maintained by heating or cooling the desiccant solution, while the concentration gradient is

maintained by setting the concentration of the desiccant solution such that the HAMP surface humidity ratio is less or more than the space humidity ratio. More details of setting the HAMP surface humidity ratio is explained in Section 2.3.11.

1.4 OBJECTIVES AND METHODOLOGY

There are two main objectives of this research. The first is to test the feasibility of the HAMP in an office building. This is done through simulating the HAMP in an office building and comparing it to other HVAC systems and testing its ability to remove the required latent load from the space. This will be done in four different cities representing four major climate conditions. The cities are Saskatoon, Chicago, Phoenix and Miami representing cold and dry, cold and humid, hot and dry, and hot and humid climates, respectively. The second objective is to test the effect of different parameters on the performance of the HAMP in different conditions. Smaller objectives include:

- Determine the effect of using the HAMP on the indoor relative humidity levels;
- Perform a sensitivity analysis to study the effect of the radiant ceiling panels area, the liquid temperature, and the HAMP desiccant solution concentration on the ability of the panels to remove the space heating and cooling loads, control space humidity level, and reduce total energy consumption.

To achieve these objectives the following tasks must be accomplished:

- Use the TRNSYS program to create a model of an office building in four different cities.
- Run simulations of the HVAC system including the HAMP and compare it to other HVAC systems including:
  - A conventional all-air VAV system.
  - A radiant panel with mechanical ventilation.
  - A radiant panel system with DOAS.

1.5 THESIS OVERVIEW

This thesis has six chapters. The first and current chapter is an introduction to radiant panels and the HAMP. The second chapter describes the office building including the floor plan, construction, infiltration, ventilation, occupancy, equipment, and lighting. It also describes the HVAC system used in the simulations including the energy wheel, heating and cooling equipment, radiant panels, and HAMP used in the simulations. Chapter three describes the computer simulation including the TRNSYS program description, weather data, and HAMP Matlab code used in the simulations. The preliminary results of the TRNSYS program for the office building theoretical loads in the four cities are also presented in chapter three. Chapter four presents the results from the simulations in the four cities including space temperature, relative humidity, and energy consumption. Chapter five shows the effect of the RCP surface area, the RCP water temperature, and the HAMP desiccant solution concentration on the performance of the heating and cooling panels including their ability to remove the space load, control the space

humidity level, and the resulting energy consumption. Finally, chapter six presents the conclusions and the recommended future work.

CHAPTER 2 BUILDING DESCRIPTION

To determine if a HAMP can control relative humidity levels in a building, a computer simulation using the TRNSYS building energy simulation package is used. An office building will be used as the test case. A description of the office building, including floor plan, construction, infiltration, ventilation and internal loads from occupants, lighting and equipment are given in this chapter.

2.1 THE OFFICE BUILDING

The office building used in this study is based on research carried out by the Pacific Northwest national Laboratory (PNL). This research classifies the United States office building stock into 25 buildings categories. Each of these buildings represents a specific percentage of the US office building stock as determined by a Commercial Building Energy Consumption Survey (CBECS) carried out by the Energy Information Administration (1986) of the U.S. Department of Energy. The building used for this investigation is chosen from a set of 20 buildings describing the existing building stock as of 1979. The selected building is a one-storey office building which represents 3.14% of the floor area of the U.S. building stock area (Briggs et al. 1987). A three-dimensional sketch of the one-storey office building is shown in Figure 2.1.

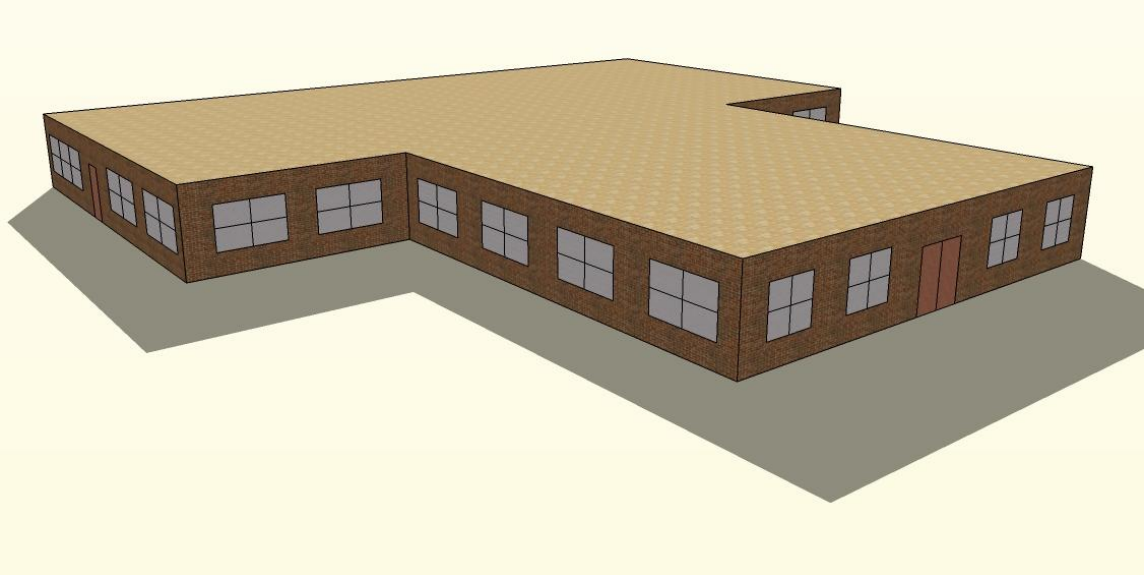

Figure 2.1: A sketch of one-storey office building used in this research.

2.1.1 Floor Plan of the Office Building

A one-storey office building with a floor area of 730 m^2 and 30% windows area (based on wall area) is selected for this study. The wall height is 3 m high. The building has dimensions as shown in Figure 2.2. The floor consists mainly of a reception area, lobby, coffee stations, a conference room, washrooms and office spaces as detailed in Table 2.1. The lobby has an entrance door facing north. There are two emergency doors on the east and west sides of the building according to Building code of Canada Section 3.3.1.5 (National Building Code 1995).

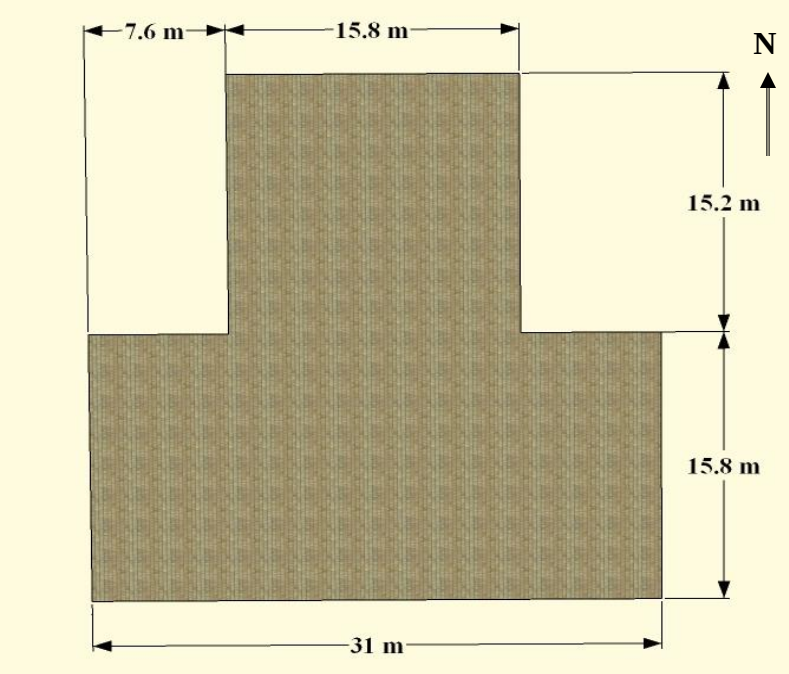

Figure 2.2: Office building plan view and external dimensions.

Table 2.1: Office building zones, areas, and categories.

Category	Floor Area (m^2)	Percentage of Floor Area (%)
Reception area	69.92	9.6
Office space	51.52	7.1
Coffee station	34.96	4.8
Main entry lobby	51.52	7.1
Coffee station	34.96	4.8
Office space	51.52	7.1
Reception area	69.92	9.6
Conference room	121.44	16.6
Office space	244.2	33.5
Total	**730**	**100**

2.1.2 Construction of the Office Building

The building description from the PNL study is based on a building located in El Paso, Texas. ASHRAE Standard 90.1 (2010) categorizes cities around the world into 8 climatic zones categories starting from the warmest cities in zone 1, and ending at the coldest cities in zone 8. El Paso, Texas is categorized by ASHRAE standard 90.1 (2010) as zone 3B. However, the cities presented in this study have different climates that vary from very cold to very hot and humid climates. This implies some modifications on the insulation of the building walls, roof, floor, and fenestration to be used in the building based on climate zone.

Table 2.2 provides a detailed description of the overall convective heat transfer coefficients: U-values for the walls, roof, floor, and fenestration. The U-value of the wall used is 66% less than the original value, while the U-value of the roof is 76% less than the original value. However, the U-value of the floor used is the same as the original value. Finally, the U-value of the fenestration used is 69% less than that of the original value. Values were based on zone 7 in ASHRAE 90.1 (2010) climate zones. This is because the coldest climate used (Saskatoon) lies in this zone.

Table 2.2: Building envelope modifications.

U-value (W/m^2K)	Wall	Roof	Floor	Fenestration
Original in PNL model	1.250	1.046	0.279	5.68
Thesis Building model	0.433	0.254	0.279	1.73
Maximum allowed, according to ASHRAE 90.1 (2010), for zone 7 (representing Saskatoon's climate)	0.513	0.360	0.496	3.24

The exterior walls of the building are made of 10.2 cm face brick, 5 cm common brick, 1.9 cm sand aggregate gypsum plaster, and 7.5 cm glass-fiber batts insulation. A sketch of the cross-Section of the wall is shown in Figure 2.3.

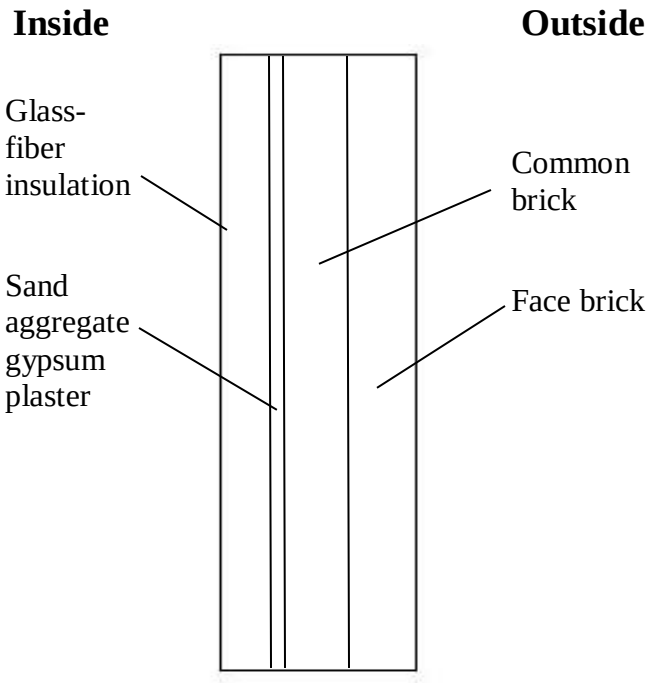

Figure 2.3: Cross-section of the wall.

The roof is made of 1.9 cm soft wood, 1 cm built-up roofing, and 8 cm insulation as shown in Figure 2.4 from bottom layer to top layer, respectively.

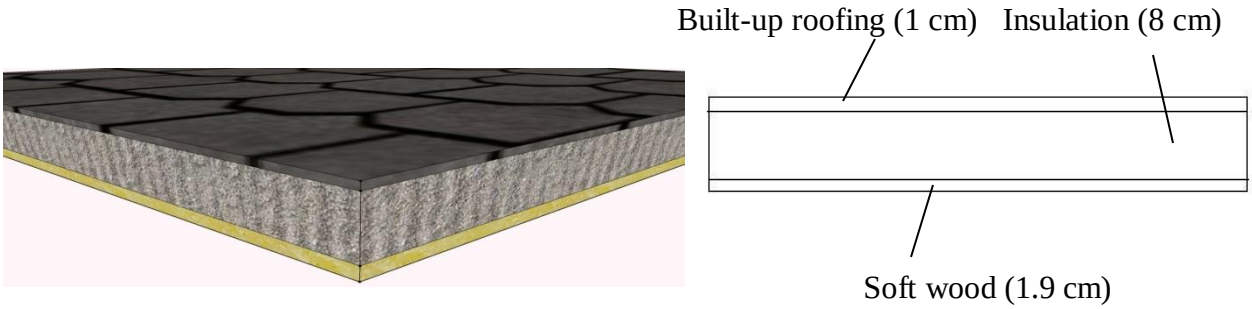

Figure 2.4: Roof cross-section.

The floor is made of 20.3 cm concrete and 11 cm insulation as shown in Figure 2.5 from bottom layer to top layer, respectively.

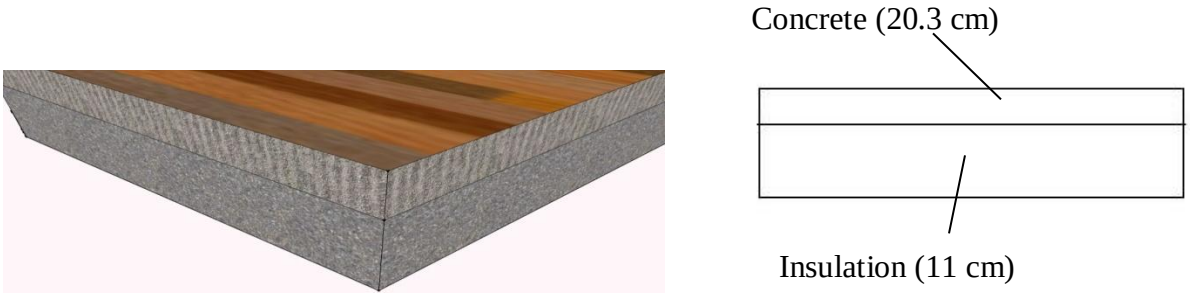

Figure 2.5: Floor cross-section.

The windows used are triple-pane windows with 5.7 mm-thick glass with 6.4 mm air gaps and wood frames. Table 2.3 shows the U-values of the different layers used in the building. The entrance door is a 1.8 m by 2.4 m single 6.4 mm glass with aluminum frame with a U-value of 5.44 W/m^{2}K. The emergency doors are each 0.9 m by 2 m with a U-value of 1.73 W/m^{2}K.

Table 2.3: U-values of building envelope.

Layer	Total thickness (m)	Total Area (m^2)	U-value ($W/m^2 \cdot K$)	UA (W/K)	Percentage of UA (%)
Wall	0.181	355.9	0.423	150	20
Roof	0.109	730	0.254	185	25
Floor	0.313	730	0.279	204	27
Window	0.0299	109.5	1.73	189	25
Entrance door	0.0064	4.32	5.63	24	3
Emergency door	0.03	1.8	1.73	3	0

The thermal capacitance of the building is set at 10 times the thermal capacity of the air in the space to account for inner space envelope mass and its furnishings. The moisture storage of the materials is set at the simple (capacitance) humidity model set by the program such that the humidity capacitance ratio is set to ten. This means that the materials in the building are assumed to have a moisture storage capacity that is ten times larger than that for the air in the space.

2.1.3 Infiltration and Ventilation in the Office Building

The infiltration rate is calculated using TESS component type 571. The infiltration rate is calculated as a function of the wind speed, indoor and outdoor temperatures, ambient pressure and relative humidity at each time step. The component uses ASHRAE (2009) semi empirical formula called the K_1, K_2, K_3 method. Equation (2.1) shows the formula used.

$$Inf(ACH) = K_1 + K_2(T_a - T_{amb}) + K_3 V_{wind} \quad (2.1)$$

K_1 is a constant coefficient, K_2 is a temperature related infiltration coefficient, and K_3 is a wind speed related infiltration coefficient. Table 2.4 shows the values of the coefficients used in this study. These values are default in the infiltration component in the TRNSYS simulation program and are typical values from ASHRAE Handbook of fundamentals (ASHRAE 2009) for medium buildings.

Table 2.4: Infiltration coefficients values.

K_1	0.1 ACH
K_2	0.017 ACH/°C
K_3	0.049 ACH·s/m

As an example, the maximum wind speed in Chicago is 15.5 m/s and it takes place on the 21st of February. Figure 2.6 shows the infiltration rate on the windiest day of the year on February 21st in Chicago, IL. The maximum infiltration in Chicago is 0.73 ACH and takes place on the 31st of December due to indoor and outdoor large temperature difference. The yearly average infiltration rate in Chicago is 0.28 ACH, and the minimum is 0.002 ACH. The average infiltration per unit wall area is 0.00075 ACH/m^2.

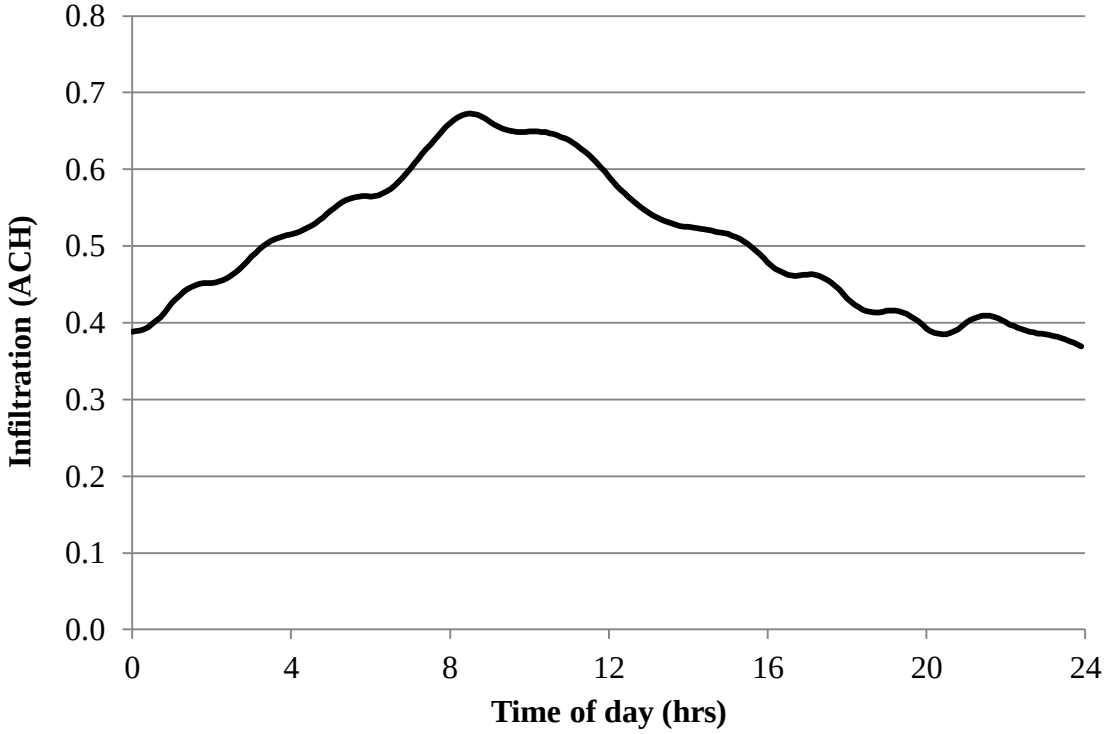

Figure 2.6: Infiltration on the windiest day in Chicago, IL, February 21.

The outdoor ventilation rate is determined according to the occupancy, area, and building type. The equation used for the calculation of the ventilation air flow rate for every space zone according to ASHRAE Standard 62.1 (2010) is

$$V=P_z \cdot R_p + R_a \cdot A \ , \tag{2.2}$$

where VA is the ventilation air flow rate in L/s, P_z is the number of persons in the space which is calculated according to the occupancy density suggested by the standard, R_p is the ventilation

flow rate per person in L/(s·person), R_a is the ventilation flow rate per unit area in L/(s·m^2), and A is the floor area. The calculation details are shown in Table 2.5.

Table 2.5: Detailed calculation of ventilation rates according to ASHRAE 62.1 (2010).

Category	**Occupancy Density**	**P_z (persons)**	**R_p (L/(s·person))**	**R_a (L/(s·m^2))**	**Required Ventilation (V) (L/s)**	**Required Ventilation (V) (ACH)**
Reception area	30	21	2.5	0.3	73	0.12
Office space	5	3	2.5	0.3	23	0.04
Coffee station	50	17	2.5	0.3	53	0.08
Main entry lobby	10	5	2.5	0.3	28	0.04
Coffee station	50	17	2.5	0.3	53	0.08
Office space	5	3	2.5	0.3	23	0.04
Reception area	30	21	2.5	0.3	73	0.12
Conference room	50	61	2.5	0.3	189	0.30
Office space	5	12	2.5	0.3	103	0.16
Total		**160**			**618**	**0.98**

The building is ventilated using a constant flow of 100% outdoor fresh air. The total outdoor ventilation rate is 0.62 m^3/s (0.98 ACH) in order to meet ASHRAE Standard 62.1 (2010) for acceptable indoor air quality for 160 people. However, the number of occupants and the ventilation rate are corrected according to the occupancy schedule presented in Section 2.1.4.

The ventilation schedule is shown in Figure 2.7. The ventilation system is turned on two hours prior to people entering the building at 6:00 and shut off after the last occupants leave at 21:00.

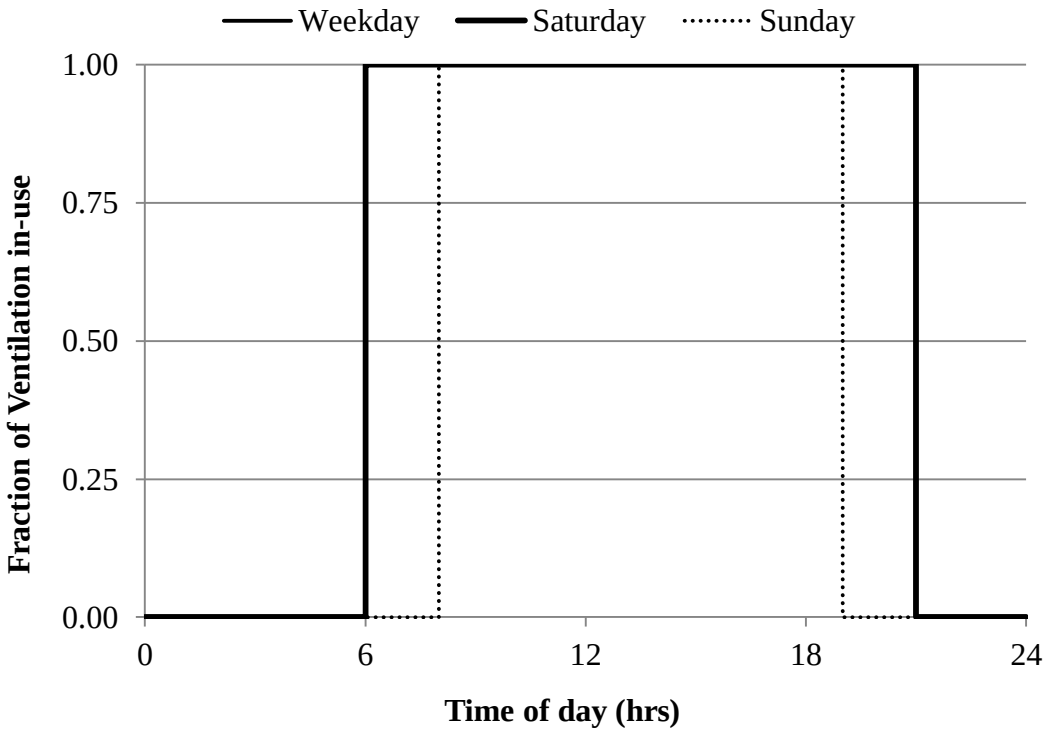

Figure 2.7: Ventilation Schedule.

2.1.4 Occupancy in the Office Building

The number of occupants in the office building based on values from ASHRAE Standard 62.1 (2010) is 160 persons. This is viewed as an unreasonable number of occupants so a value of 5 people/100 m^2 is suggested for the office space, which results in a total of 37 people. In order to correct for the ventilation, ASHRAE Standard 62.1 (2010) recommends the calculation of the

occupant diversity, D, such that D is the fraction of the actual occupants from the calculated number of components P_z. D is 0.23 for the suggested number of components. The new ventilation rate is thus calculated from Equation (2.3). The new ventilation rate is 0.38 m^3/s (0.60 ACH).

$$V_{corr} = D(R_p \cdot P_z) + R_a \cdot A \tag{2.3}$$

The occupancy schedule for weekdays and weekends is shown in Figure 2.8. The activity level of the occupants doing moderately active office work in offices is recommended by AHSRAE (2009) to be 130 W per person such that 75 W is a sensible load and 55 W is a latent load. However, TRNSYS gives only limited choices of activity levels of the occupants. The nearest activity level to the ASHRAE (2009) recommendation is chosen to be 120 W such that 65 W is a sensible load and 55 W is a latent load. An extra sensible load of 10 W is also added as a separate extra gain to account for the difference to meet the ASHRAE (2009) recommendation.

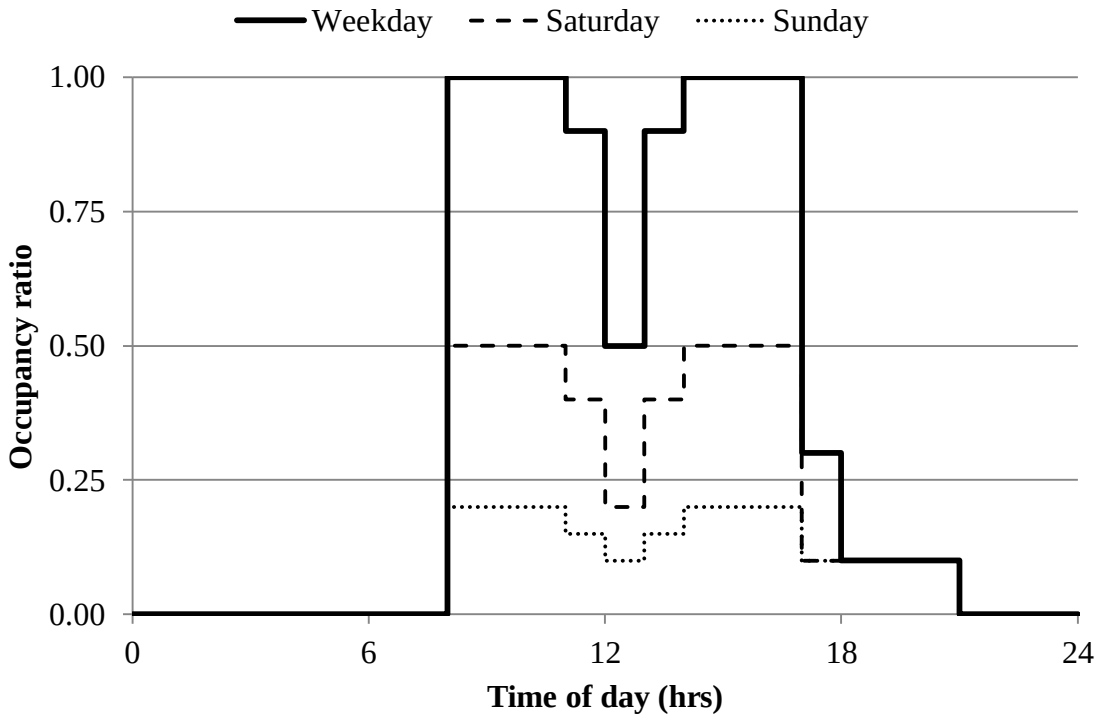

Figure 2.8: Occupancy schedule.

2.1.5 Equipment and Lighting in the Office Building

It is assumed that every person in the building has a computer with colored monitor. This makes a total of 34 computers. The TRNSYS program gives a value of 230 W for each of these computers which are similar to the heat gain values given in ASHRAE (2009). The equipment gain contributes 10.7 W/m^2 which is very close to the value suggested by ASHRAE (2009) which is 10.8 W/m^2 for medium office work. The schedule of the computers is shown in Figure 2.9.

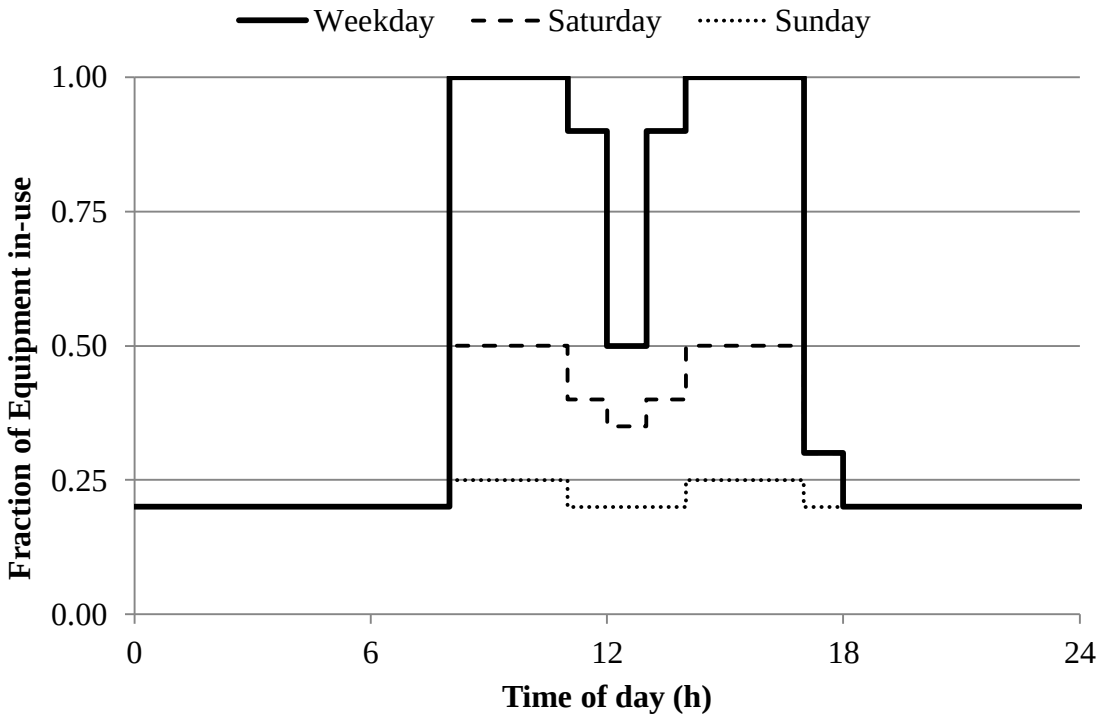

Figure 2.9: Equipment schedule.

According to ASHRAE Standard 90.1 (2010) the lighting in office buildings based on the building area should be limited to 10.8 W/m^2. Accordingly, the heat gain from the lighting is selected from a table in the computer program to be 13 W/m^2 distributed over an area of 606 m^2 which is 83% of the floor area, such that the overall lighting density is 10.8 W/m^2 in order to meet ASHRAE requirements. The heat gain from the lights is assumed to be 40% convective. The schedule for the lighting is shown in Figure 2.10 during weekdays and weekends. The lights are left on at 27% during the evenings.

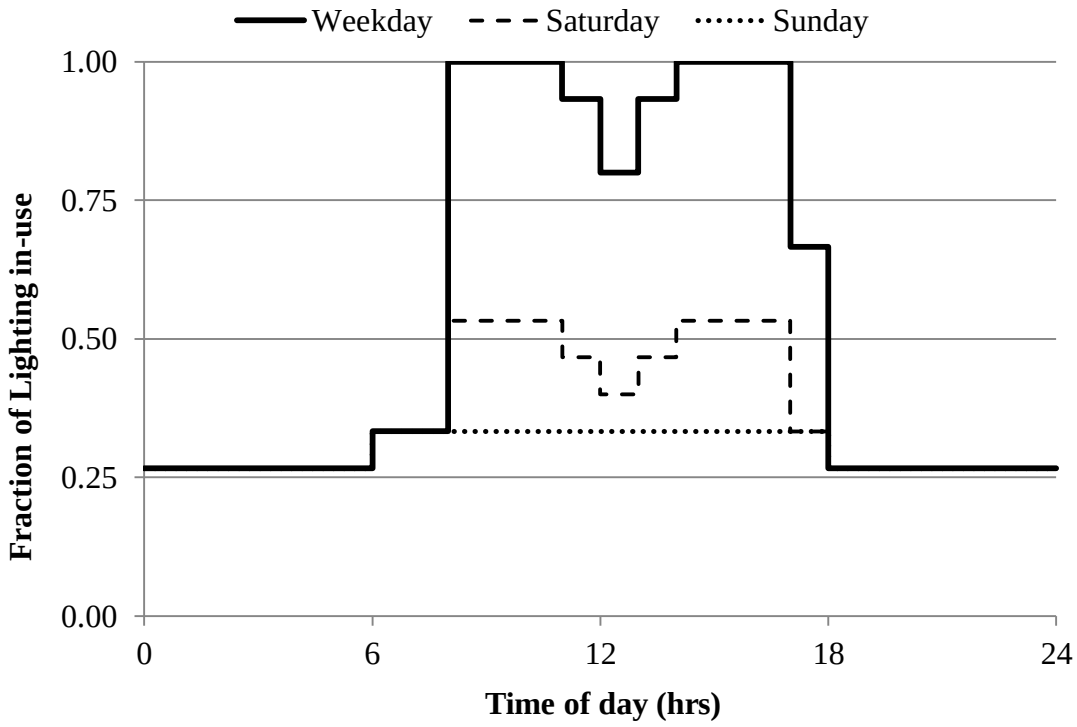

Figure 2.10: Lighting schedule.

2.2 HVAC SYSTEMS

In this thesis, four HVAC systems will be studied:

- System A: A conventional all-air system with an energy wheel.
- System B: A radiant ceiling panel system with a 100% outdoor air mechanical ventilation system.
- System C: A radiant ceiling panel system with HAMP and a 100% OA mechanical ventilation system.

- System D: A radiant ceiling panel system with DOAS.

In this section, Section 2.2, the four systems will be described. The detailed components models used to simulate each component of the systems will be described in Section 2.3.

2.2.1 System A: All-air VAV system

The schematic of system A is shown in Figure 2.11. In system A, which is the base system, air is taken from outside and passed through an energy wheel. The energy wheel transfers heat and moisture between the outdoor air (OA) entering the system and the exhaust air (EA) leaving the system. After exchanging heat and moisture with the exhaust air in the energy wheel, the OA is mixed with the return air (RA) in the economizer (E). The economizer controls the fraction of OA and RA delivered to the building. The economizer will increase the percentage of OA used under favorable outdoor temperature and humidity conditions. This will reduce the amount of cooling energy required in mild climates and during moderate weather conditions. The energy wheel is normally bypassed when the economizer is operating in order to reduce the fan power. The minimum OA flow rate is used as the required minimum rate stated in Section 2.1.3 according to the schedule in Figure 2.7, while the rest of the required supply air is supplied from the return air. However, when heating and/or cooling is required outside of the ventilation hours shown in Figure 2.7, the supply air (SA) provided to the building is 100% RA.

As shown in Figure 2.7, the mixture of OA and RA is conditioned by passing through the heating and cooling units, as needed. The conditioned air is then supplied to the space by the supply

fan (SF). The SA enters the building at 30°C for heating and 14°C for cooling. The exhaust fan (EF) extracts air from the building and a portion of this air is used for recirculation (RA) and the rest is exhausted from the building (EA). Both the SF and the EF are constant volume fans.

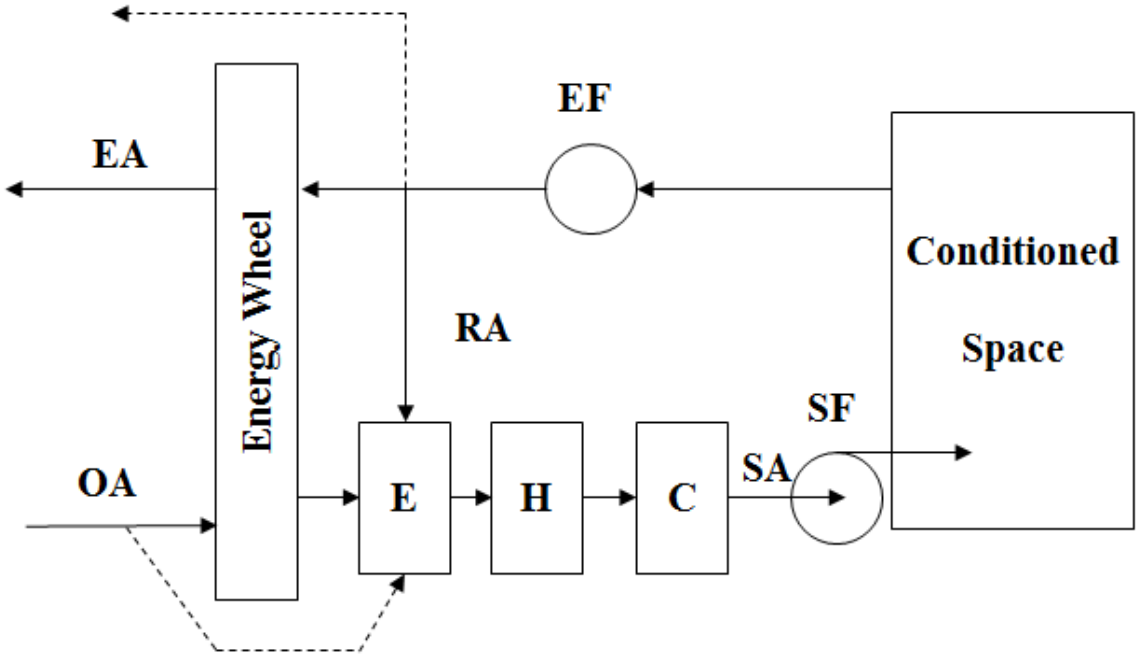

Figure 2.11: Schematic of the all-air VAV system (System A) [EA: Exhaust Air, EF: Exhaust Fan, OA: Outdoor Air, E: Economizer, H: Heating unit, C: Cooling unit, SA: Supply Air, SF: Supply Fan].

The space temperature is controlled using an on/off control strategy such that the fans are turned on if the indoor temperature is less than the heating set point or higher than the cooling set point. If the indoor temperature is within the heating and cooling set points, then the fans are turned off. The only exception is heating in Miami as the temperature in winter is allowed to be lower than the set point temperature because no heating is used in Miami. This is because the heating load in Miami is

very small and seen as unnecessary as the minimum temperature reached in the space is 20°C even with no heaters.

Table 2.6 shows the SA flow rates for each city. The detailed calculations of the SA are given in Appendix A. The SA flow rates were calculated using

$$Q=\dot{m}_{SA}(h_{out}-h_{in}) \ , \tag{2.4}$$

where Q is the heat transferred to or from the space, h_{out} is the enthalpy of the air leaving the space which is assumed to be at the space design condition, and h_{in} is the enthalpy of the air entering the space which is assumed to be at the supply design conditions.

Table 2.6: System A supply air flow rates for different cities.

City	SA flow rate (m^3/s)
Saskatoon, Saskatchewan	8.4
Miami, Florida	4.3
Phoenix, Arizona	3.6
Chicago, Illinois	7.3

2.2.2 System B: Radiant Ceiling Panels with 100% Mechanical Ventilation

The schematic of system B is shown in Figure 2.12. In system B, only the minimum ventilation flow rate required by ASHRAE Standard 62.1 (2010) of 0.38 m^3/s stated in Section 2.1.3 is supplied to the space. The ventilation system provides 100% outdoor air to the space. The space sensible load is handled by the radiant ceiling panels (RCP) shown in Figure 2.12.

Normally, there must be a parallel system with the RCP system to remove the latent load. An example of such a system is the dedicated outdoor air system (DOAS) which provides an air flow rate sufficient to remove the space latent load and also removes some of the space sensible load with the RCP system. Since the applicability of the HAMP in this thesis is tested by comparing relative humidity levels in the space, the RCP system is presented in system B without a DOAS but only the minimum mechanical ventilation. However, the DOAS will be presented later in a separate system in Section 2.2.4.

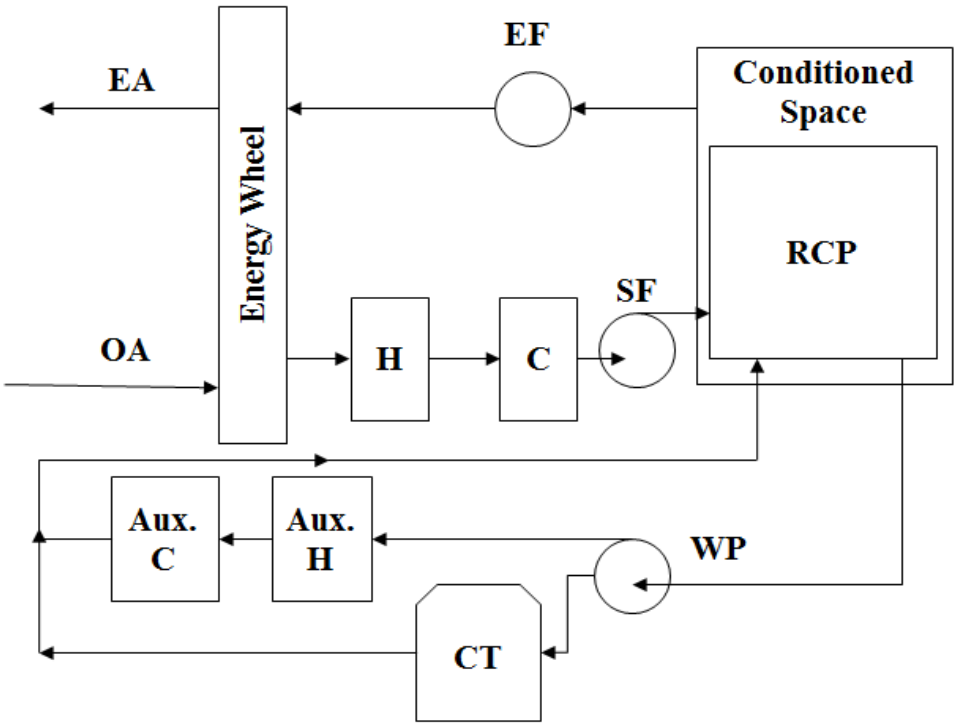

Figure 2.12: Schematic of the radiant ceiling panel system with mechanical ventilation (System B) [EA: Exhaust Air, EF: Exhaust Fan, OA: Outdoor Air, H: Heating unit, C: Cooling unit, SF: Supply Fan, Aux. C: Auxiliary Cooling unit, Aux. H: Auxiliary Heating unit, CT: Cooling Tower, WP: Water Pump, RCP: Radiant Ceiling Panels].

The RCP is chosen to cover 60% of the ceiling area. However, a sensitivity study will be presented in CHAPTER 5 for different RCP areas to show how this will affect the space temperature. The heated or chilled water passes through tubes to remove the loads directly from the space by radiation and convection. The return water (RW) from the RCP is pumped by a water pump (WP) to the auxiliary heater or auxiliary cooler as required, then enters the RCP tubes again. The water also passes by a cooling tower (CT) to make use of natural cooling which reduces the cooling load required. The temperature of the water for cooling and heating is given in Table 2.7 for each city.

Table 2.7: Water temperature in RCP in system B

City	Heating Temperature (°C)	Cooling Temperature (°C)
Saskatoon, Saskatchewan	50	14
Miami, Florida	-	14
Phoenix, Arizona	30	12
Chicago, Illinois	45	12

The heating temperature is high in Saskatoon and Chicago to cover the heating load, while 30°C covers the small heating load in Phoenix. This is due to the low heating convective heat transfer coefficient of RCP. To improve the convective heat transfer coefficient, it would be recommended to use floor heating panels. The set point temperature of water during cooling temperature used is very low and condensation of water vapor on the RCP surface will take place in Chicago and Miami due to the humid climates and the absence of a parallel system to remove the space latent load completely. However, since the cities chosen for this study have high cooling loads and no parallel system is used in system B, it is important to use a low cooling

water temperature in order to remove most of the cooling load. In order to avoid condensation, the temperature of the water should not be lower than 17°C (Olesen 2008). This will be used in Section 2.2.4 in system D which will utilize a parallel system to remove the space latent load.

2.2.3 System C: RCP with 100% OA Mechanical Ventilation and HAMP

The schematic of system C is shown in Figure 2.13.

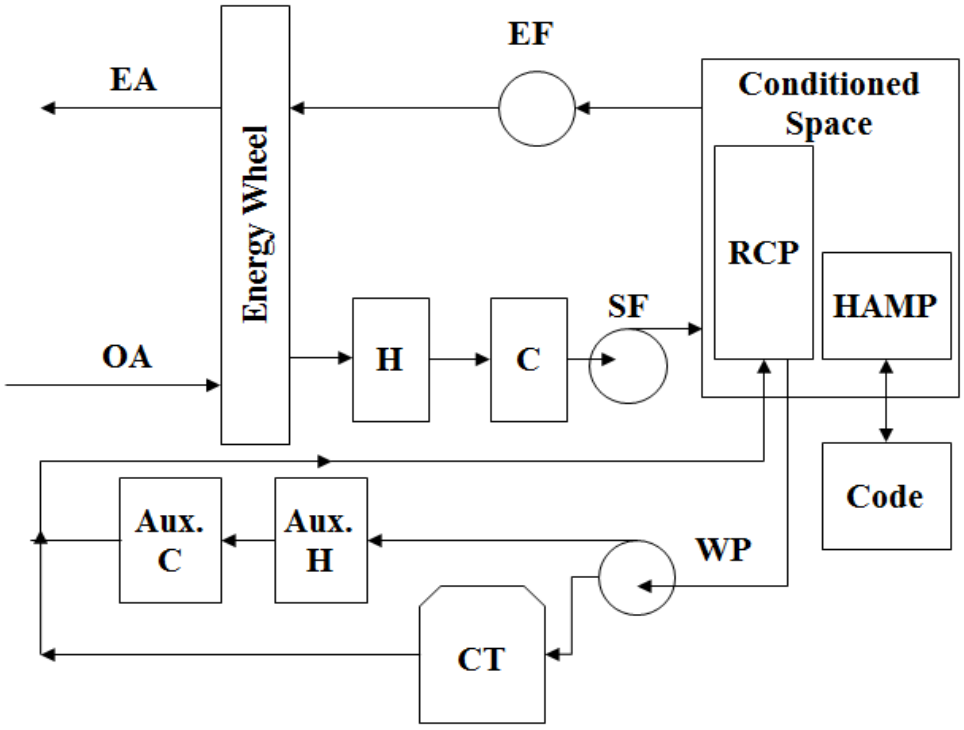

Figure 2.13: Schematic of System B with the HAMP (System C) [EA: Exhaust Air, EF: Exhaust Fan, OA: Outdoor Air, H: Heating unit, C: Cooling unit, SF: Supply Fan, Aux. C: Auxiliary Cooling unit, Aux. H: Auxiliary Heating unit, CT: Cooling Tower, WP: Water Pump, RCP: Radiant Ceiling Panels, HAMP: Heat And Moisture transfer Panel].

System C is similar to system B RCP with a 100% OA ventilation except that the HAMP is added to remove the space latent load. The moisture that should be added or removed from the space by the HAMP to remove the latent load of the space is calculated in a Matlab code. The Matlab code is called by Type155 in TRNSYS simulation studio. The calculated gain is then added or removed to/from the space through a defined variable gain in the building. The code is presented in Appendix B. The HAMP is chosen to cover 10% of the ceiling area as it is found sufficient to remove the latent loads in different cities. The water temperature used in the RCP is the same as system B to be able to remove the cooling load and the heating load but minimal or no condensation takes place as will be shown in CHAPTER 5.

2.2.4 System D: RCP with Dedicated Outdoor Air System (DOAS)

The schematic of system D is the same as that of system B shown in Figure 2.12. System D is introduced to overcome the drawback of system B of not being able to control the latent load. In system D, the ventilation air is calculated such that it removes the latent load of the space. The flow rate needed to remove the space latent load is 5-6 times the minimum ventilation flow rate used in system B. The dedicated outdoor air system (DOAS) used in parallel with the RCP system is defined as the ventilation system that is able to control the space latent load using 100% OA. This means that system D is expected to consume more energy than system A and B as it uses a higher ventilation flow rate while there is no recirculation. Table 2.8 shows the constant ventilation rate required in each city and Appendix A shows more calculations of the ventilation rates. The equation used to calculate the DOAS ventilation rate is

$$Q_{lat} = \dot{m}(W_{out} - W_{in})h_{fg} \ , \qquad (2.5)$$

where Q_{lat} is the space latent load, W_{out} is the humidity ratio of the air flowing out of the space, W_{in} is the humidity ratio of the air flowing into the space, and h_{fg} is the latent heat of vaporization of air. The space sensible load is partially removed by the DOAS and mostly removed by the RCP. The temperature of the water in the RCP is maintained 17°C for cooling to avoid condensation on the surface of the panels. For heating, it is recommended to keep the water at 27°C to avoid temperature asymmetry for thermal comfort (Olesen 2008). This is used in Phoenix due to the low heating load, while water at 40°C and 45°C is used in Chicago and Saskatoon, respectively.

Table 2.8: System D DOAS ventilation flow rates for different cities.

City	DOAS Ventilation Flow Rate (m^3/s)
Saskatoon, Saskatchewan	2.6
Miami, Florida	5.5
Phoenix, Arizona	1.6
Chicago, Illinois	2.1

A parallel system with the RCP that removes the latent load and does recirculation so that it saves energy can be used instead of a DOAS. This system is a hybrid between system A and B. However, the DOAS is studied in this thesis.

2.3 HVAC COMPONENTS

2.3.1 Energy Wheel

In order to reduce the amount of energy a building uses, the use of an energy wheel became necessary in modern buildings. Energy wheels transfer sensible and latent heat between exhaust and supply air streams of a building. This leads to significant energy savings in conditioning outdoor air which is beneficial for the environment and also reduces running costs of the building by reducing the amount of electricity or any other energy source.

For modeling an energy wheel in an HVAC system, two important parameters should be determined: the sensible and latent effectivenesses and the pressure drop across the energy wheel. The pressure drop is assumed to be 200 Pa (0.8 inH_2O) on both the supply and exhaust sides (Fauchoux 2006). The effectivenesses of the energy wheel are assumed to be constant throughout the year (Fauchoux 2006). The constant effectiveness is chosen to be 75% for both sensible and latent heat transfer (Fauchoux 2006).

Although energy wheels can help to significantly reduce the energy required to condition the ventilation air for buildings, under certain weather conditions, the use of an energy wheel can actually increase the building cooling demands. Studies have shown that energy wheels should be operated at maximum capacity when the building requires heating (defined as the heating season) as it reduces the heating and humidification loads significantly (e.g. Rasouli et al. 2010). However, the energy wheel should be controlled when the building requires cooling (defined as the cooling season) as it can increase the cooling required (Fauchoux 2006). During these

conditions, it is desirable to reduce or eliminate the energy transfer through the energy wheel. To further explain, Figure 2.14 shows a schematic of a psychrometric chart presenting the various outdoor conditions that can occur in different cities in different times of the year.

State 3 represents the suggested supply air to the building. In this thesis research, as was mentioned in Section 2.2.1, the air is supplied in the cooling season at 14°C. State 4 is the indoor air condition. The shaded zone from a temperature of 0°C to $T_{heating}$ represents the region when the energy wheel is used for heating where $T_{heating}$ is the outdoor temperature under which the space requires heating and the heating system starts operating. If the outdoor air is anywhere in the unshaded zone, the outdoor air will be heated rather than cooled as it flows through the energy wheel which will increase the energy load. For example, if the outdoor air enters at 20°C while the exhaust air exits at 24°C, the outdoor air can be heated by the energy wheel to 22.2°C rather than cooled. The air will then need to be further cooled to the supply temperature of 14°C but instead of cooling the air from 20°C, it will be cooled from a higher temperature of 22.2°C which means more cooling will be required in every time step. This is undesirable and should be avoided.

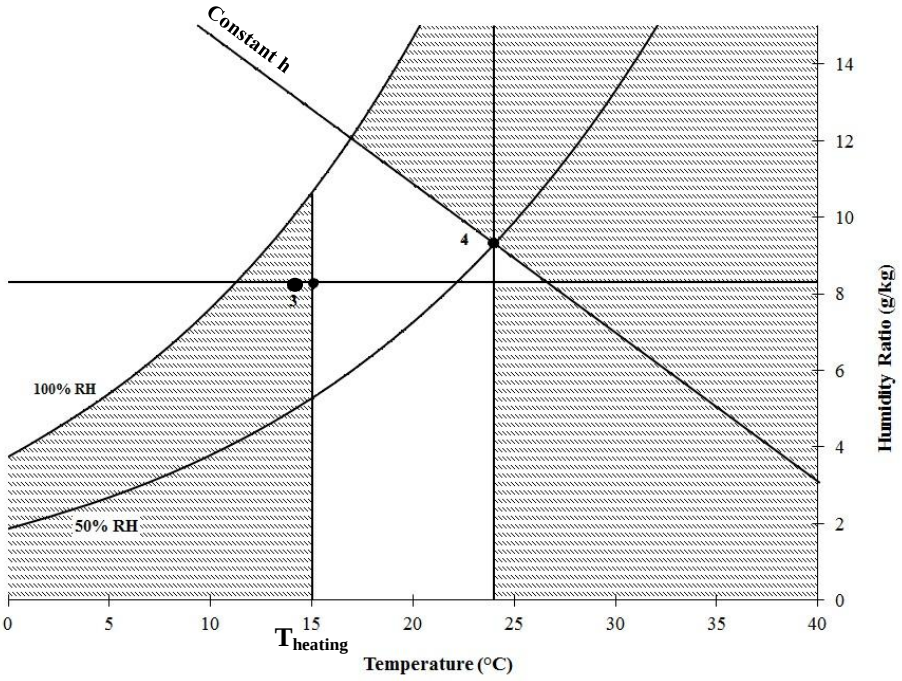

Figure 2.14: Psychrometric chart showing the shaded area at which the energy wheel should operate to save energy and unshaded area at which the energy wheel should be off.

Rasouli et al. (2010) suggests a control strategy for energy wheels to control both heat and moisture transfer through using enthalpy control based on an effectiveness ratio (energy when sensible effectiveness/latent effectiveness) of 1. This control allows the energy wheel to operate in summer only under two control conditions. This first is that the outdoor enthalpy must be greater than the indoor enthalpy. The second is that the humidity ratio of the outdoor air must be lower than that of the supply air and outdoor temperature is greater than the indoor temperature. This is the control strategy used in this thesis to avoid over heating of to the outdoor ventilation air when the building needs cooling. On the other hand, the unshaded zone represents the economizer operation condition (Rasouli 2010).

2.3.2 Economizer

The percentage of OA in System A is different for every city and ranges between 4-9% of the SA. However, sometimes it is more beneficial to use a larger percentage of OA. The economizer is utilized to control the percentage of OA used by allowing a certain fraction of OA to be supplied to the conditioned space through valves which are controlled by the outdoor temperature.

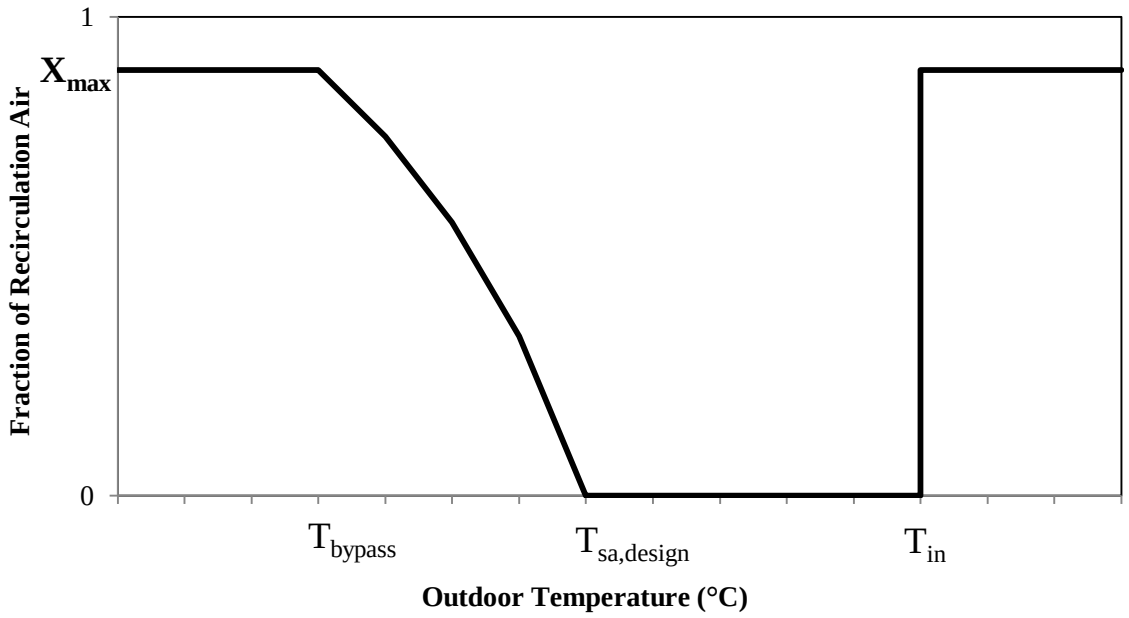

Figure 2.15 shows the fraction of recirculation air, X, allowed by the economizer based on the outdoor temperature. The economizer allows a maximum fraction X_{max}, given in Table 2.9 for every city, of RA in the SA as long as the outdoor temperature is less than a certain temperature defined by Simonson et al. (2000) called bypass temperature, T_{bypass}, calculated by

$$T_{bypass} = \frac{T_{sa,design} - X_{max} . T_{in}}{1 - X_{max}} , \qquad (2.6)$$

where $T_{sa,design}$ is the outdoor air temperature at which the cooling load of the space will be just satisfied with no additional cooling and is taken to be 14°C, T_{in} is the indoor temperature, and X_{max} is the maximum allowable fraction of RA.

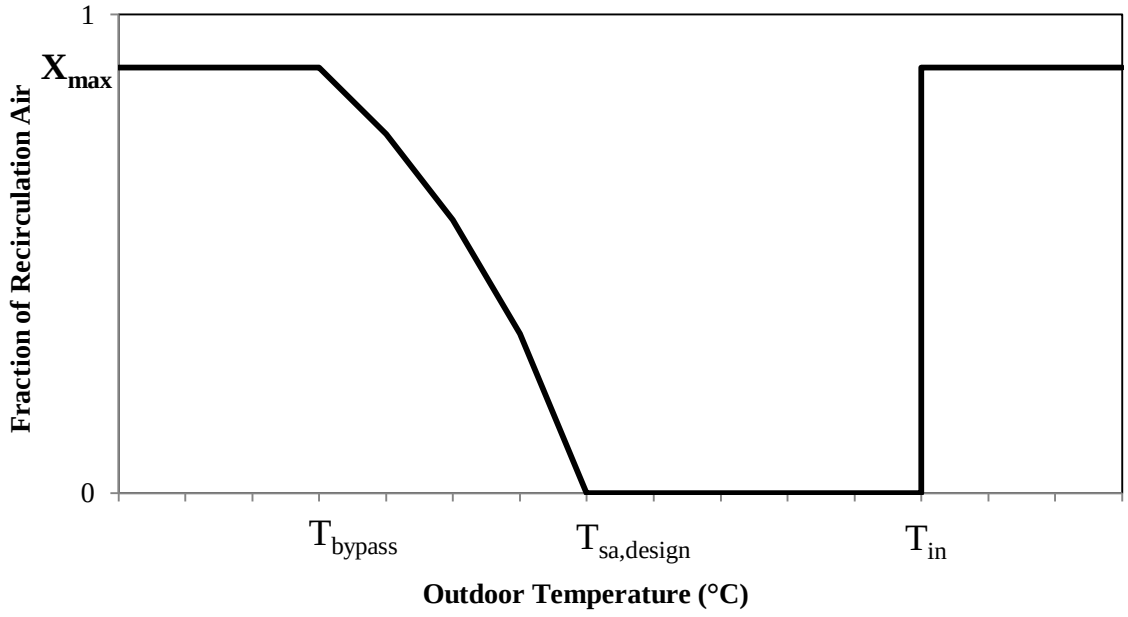

Figure 2.15: The fraction of recirculation air allowed by the economizer based on the outdoor temperature

The calculation of X_{max} is given in Appendix A. If the outdoor temperature is between T_{bypass} and $T_{sa,design}$, the economizer will increase the percentage of OA in the SA. X will then be calculated as

$$X=\frac{T_{sa,design}-T_{out}}{T_{in}-T_{out}}\ , \qquad (2.7)$$

where T_{out} is the outdoor temperature. If the outdoor temperature is greater than $T_{s,design}$ and less than the T_{in}, then X will be 0 and all the SA will be OA. If the outdoor temperature is greater than T_{in}, then X will just be X_{max}.

Table 2.9: System A maximum RA fraction in SA

City	Maximum Fraction of RA in SA, X_{max}
Saskatoon, Saskatchewan	0.962
Miami, Florida	0.927
Phoenix, Arizona	0.914
Chicago, Illinois	0.957

2.3.3 Heating Unit

The design indoor air temperature in the heating season is set as shown in Figure 2.16. The set point temperature is 22ºC for the maximum occupied times of day. The set point temperature varies according to the building load. In winter, the set point temperature is lower during the night as shown in Figure 2.16; however, it does not go lower than 15ºC during weekdays and 10°C during weekends.

When the air temperature in the space is below this set point temperature, the SA must be heated. This is accomplished using a natural gas heating coil. The efficiency of the heater is 90%

according to ASHRAE Standard 90.1 (2010). The efficiency of the heater is calculated based on the outdoor standard rating conditions of 8.3°C dry-bulb temperature and 6.1°C wet-bulb temperature given by AHRI Standard 340/360 (AHRI 2007). Appendix D presents the variation of the heater efficiency with operating conditions. When the heater is on, the air is heated to 30°C. The size of the heater is set to a large value as the capacity of the heater is not limited to a certain value.

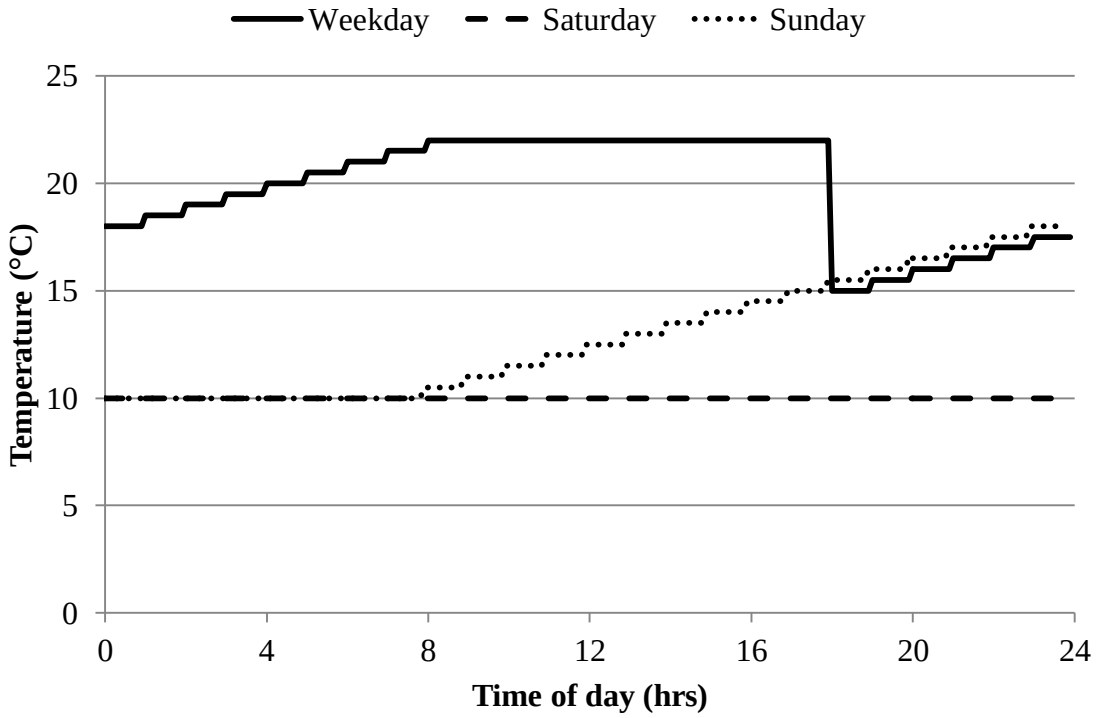

Figure 2.16: Indoor heating set point temperature through the day.

2.3.4 Cooling Unit

The design indoor air temperature in the cooling season is set as shown in Figure 2.17. The set point temperature is 24ºC for the maximum occupied times of day. The set point temperature varies according to the building load. In summer, the set point temperature is higher during the night as shown in Figure 2.17; however, it does not go higher than 28ºC during weekdays and 30°C during weekends.

When the temperature in the building is above the set point temperature, the SA must be cooled and thus the cooling unit is turned on. The cooling unit selected for use in the model is a simple cooling unit using bypass fraction method. The bypass fraction is assumed to be 0.15 and the set point temperature of the cooled air is 14°C as mentioned previously. The capacity of the cooling coil is also unlimited.

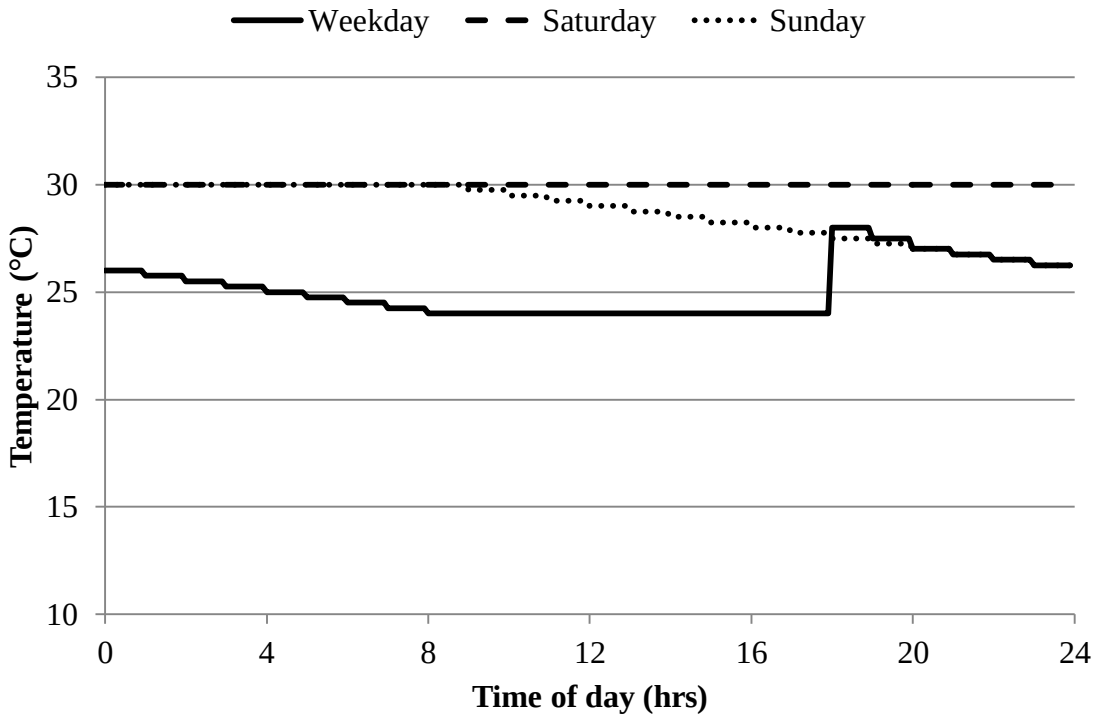

Figure 2.17: Indoor cooling set point temperature through the day.

The COP of the cooling unit is 3 to satisfy the minimum requirement of ASHRAE Standard 90.1 (2010). The COP of 3 for the cooling unit is determined at the outdoor standard rating conditions of 35°C dry-bulb temperature and 23.9°C wet-bulb temperature given by AHRI Standard 340/360 (AHRI 2007). The COP varies with operating conditions in the simulation. Appendix D presents the variation of the cooler COP with operating conditions.

2.3.5 Auxiliary Heater

The auxiliary heater is used to heat the water which is pumped to the radiant ceiling panel tubes in the space. When the air temperature in the space is below the heating set point temperature (shown in Figure 2.16), the heater is turned on. The efficiency of the heater is 90% according to ASHRAE Standard 90.1 (2010). When the heater is on, the water is heated to the required supply temperature. The size of the heater is set to a large value as the capacity of the heater is not limited to a certain value. The efficiency of the heater is calculated based on the outdoor standard rating conditions of 8.3°C dry-bulb temperature and 6.1°C wet-bulb temperature given by AHRI Standard 340/360 (AHRI 2007).

2.3.6 Auxiliary Cooler

The auxiliary cooler is used to cool the water which is pumped to the radiant ceiling panel tubes in the space. When the air temperature in the space is above the cooling set point temperature (shown in Figure 2.17), the cooler is turned on. When the cooler is on, the water is cooled to the required supply temperature. The cooler capacity is also unlimited. The COP of the cooling unit is 3 to satisfy the minimum requirement of ASHRAE Standard 90.1 (2010). The COP of 3 for the cooling unit is determined at the outdoor standard rating conditions of 35°C dry-bulb temperature and 23.9°C wet-bulb temperature given by AHRI Standard 340/360 (AHRI 2007). The COP varies with operating conditions in the simulation.

2.3.7 Supply and Exhaust Fan

Fans are important components in all HVAC systems. There are two constant volume fans, a supply fan, and an exhaust fan. The supply fan has a pressure drop of 1250 Pa (5 inH_2O) and the exhaust fan has a pressure drop of 500 Pa (2 inH_2O). Both fans have an efficiency of 70%. These values are based on the study done by Fauchoux (2006). The fan power is determined from the flow rate, pressure drop and efficiency of the fan.

2.3.8 Water Pump

A constant flow water pump is used to create water flow in the radiant panel tubes. The pump has an overall pump efficiency of 90% and a motor efficiency of 90%. The pump power is determined from the flow rate and efficiency of the pump.

2.3.9 Cooling Tower

Type 510 closed circuit (indirect) cooling tower component is used to naturally cool the RCP water. This is achieved by evaporating water from the outside of coils containing the RCP water. The RCP water is completely isolated from the ambient air and water in this type of cooling tower. This provides natural cooling to the water and saves cooling energy.

2.3.10 Radiant Ceiling Panels (RCP)

The radiant ceiling panels (RCP) are modeled in the building component (Type 15-6) in TRNSYS. The general RCP heat transfer equation is given by

$$Q_{RCP}=UA(T_p-T_a)\ , \tag{2.8}$$

where U [$W/m^2 \cdot K$] is the total heat transfer coefficient of the RCP, A [m^2] is the RCP area, T_p [K] is the panel temperature, and T_a [K] is the space temperature. T_p is the active layer surface temperature. The TRNSYS allows an active layer in the building. This layer can be in the floor, wall, or ceiling. TRNSYS allows two choices for the active layer: (a) define the parameters of the active layer including the specific heat coefficient of water, pipe spacing, pipe outside diameter, pipe wall thickness, and pipe wall conductivity, or (b) to use an expert mode where the user will have to define the specific heat transfer coefficient of water, and the equivalent heat transfer coefficient of the panels. The expert mode is used in this thesis so that the heat transfer coefficients would be defined. The convective heat transfer coefficient is assumed to be due natural convection as the ventilation is introduced into the space to very low flow rates. The convective heat transfer coefficient is calculated in a separate component for every time step depending on the panel temperature and the space air temperature. Equations (2.9) and (2.10) are used to calculate the convective heat transfer coefficients for heating and cooling ceiling panels, respectively (ASHRAE 2012).

$$h_c = 0.134(T_p - T_a)^{0.25} \tag{2.9}$$

$$h_c = 2.13\left|T_p - T_a\right|^{0.31} \tag{2.10}$$

where h_c is in $W/m^2 \cdot K$, T_p and T_a are in K. The radiation heat transfer coefficient is also calculated in a separate component and the total heat transfer coefficient is calculated and given to the building as an input each time step. The radiation heat transfer coefficient is calculated using equation (2.11) (ASHRAE 2012). In equation (2.11), both T_p and T_a must be in K.

$$h_r = 5\times10^{-8}\times\left|\frac{T_p^4 - T_a^4}{T_p - T_a}\right| \tag{2.11}$$

The total heat transfer coefficient is calculated using equation (2.12).

$$U = h_c + h_r \tag{2.12}$$

The U is given as an input value in every time step to the building component together with the water inlet temperature and mass flow rate. The outlet water temperature from the building is calculated in the building component in every time step and is given as input to the boiler or chiller as required.

2.3.11 HAMP

2.3.11.1 General Description

The main purpose of the HAMP is moisture transfer. Heat transfer also takes place but it is not as effective as moisture transfer. Convective heat transfer by the HAMP is experimentally investigated by Fauchoux et al. (2008, 2009). Heat transfer by radiation also takes place due to the temperature difference between the HAMP surface and the wall surfaces of the space. At this stage of the research, however, the method of regeneration of the HAMP desiccant solution is still under investigation. For this reason, the HAMP in this research is mainly used for moisture transfer to remove the latent load while the radiant panels are used in conjunction with the HAMP to remove the sensible load.

As stated in Section 1.3, the HAMP used in the office building uses lithium chloride (LiCl) as the salt solution. The temperature and concentration of the desiccant solution will determine the direction of heat and moisture transfer, thus a selection of a temperature and concentration for (a) heating and humidification, and (b) cooling and dehumidification must first be done. In order to decide on the desiccant solution concentration to achieve a concentration gradient between the surface of the HAMP and the space air, it is important to define the set point humidity ratio and look closely at how the HAMP surface humidity ratio changes with LiCl concentration and temperature. Figure 2.18 shows the relation between the HAMP surface humidity ratio with the solution concentration at six different desiccant solution temperatures. The surface humidity ratio values are calculated using empirical equations (Afshin 2010).

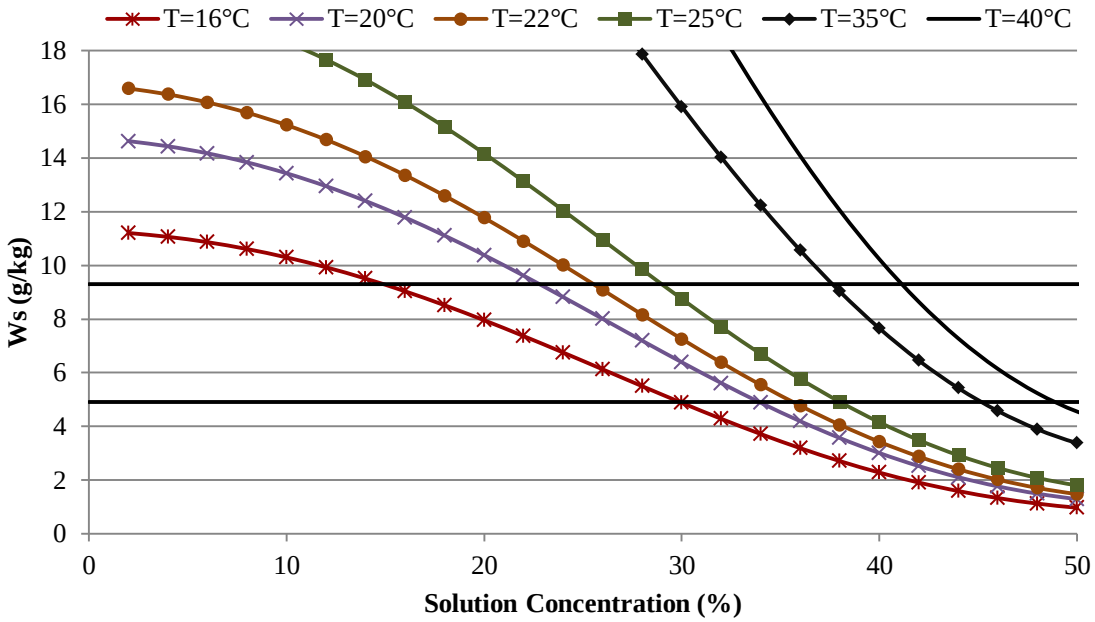

Figure 2.18: Relation between the HAMP surface humidity ratio (W_s) and the salt solution concentration at different solution temperatures for LiCl.

Figure 2.18 shows that at a certain solution temperature, as the solution concentration increases the surface humidity ratio of the HAMP decreases. Figure 2.18 also shows the indoor set point humidity ratio for humidification at 4.91 g/kg which corresponds to a temperature of 22ºC and relative humidity of 30% RH. Thus, it is required to keep the HAMP surface humidity ratio (W_s) above this value to create a mass transfer potential. In order to use a suitable temperature for heating and dehumidification, a temperature greater than 20ºC shall be used while for cooling and dehumidification, a temperature lower than 20°C shall be used. The salt solution is thus selected to be provided at 40ºC and 38% concentration for heating and humidification (W_s = 12.05 g/kg), and at 35°C and 50% concentration for heating and

dehumidification (W_s = 4.56 g/kg). Heating and humidification solution will create a value of 7.14 g/kg difference in the humidity ratio between the surface of the HAMP and the room design conditions.

Figure 2.18 shows the indoor set point humidity ratio for dehumidification at 9.30 g/kg which corresponds to a temperature of 24ºC and 50% RH. Therefore, W_s must be below 9.30 g/kg to allow moisture transfer from the indoor air to the HAMP. The salt solution is thus selected to be provided at 16ºC and 32% concentration for cooling and dehumidification (W_s = 4.28 g/kg), and at 16°C and 6% concentration for cooling and humidification (W_s = 10.86 g/kg). During cooling and dehumidification the solution will create a value of 5.02 g/kg difference in the humidity ratio between the surface of the HAMP and the room design conditions which is considered suitable for the dehumidification process.

2.3.11.2 Heat and Moisture Transfer Calculation

The methods used to calculate the moisture transfer between the HAMP and the space are presented in this section. Sensible heat transfer (both convection and radiation) between the HAMP and the space is neglected in this thesis because the HAMP area is generally small (10% of the ceiling area). However, the importance of the sensible heat transfer between the HAMP and the space will be studied in a sensitivity study in Appendix C.

The moisture added or removed by the HAMP is added or removed as a variable gain to the space. TRNBuild allows the user to add variable gains to the space that can be positive or

negative. The positive gain resembles sources of gains in a space such as occupants producing water vapor by breathing. The negative gain resembles sinks of moisture in a space such as building materials or furniture absorbing moisture from space. This gain is calculated using a Matlab code with input information from the building space. The code is presented in Appendix B. The Matlab code is integrated into TRNSYS using Type 155 which calls the Matlab code every time step. The moisture is calculated using heat and mass transfer analogy.

The general heat transfer equation is

$$Q = UA\Delta T \ , \tag{2.13}$$

where Q [kW] is the heat transferred, U is the overall heat transfer coefficient, A is the area, and ΔT is the temperature difference. This equation shows that the heat transfer depends on boundary layer conditions, which are influenced by surface geometry, nature of the fluid motion and thermodynamic and transport properties.

The general moisture transfer equation is

$$\dot{m} = U_m A\Delta W \ , \tag{2.14}$$

where $\dot{m}$ [kg/s] is the rate of mass transferred, U_m [m/s] is the mass transfer coefficient, and ΔW is the humidity ratio difference. This equation shows that moisture transfer mainly depends on

humidity ratio between the HAMP surface and the space, surface geometry, and transport properties.

The overall convective heat transfer coefficient is given by

$$U_c = \frac{1}{\frac{1}{h_{c1}} + \frac{t}{k_{th}} + \frac{1}{h_{c2}}} \quad , \tag{2.15}$$

where h_{c1} [W/m^2·K] is the convective heat transfer coefficient between HAMP external surface and space air calculated from Equations (2.9) and (2.10), t [m] is the thickness of the membrane between the air layer and liquid layer, k_{th} [W/m·K] is the thermal conductivity of the HAMP, and h_{c2} is the convective heat transfer coefficient between the HAMP internal surface and the desiccant solution (Incropera and DeWitt 2002). Since the convection heat transfer coefficient in liquids is around 1000 times greater than the convective heat transfer coefficients in air, the term $1/h_{c2}$ is neglected and Equation (2.15) is reduced to

$$U_c = \frac{1}{\frac{1}{h_{c1}} + \frac{t}{k_{th}}} \tag{2.16}$$

The Nusselt number is calculated using equation (2.17)

$$Nu=\frac{U_c L}{k_f}\ , \tag{2.17}$$

where L [m] is the characteristic length of the space calculated using equation (2.18),

$$L=\frac{4A_s}{P}\ , \tag{2.18}$$

where A_s [m^2] is the cross-sectional area of the HAMP, and P [m] is the perimeter of the HAMP (Incropera and DeWitt 2002). The HAMP is selected to cover 10% of the ceiling area. The surface humidity ratio of the HAMP, W_s, is calculated from equation (2.19) using the vapour partial pressure and the atmospheric pressure values,

$$W_s=0.62198\times\frac{p_v}{\frac{P_{atm}}{1000-p_v}}\ , \tag{2.19}$$

where p_v [kPa] is the vapour partial pressure and P_{atm} [kPa] is the atmospheric pressure (Incropera and DeWitt 2002). Appendix C gives a brief sensitivity on the effect of the atmospheric pressure value on the results. The vapour partial pressure is calculated using empirical formulae given in the Matlab code in Appendix B. The density of dry air is calculated using

$$\rho_{dryair} = \frac{p_a}{R \cdot T_a} \ , \tag{2.20}$$

where p_a [kPa] is the air partial pressure calculated using empirical formulae given in Appendix B, and R is the air gas constant.

The Sherwood number, Sh, which is the dimensionless concentration gradient at the surface of the HAMP, is calculated using the heat and mass transfer analogy. The analogy of heat and mass transfer applies when each of the equations is composed of advection (bulk motion) and diffusion terms of the same form. As a result, the boundary layer temperature and concentration profiles must have the same functional form. Accordingly, heat and mass transfer relations for a particular geometry are interchangeable. Equation (2.21) may be used to directly relate the two convection coefficients

$$\frac{Nu}{Pr^n} = \frac{Sh}{Sc^n} \ , \tag{2.21}$$

where Pr is Prandtl number, and Sc is Schmidt number. For most applications it is reasonable to assume a value of n = 1/3 (Incropera and DeWitt 2002). Equation (2.21) can be used to calculate Sh. The Schmidt number, Sc, which is defined as the ratio of the momentum diffusivity (viscosity) and the mass diffusivity, is calculated using equation (2.22)

$$Sc = \frac{\upsilon}{D_{AB}} \ , \tag{2.22}$$

where ν [kg/s·m] is the kinematic viscosity and D_{AB} [m^2/s] is the diffusivity of moisture into air. These properties are calculated according to the zone temperature by interpolation from input values.

The convective mass transfer coefficient, U_m, is calculated using equation (2.23)

$$Sh = \frac{U_m L}{D_{AB}} \tag{2.23}$$

The final equation used to calculate the rate at which moisture is added to or removed from the space is

$$H = U_m A \rho_{dryair} (W_s - W_a) \ . \tag{2.24}$$

Although equation (2.24) provides an estimate of the moisture transfer between the HAMP and the room air, it should be noted that it is not totally correct because it applies the analogy between heat and moisture transfer to the overall thermal resistance rather than the convective heat transfer coefficient only (see equation (2.17)). In order to obtain more correct values of the mass transfer coefficient from the heat-mass transfer analogy, the calculated Nu should be based on the convection heat transfer coefficient only rather than the overall heat transfer coefficient. The moisture resistance of the membrane should then be added to the obtained mass transfer coefficient to determine the overall moisture resistance of the HAMP. This is demonstrated and

studied in appendix C to show how this corrected moisture transfer calculation changes the simulation results in the most humid climate (Miami).

2.3.11.3 Regeneration Energy

The energy required for the regeneration of the desiccant solution flowing in the HAMP depends on the method used for the regeneration process. In this stage of research, it is challenging to decide on how the salt solution will be practically regenerated. More research is needed to estimate the amount of energy that will be needed to regenerate the HAMP desiccant solution. Thus, the ideal regeneration method is considered out of the scope of this thesis and left for further future research. The gain added or removed by the HAMP in the space is used to calculate the theoretical latent load added or removed defined as

$$Q_{lat} = H \cdot h_{fg} \ , \tag{2.25}$$

where H [kg/s] is the moisture added or removed to or from the space calculated using equation (2.24) and h_{fg} [kJ/kg] is the latent heat of vaporization of water. This is then added to the space as a separate gain that can be positive (heat added to the space) or negative (heat removed from the space). This theoretical latent load is presented in the figures. This is just an assumption to be able to estimate the required regeneration energy.

2.3.12 Summary

The building envelope, building schedules, HVAC systems, and HVAC components used were described in this chapter. Table 2.6 briefly summarizes the loads removed from each system. The space load includes the heating or cooling required due to the temperature different between the space and the outdoors, the air infiltration into the building, the internal load including lighting, equipment, occupants, and other sources or sinks of heat inside the building, while the ventilation load is the energy required to heat or cooling the ventilation air that is required by ASHRAE Standard 62.1 (2010) to maintain a healthy environment inside the building.

Table 2.10: A summary of different systems studied showing how each system handles the space and ventilation sensible and latent loads.

	Space		Ventilation	
	Sensible	**Latent**	**Sensible**	**Latent**
System A	VAV	None	VAV	VAV
System B	RCP	None	MV	MV
System C	RCP	HAMP	MV	MV
System D	RCP	DOAS	DOAS	DOAS

Where,

- VAV: Variable air volume system.
- RCP: Radiant ceiling panel system.
- MV: 100% OA mechanical ventilation system.
- HAMP: Heat and moisture transfer panel.
- DOAS: Dedicated outdoor air system.

CHAPTER 3 SIMULATION DESCRIPTIONS

The TRNSYS simulation package is chosen for this study according to a study performed by Fauchoux (2006) on different types of building simulation programs that are commercially available. TRNSYS was found to be the best out of 11 programs that suits the required characteristics for this research. TRNSYS is a FORTRAN-based transient system simulation program which is designed to solve complex thermal systems by breaking them down into less complicated components. As is shown by Beckman et al. (1994), TRNSYS is characterized by its capability to solve each thermal component independently and then couple them to solve the main thermal system. Thermal Energy System Specialists, TESS, is one of the major developers of TRNSYS component libraries. TRNSYS 17 and the second version of TESS libraries are used in this study. Research on radiant ceiling panel using TRNSYS simulation program has been verified by experimental results (such as Miriel et al. (2002) and Vangtook & Chirarattananon (2006, 2007)) showing its ability to produce accurate and reliable results.

TRNSYS is made up of two parts (Klein 2000). The first is an engine that reads and processes the input file. This engine also performs the mathematical processes. The second part is a huge library of components. Each component is used to model one part of the system and the components are connected together (Klein 2000). The library includes fans, pumps, multizone buildings, weather data processors, and basic HVAC equipment such as chillers, boilers, cooling towers, heat exchangers, and other equipment.

The TRNSYS user interface is divided into two connected programs: TRNBuild and TRNSYS Simulation Studio. The TRNBuild allows the user to define the building zones, their volumes, and air capacitance. In every zone the roof, walls, and floor materials are defined. The users can create their own material or use materials from different libraries including the ASHRAE (2012) library of materials. Every wall windows and doors can also be defined either by the user or from different libraries. Ventilation, cooling, heating, infiltration, heat and moisture gains, humidity model and thermal comfort parameters of every zone can also be defined in TRNBuild. Different schedules can also be defined to control the heating, cooling, and other important variables.

As previously mentioned in Section 2.2.8, TRNBuild also allows the user to define an active layer which acts as the radiant panels. This layer is added to the ceiling layers as the panels are placed on the ceiling in this research. TRNBuild has two models for humidity calculation inside buildings. The first is the "Simple Humidity Model" or "Capacitance Humidity Model" which considers sorption effects with an enlarged moisture capacity of the air where the user defines the humidity capacitance ratio which can be set to 1 or more. The second model is the "Moisture Capacitance Model" or "Buffer Storage Model" which is a more sophisticated model offering a surface and a deep moisture buffer in the walls of the space. The first model is used in this research to account for moisture storage in space materials.

TRNSYS Simulation Studio is the second part of the user interface where the building designed in TRNBuild is called as a multizone building component and connected to other

components such as fans, heating and cooling equipment, infiltration calculation component, weather data components, and other components which together form the complex thermal system under investigation. Figure 3.1 shows a part of a system in the simulation studio. The simulations can be executed in the simulation program and the results are written in external files which are analyzed separately. The results can also be directly plotted while the program is progressing.

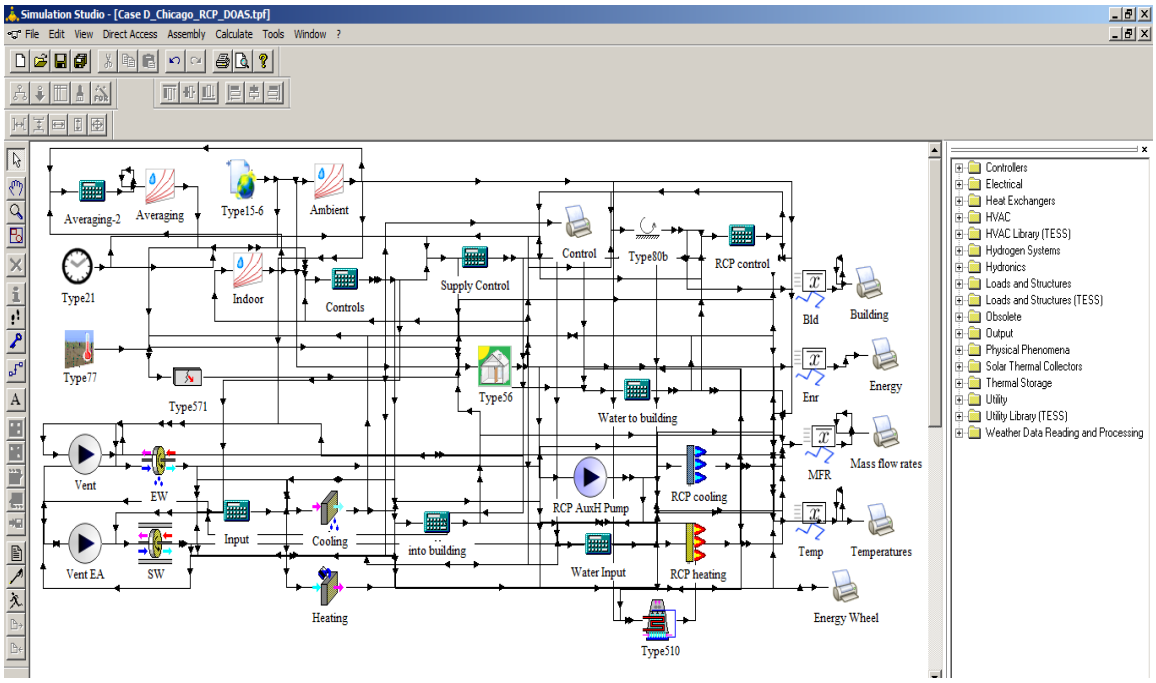

Figure 3.1: A part of a complex thermal system in TRNSYS 17 Simulation Studio.

The simulation time step is a very important variable that directly affects the quality of the results. The user can control the simulation time span and time step from the control cards in the simulation studio. Figure 3.2 shows the space temperature fluctuation on the coldest day in

Saskatoon using different time steps. As the time step decreases the temperature fluctuations decrease and the temperature follows the set point closer.

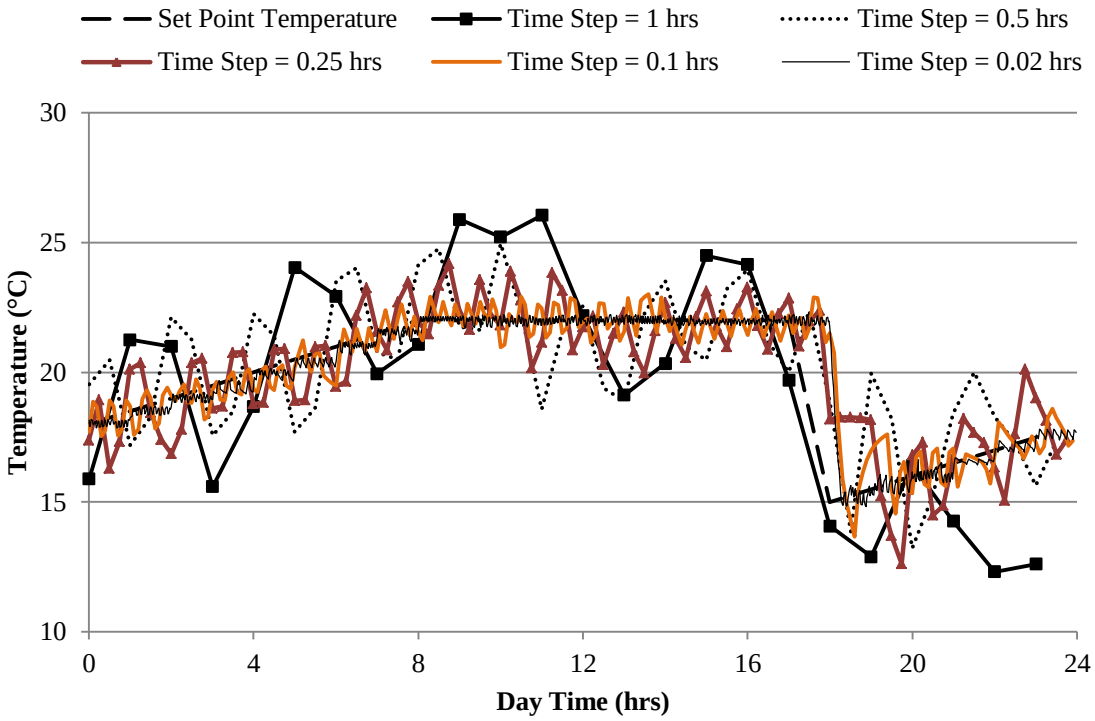

Figure 3.2: Temperature fluctuation with different time steps on the design cooling day in Saskatoon without averaging.

TRNSYS has been used for over 35 years and has proven to be a reliable tool used by many researchers (e.g. Sodec 1999, Vangtook & Chirarattananon 2006 and Fauchoux 2006). It also allows the user to edit the source codes of its components, which are written in FORTRAN, which makes it a very flexible tool as it allows users to write their own components as well as

call other external programs such as Matlab and Fluent, making TRNSYS a very good tool for energy simulation in buildings.

3.1 WEATHER DATA

The simulations are performed in four different cities: Saskatoon, Saskatchewan; Miami, Florida; Phoenix, Arizona; and Chicago, Illinois. The global position and elevation of each of these cities are shown in Table 3.1. The weather data files that are used in TRNSYS program contain this information and hourly weather data of each city for a typical meteorological year. The weather files used in this thesis are in the TMY2 format and are obtained from the National Renewable Energy Laboratory (2009). When the simulation is run at intervals of less than one hour the data in the weather file are interpolated to give data at each time step. In this research, the time step used is 0.1 hours. This is based on a sensitivity study done by running the simulations at time steps of 1, 0.5, 0.25, 0.1 and 0.01 hours. The accuracy of the results and the time efficiency were compared and the time step of 0.1 hours proved to compromise the optimal time efficiency with acceptable accuracy of the results.

Table 3.1: Location of the four different cities.

	Saskatoon, SK	Miami, FL	Phoenix, AZ	Chicago, IL
Latitude	52.17° N	25.80° N	33.43° N	41.98° N
Longitude	106.68° W	80.30° W	122.02° W	87.90° W
Elevation (m)	500	3	338	205

Briggs et al. (2003) developed a new climatic classification method of the world is different climates to be used for building energy analysis. This classification divided the cities into eight different climatic zones based on temperature ranging from very hot to subarctic. These climatic zones take numbers from number 1 which is very hot to number 8 which is subarctic. Afterwards, these zones were further divided into three humidity based subdivisions which are humid, marine and dry. These were designated with the letters of A for humid, B for dry, and C for marine. The combination of temperature based and humidity based classification resulted in 17 climatic zones and U.S. sample cities were introduced as representatives of each climate. Table 3.2 presents a summary of the climatic zones studied in this thesis and the representative city, dry bulb (DB) and wet bulb (WB) temperatures for heating and cooling seasons (ASHRAE 90.1 2010).

Table 3.2: Climatic zones and representative cities used.

Climatic Zone	Very Hot-Humid	Warm-Dry	Cool-Humid	Very Cold-Dry
Representative city	Miami, FL	Phoenix, AZ	Chicago, Illinois	Saskatoon, SK
Heating DB (°C)	8	1	-21	-35
Cooling DB (°C)	32	42	31	29
Cooling WB (°C)	25	21	23	17
Climatic Zone Number	1A	3B	5A	7

Figure 3.3 presents the hourly TMY2 weather data on the psychrometric chart and the distribution of outdoor condition in different regions for one year in Miami. Region 1, 2, 3, 4, 5, and 6 represent cold & dry, cool & dry, mild & dry, hot & dry, hot & humid, and mild & humid

weather, respectively. The hourly weather data from Miami are 59% in region 5 and 88% in regions 5 and 6 which agrees with its very hot humid climatic zone.

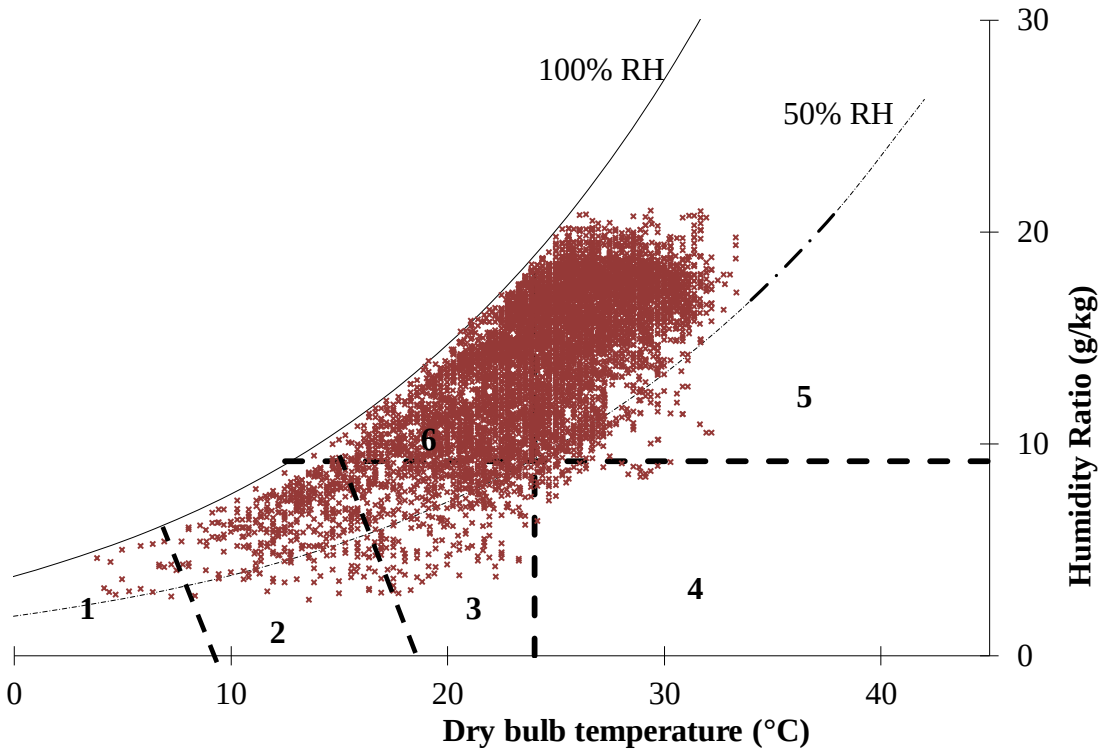

Figure 3.3: Hourly ambient condition in one year in Miami.

To further ensure that different climatic zones are applicable to selected cities, Figure 3.4 presents the fraction of outdoor conditions in each psychrometric region in every selected city. There is a good agreement between Briggs et al. (2003) and Figure 3.4. Phoenix has 46% of the time in a year in regions 4 and 5 which are the hot regions. It also had 50% of the time in regions 3 and 4 which are the warm dry regions.

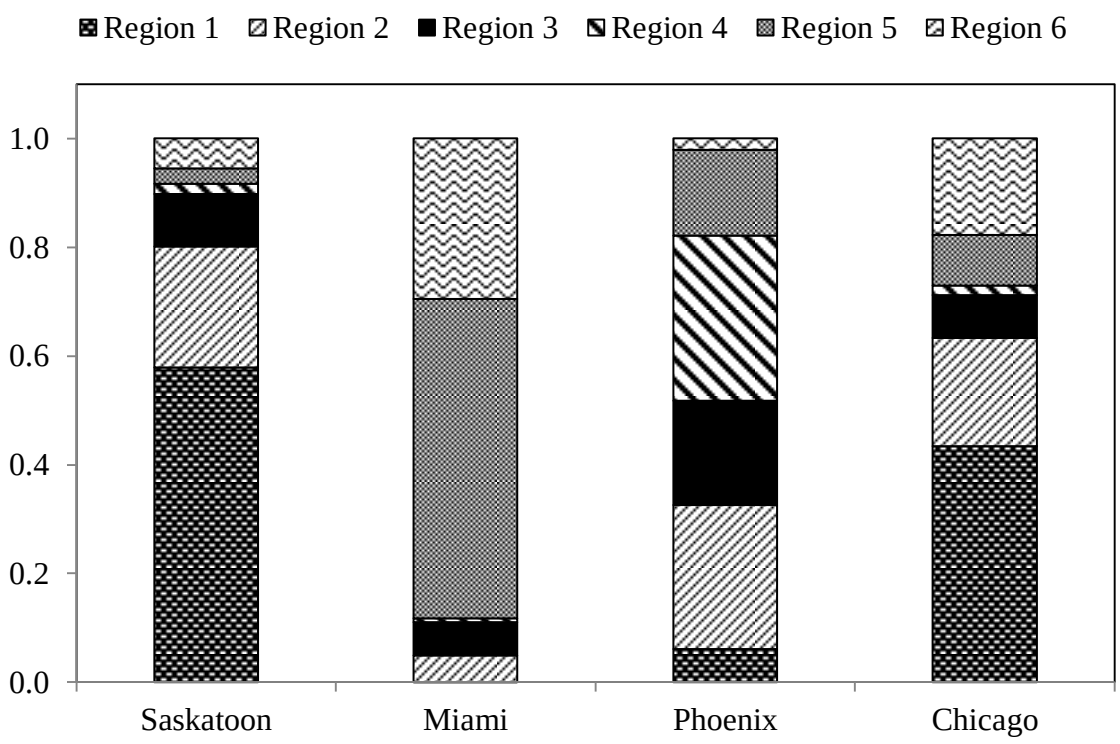

Figure 3.4: Yearly distribution of outdoor conditions in different psychrometric chart regions.

In Saskatoon, the weather is in region 1 58% of the time of the year and in regions 1 and 2 80% of the time of the year. This means that Saskatoon has a very cold and dry weather. Finally, Chicago has 43% of the time in a year in region 1 and 71% in regions 1, 2 and 3 showing cool weather. Chicago also has 18% of the time in a year in region 6 which is the cool humid region.

The cumulative outdoor temperature, humidity ratio and enthalpy distributions for each of these cities are given in Figure 3.5, Figure 3.6, and Figure 3.7, respectively.

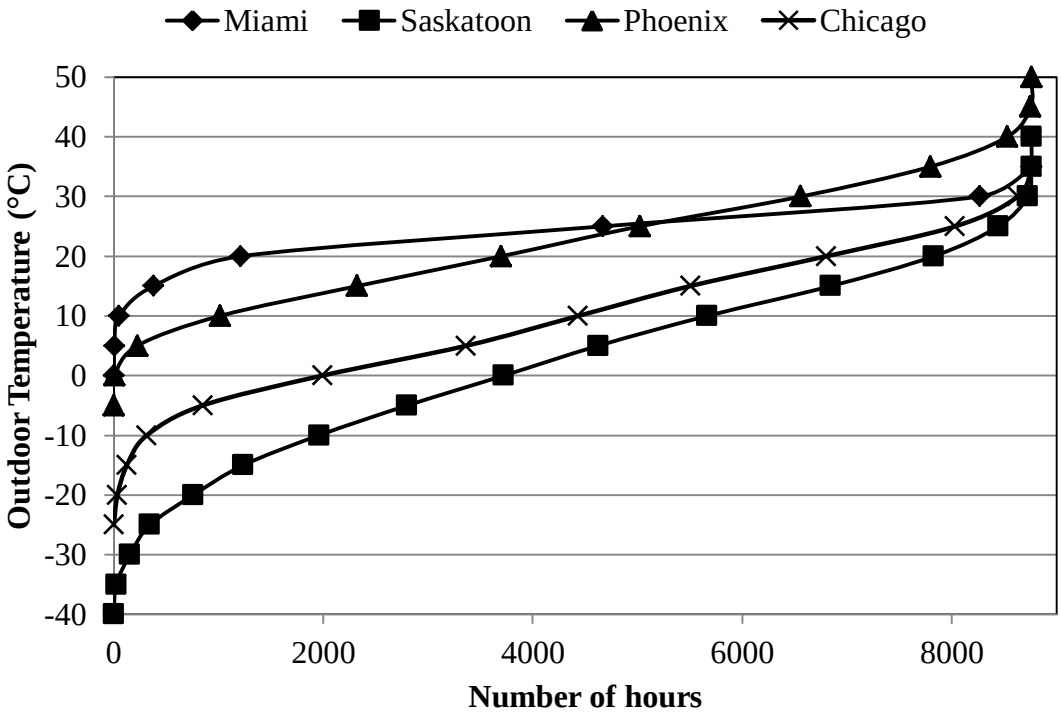

Figure 3.5: Cumulative outdoor temperature distributions in the four cities.

Figure 3.5 shows that each city has a different outdoor temperature profile. In Saskatoon the temperature gets as cold as -36°C, and the temperature is below 20°C more than 7800 hours or 89% of the year. The maximum temperature in Saskatoon is 34°C and the temperature is above 25°C for only 4% of the year. Chicago is the next coldest city with a minimum temperature of -22.5°C and 6800 hours (78% of the year) where the temperature is below 20°C. The maximum temperature reached in Chicago is 35°C and the temperature is above 25°C only 8% of the year.

Phoenix has a rather hot climate with a maximum temperature of 46°C which is the highest temperature reached in the four cities. The outdoor temperature in Phoenix is above 25°C 43% of

the year. The minimum temperature than can be reached in Phoenix is -3°C and the temperature is below 20°C 42% of the year. The slope of the cumulative temperature curve in Miami is large at first and the temperature reaches 20°C quickly, but it then flattens out in the middle. Another slight increase occurs at the end of the profile and the temperature reaches about 33°C. The maximum temperature in Miami is 33°C but the temperature is above 25°C 47% of the year. The minimum temperature in Miami is 4°C. The temperature in Miami is below 20°C only 14% of the year and most of the winter heating is not needed at all.

The cumulative outdoor humidity ratio is shown in Figure 3.7 for each city. Saskatoon, Phoenix and Chicago have very similar profiles, showing many hours at the lower humidity levels and gradually increasing up to values around 14 g/kg, 18 g/kg, and 21g/kg, respectively. Saskatoon has the driest weather as the humidity ratio is the least in all hours. Miami shows only a few hours at low humidity levels and many hours at higher humidity levels. Miami peaks around 21 g/kg. Chicago has generally lower humidity ratios than Phoenix half of the time or in the dry season, but is relatively more humid in summer as it even hits the highest humidity level around 21 g/kg.

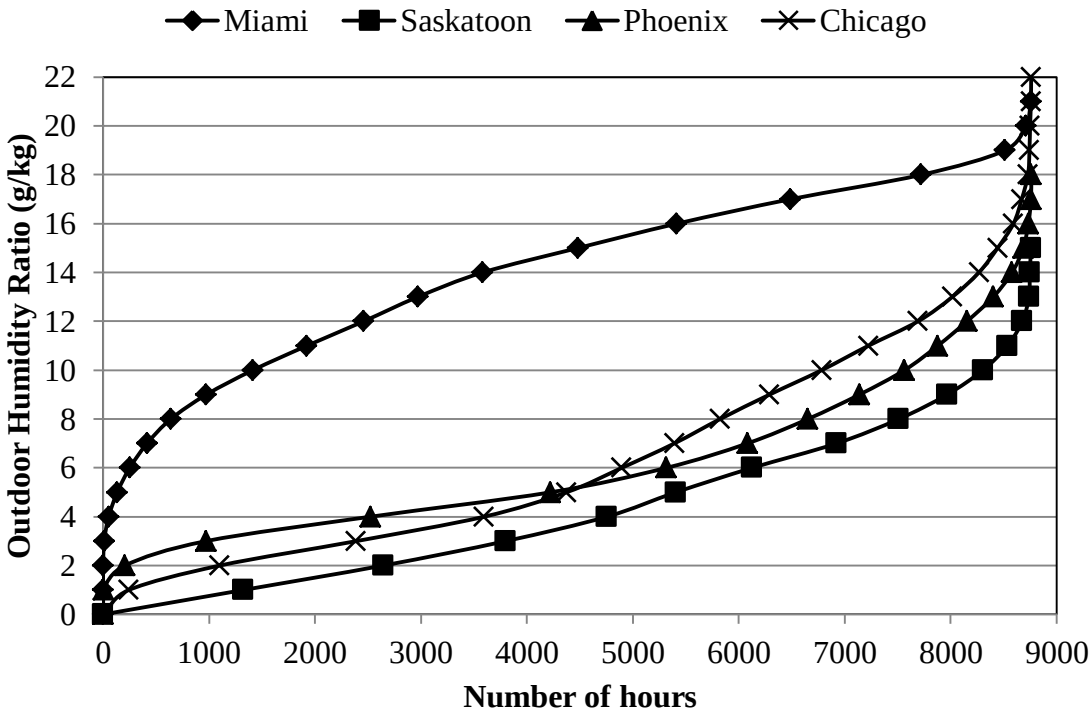

Figure 3.6: Cumulative outdoor humidity ratio distributions in the four cities.

The cumulative outdoor enthalpy distribution for each city is shown in Figure 3.7. Saskatoon has the lowest enthalpies, because of its low temperatures and humidity levels. Chicago has enthalpies greater than Saskatoon but generally lower than Phoenix although the maximum enthalpy in Chicago is higher than that of Phoenix. Actually the enthalpy in Phoenix is slightly higher than Chicago, because of its warmer temperatures. Miami has the highest enthalpies, because of its high temperatures and humidity levels.

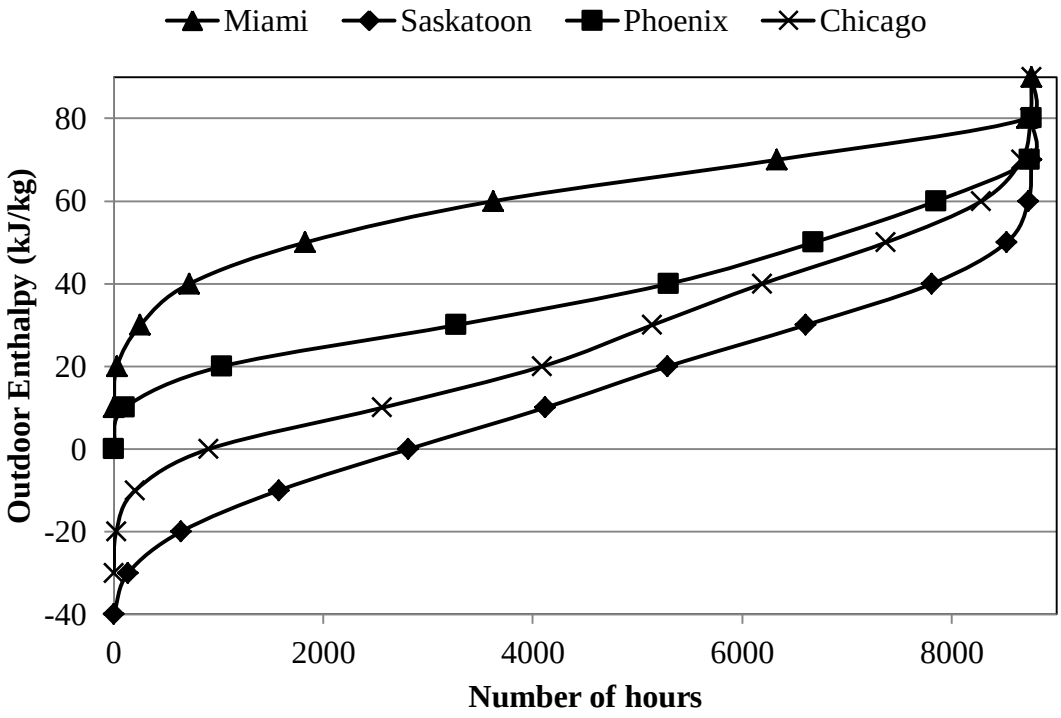

Figure 3.7: Cumulative outdoor enthalpy distributions for the four cities.

3.2 THEORETICAL LOADS (PRELIMINARY RESULTS)

The simulations were first run without HVAC equipment to calculate the theoretical space heating and cooling loads of each city. The minimum ventilation required by ASHARE Standard 62.1 (2010) is included in this calculation. The weather file type 15-6 is changed for different cities. The time step used to calculate the loads is 0.1 hours. The results presented here are hourly averages, which mean that the results were averaged over 10 time steps. The design space heating and cooling loads of each city are given in Table 3.3. Miami has the hottest climate and thus the highest design cooling load. In spite of the fact that Phoenix has the highest outdoor

temperature as is shown in Figure 3.5, both Miami and Chicago have higher design cooling loads. This is because Miami and Chicago have more humid climates and thus higher dehumidification loads.

Table 3.3: Design space loads for each city.

City	Design Heating Load (kW)	Design Cooling Load (kW)
Saskatoon, SK	102	47
Miami, FL	16	66
Phoenix, AZ	34	56
Chicago, IL	74	61

It is also shown in Figure 3.5 that the minimum temperature takes place in Saskatoon, SK, and thus the maximum cooling load is in Saskatoon followed by Chicago.

Table 3.4 presents a comparison of energy intensity in each city between the current research and another research on a different building done by Rasouli (2010).

Table 3.4: Comparison of energy intensity of each city.

	Current Space	Rasouli (2010)
City	Energy Intensity ($MJ/(m^2 \cdot year)$)	Energy Intensity ($MJ/(m^2 \cdot year)$)
Saskatoon, SK	471	726
Miami, FL	617	780
Phoenix, AZ	464	519
Chicago, IL	342	526

Table 3.4 shows that the loads in Rasouli's work in the cold climates (Saskatoon and Chicago) are 54% higher. This might be explained by Table 3.5 which shows that Rasouli (2010) used relatively low resistance values for the roof and floor, which are each more than double the wall area, while he used a higher resistance for the walls. Rasouli (2010) did not specify the resistance value of the windows used but only mentioned they were double pane windows. The windows used in the current research are triple pane as detailed in Section 2.1.2. In Miami, Rasouli's load is 27% higher than the current space load and in Phoenix 12% higher than the current space load. In both cases the loads are close. Differences might be due to different lighting, occupancy, temperature, and relative humidity schedules in addition to other reasons mentioned previously.

Table 3.5: Comparison of building envelope resistances between the current research and research by Rasouli (2010).

	Current	**Rasouli (2010)**
	Resistance (m^2·K/W)	**Resistance (m^2·K/W)**
Wall	2.36	2.72
Roof	3.94	3.64
Floor	3.58	3.45

The Building Energy Consumption Survey (CBECS) (1986) reported an average energy intensity of 533 MJ/(m^2·year) for HVAC energy consumption in US office buildings. The values of the four cities in the study range from 519 and 780 MJ/(m^2·year) which is a relatively good range of this value. The average energy intensity of the four cities in the current research is 474 MJ/m^2·year, which is 12% lower than the reported average, while the average of Rasouli (2010)

is 638 MJ/m^2·year which is 20% higher than the reported average. Thus the average energy intensity in the current research is relatively closer than the reported average.

The results of the theoretical load case simulation in Saskatoon, SK, are presented in this section for a two-day design period corresponding to the coldest and the hottest periods of the year. The indoor temperature at each hour over two days in January and August can be seen in Figure 3.8 and Figure 3.10, along with the outdoor temperature, design temperature and the heating or cooling demand.

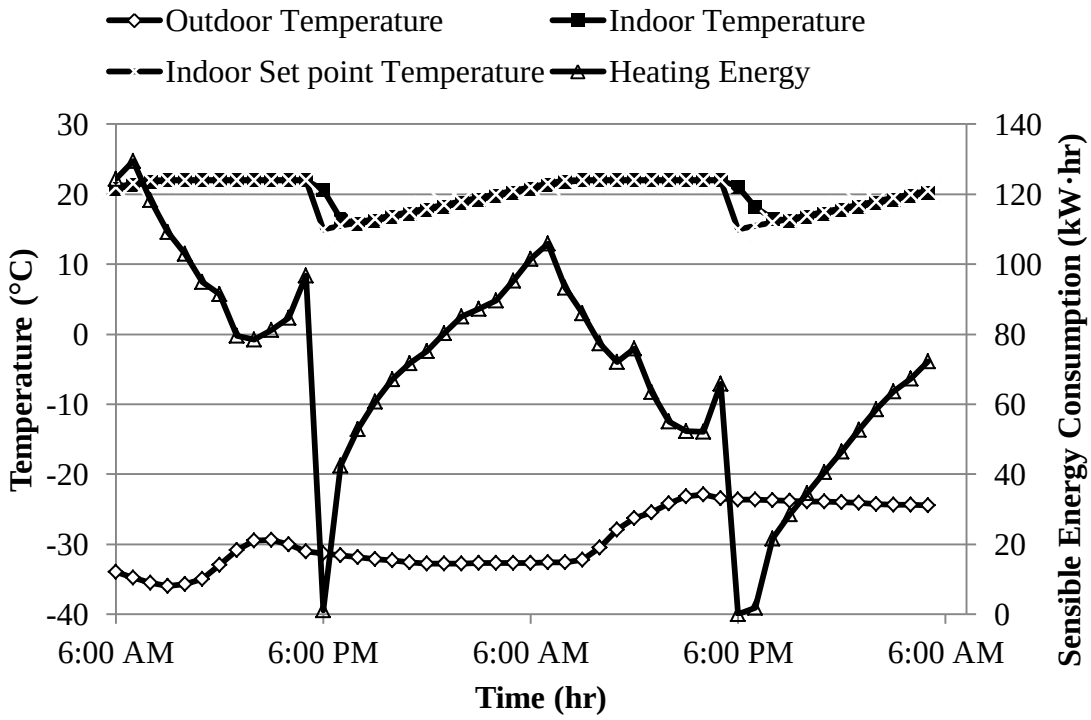

Figure 3.8: Building hourly average outdoor temperature, indoor temperature, and the heating energy consumption in Saskatoon over two days in January.

The results in Figure 3.8 begin at 6:00 am on January 14th when the indoor temperature is 21°C due to the night setback. At 6:00 am, the thermostat calls for additional heat to heat the building to 22°C. The ventilation system is also turned on at 6:00 am resulting in the peak heating consumption of 106 kW·hr at 7:00 am on January 15. The temperature in the space begins to heat up so that it is at a comfortable temperature when the occupants of the building arrive at 8:00 am. Between 8:00 am and 2:00 pm the heating energy consumption decreases, because of the heat given off by the internal heat sources (occupants, lights, equipment) in the space. At 9:00 am the temperature reaches 22°C and is nearly constant until 5:00 pm when the night set back is initiated. The heating energy consumption goes to zero at this point. The building cools at a rate slower than the indoor set point temperature which decreases during the next two hours from 22°C to 16°C. At 7:00 pm, heating comes on to keep the indoor temperature above 18°C. This process is repeated again the next day. The indoor temperature is very similar on the second day, but the energy consumption is slightly lower because the outdoor temperature is higher.

The relative humidity of the space during the two day period in January is shown in Figure 3.9, along with the outdoor relative humidity and the heating energy. This profile is more random than the temperature distribution as the relative humidity levels in the building are not controlled. The relative humidity levels depend on the people in the space, as well as the outdoor relative humidity. At 6:00 am, the indoor space has a relative humidity of about 2% RH. When the people enter the building at 8:00 am the relative humidity level begins to increase, reaching 13% RH by 11:00 am. There is a slight decrease in the relative humidity between 11:00 am and

1:00 pm when some of the occupants leave for lunch. The relative humidity increases again during the afternoon as the occupants return.

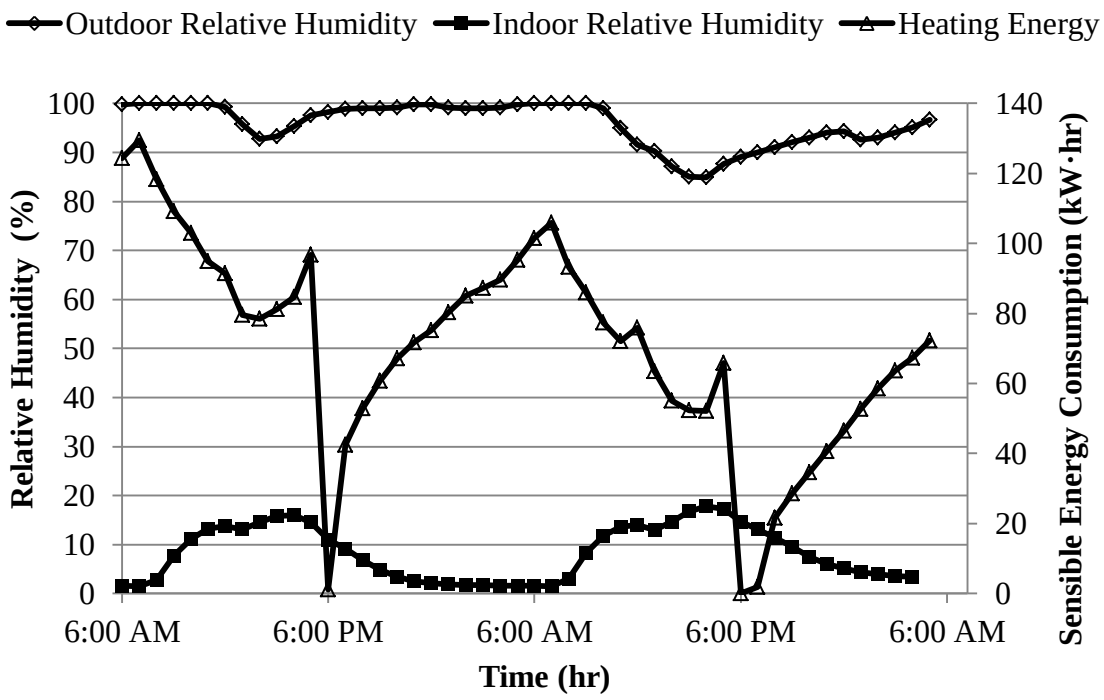

Figure 3.9: Building hourly average outdoor relative humidity, indoor relative humidity of the space, and the heating energy consumption in Saskatoon over two days in January.

At 5:00 pm, the majority of the occupants leave the building and the relative humidity level decreases again. By 9:00 pm, all of the occupants have left and the relative humidity levels out at about 5% RH. The process follows the same pattern for the next day but with slightly higher humidity values. These higher values are due to higher outdoor temperatures and consequently

higher outdoor humidity ratios on January 15. The average outdoor humidity ratio is 0.19 g/kg on January 14th and 0.36 g/kg on January 15. The initial relative humidity when the ventilation system turns on is about 2% RH on the first day and increases by 14% RH. On the second day the initial value is 5% RH so an increase of 14% RH makes the relative humidity around 19% RH.

Figure 3.10 shows the indoor temperature distribution for a two day period in August along with the outdoor temperature, design temperature, and the cooling energy. The indoor temperature is 24.5°C at 6:00 am on August 19th and begins to decrease as the occupants enter the building and the cooling energy increases, reaching 24°C at 9:00 am. The cooling system is turned on to keep the space temperature from exceeding 24°C. The required cooling energy starts out small, but increases as the outdoor temperature increases and radiative gains from previous hours become cooling loads. Radiative gains from previous hours are due to thermal storage in the different building masses such as the walls and the furniture. The cooling energy drops between 11:00 am and 1:00 pm as occupants leave the building for lunch. At 5:00 pm, some of the occupants begin to leave the building so the amount of cooling required to maintain a temperature of 24°C decreases. When all the occupants leave the building, the cooling energy is turned off and the temperature in the space begins to increase at 9:00 pm. After 9:00 pm the cooling energy starts increasing again due to the night set back and due to the lighting which is left on at 10% all night. The cooling energy does not increase to high levels except when occupants enter the building again the next morning. The same pattern is repeated the next day except that the cooling energy is less than the previous day due to lower outdoor temperatures.

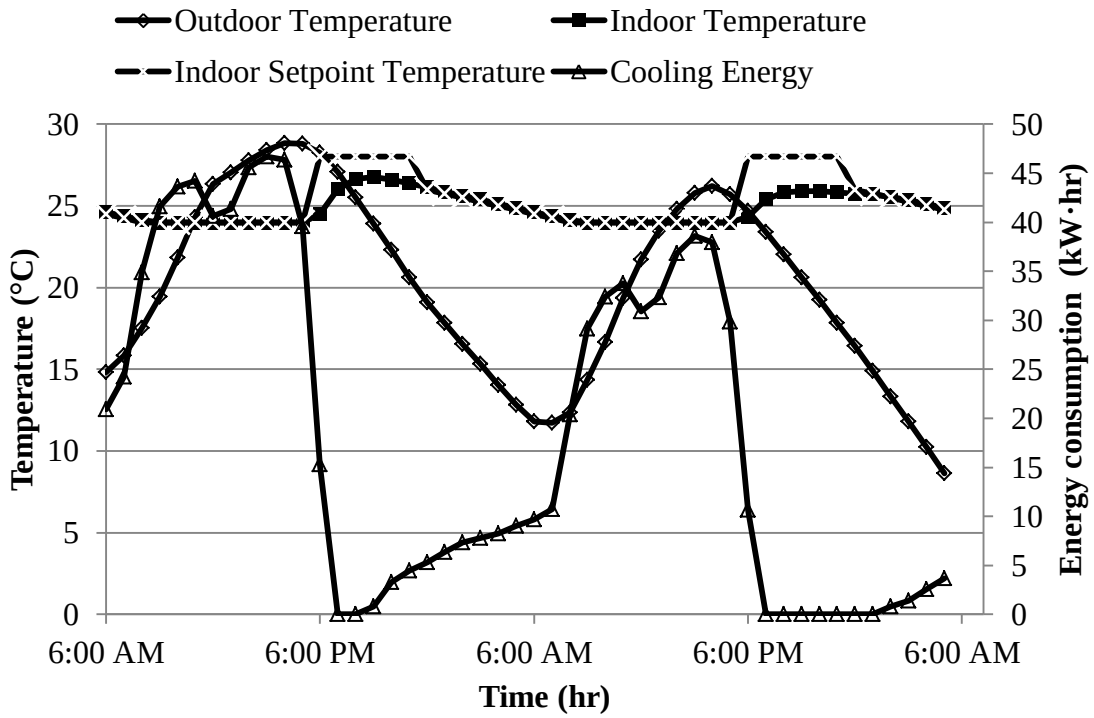

Figure 3.10: Building hourly average outdoor temperature, indoor temperature, and the cooling energy consumption in Saskatoon over two days in August.

Figure 3.11 shows the indoor relative humidity, outdoor relative humidity and cooling energy over the two day period in August. The indoor relative humidity is initially at 56% RH at 6:00 am on August 19th, but decreases when the ventilation system is turned on because the outdoor humidity ratio is lower than the indoor humidity ratio. The occupants of the building enter at 8:00 am and the relative humidity increases slightly again. When the occupants leave the building at 6:00 pm and the amount of cooling required is reduced, the indoor relative humidity begins to decrease slightly again. At 11:00 pm the ventilation system is turned off and the relative humidity level within the space remains almost at a constant value until the next

morning. This process is repeated again the next day. Generally, the relative humidity is mainly constant throughout the day.

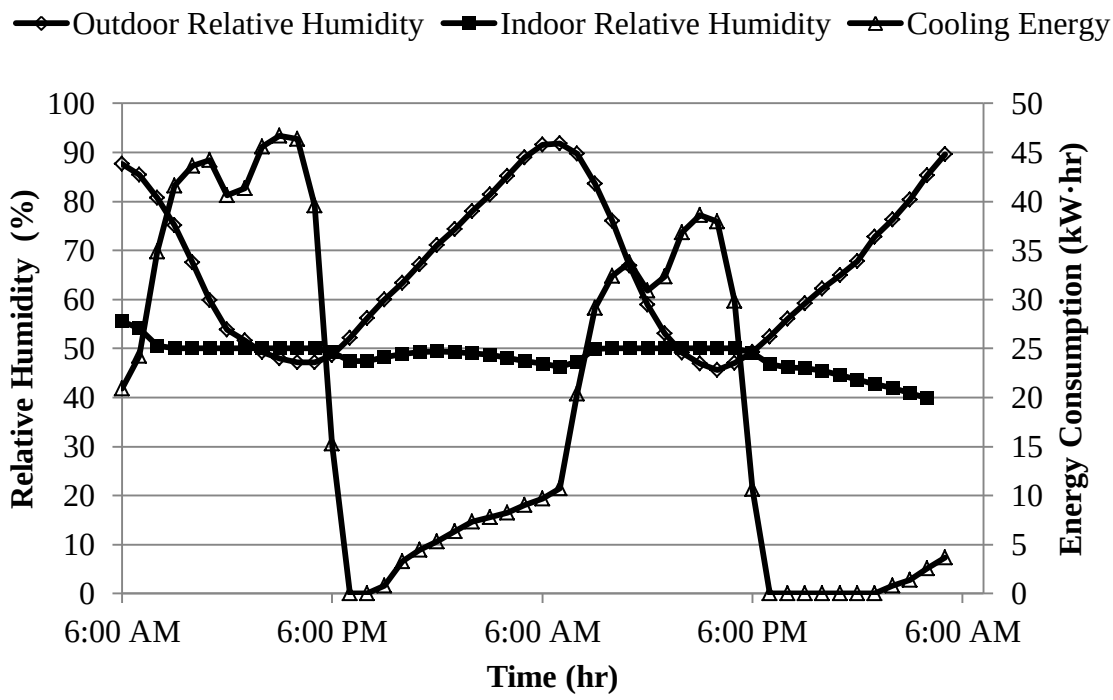

Figure 3.11: Hourly average outdoor relative humidity, indoor relative humidity of the space, and the cooling energy consumption in Saskatoon over two days in August.

CHAPTER 4 RESULTS

This chapter will discuss the results of the simulations pertaining to the improvement of space relative humidity levels while maintaining or improving heating energy and cooling energy consumption levels. The results from the four systems described in Section 2.2 will be presented and compared (system A: conventional all-air system; system B: radiant ceiling panel system with 100% OA mechanical ventilation; system C: radiant ceiling panel system with HAMP and 100% OA mechanical ventilation; and system D: radiant ceiling panel system with DOAS) in the four different cities representing the major climatic conditions (as discussed in Section 3.1).

4.1 SPACE TEMPERATURE

To be able to ensure that the radiant ceiling panels system is capable of removing the heating and cooling loads, the temperature inside the zone is monitored and compared to the set point temperatures in Figure 2.16 and Figure 2.17, respectively. In order to do that, the space temperature in a selected winter day with the highest heating load and on a selected summer day with the highest cooling load will be compared in system A (all-air system) and system B (radiant ceiling panel system) in each city. The space temperature variation of systems C and D are very close to that of system B as the radiant ceiling panel (RCP) system is common in the three systems. Thus, the space temperature of system B only is represented.

Figure 4.1 shows the variation of the space temperature on December 31 in Chicago. Chicago has a cold winter as the ambient temperature reaches -22°C. In the all-air system, the

space temperature follows the set point temperature closely showing the ability of the system to cover the load and responding quickly to changes in space load. In the RCP system, the space temperature also follows closely with the set point temperature except when there is a sharp drop in the ambient temperature near 5:00 am. However, the drop in space temperature is relatively low and the panels are capable of responding and covering the load.

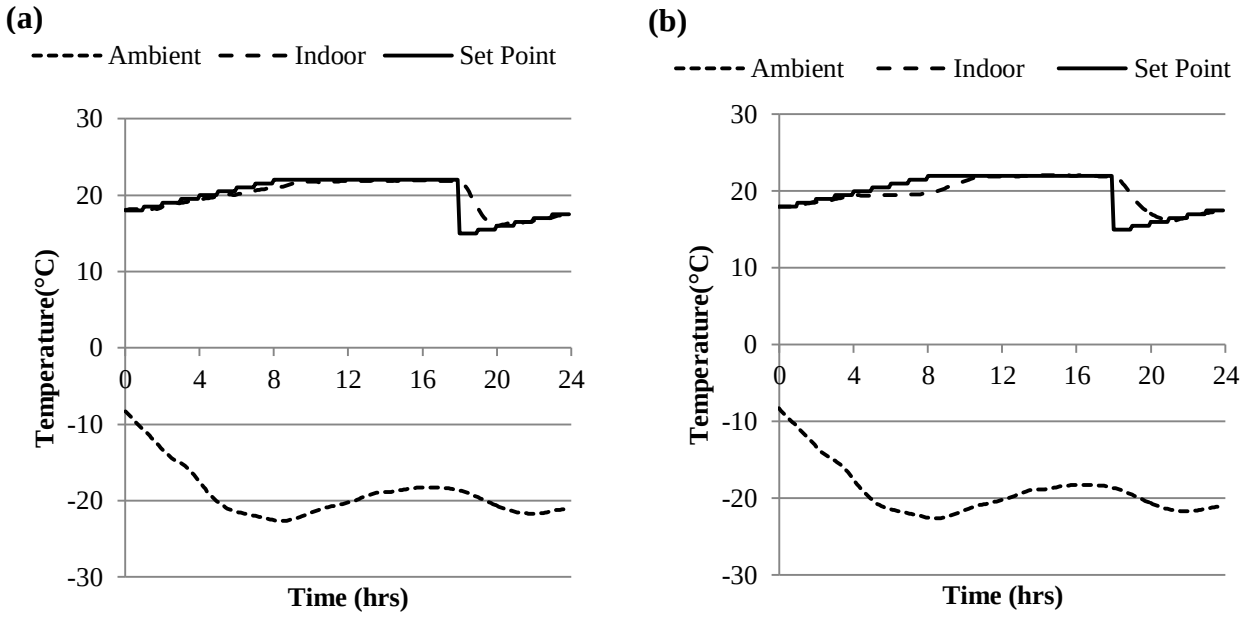

Figure 4.1: Heating space temperature variation with respect to set point temperatures on the design heating day in Chicago: (a) All-air system and (b) RCP system.

The response of the panels can be viewed as slow compared to the all-air system due to the fact that the ceiling panels have a lower heat transfer coefficient for heating. Generally, floor

radiant panels have a higher heat transfer coefficient for heating and thus it is recommended for heating. The space temperature goes back to the set point temperature overnight slowly such that less heating is required overnight in Figure 4.1 (b). This is caused by the hot liquid in the panels. This means that, although the flow of water is stopped and the heating or cooling equipment is turned off, it takes some time for the water in the tubes to reach steady state with the space air.

Figure 4.2 shows the variation of the space temperature on July 9 in Chicago.

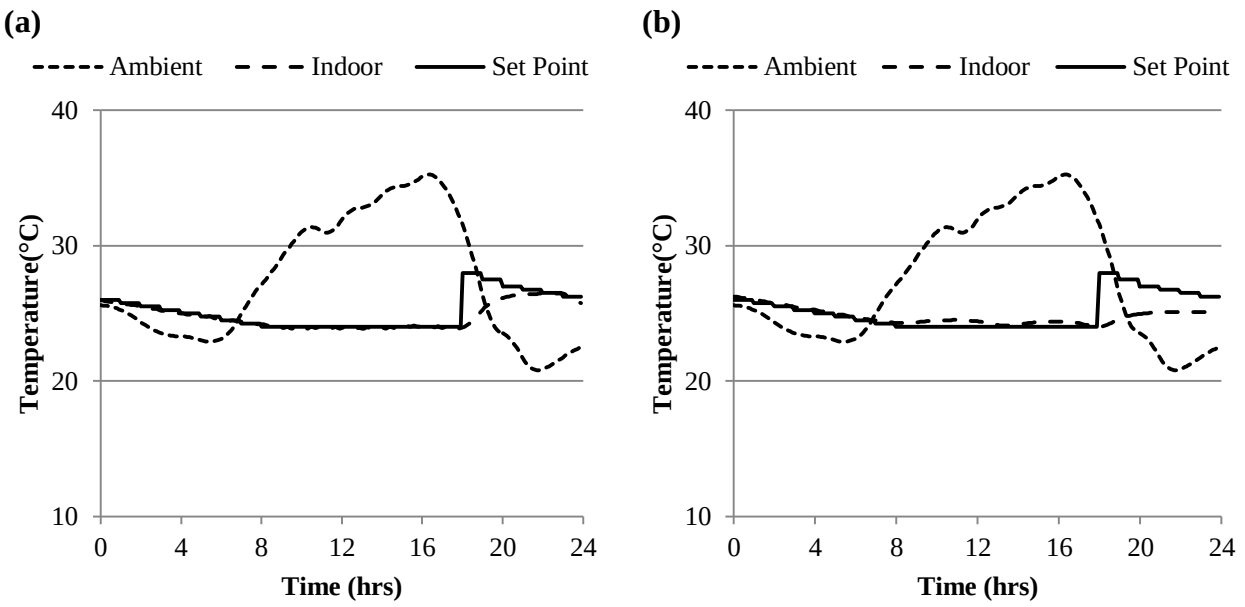

Figure 4.2: Cooling space temperature variation with respect to set point temperatures on the design cooling day in Chicago: (a) All-air system and (b) RCP system.

The space temperature is close to the set point temperature in the all-air system proving its ability to respond quickly to changes in the ambient temperature and space load. The RCP system shows a good performance in cooling as the space temperature is much closer to the set point temperature. It is however noted that there is a very slight increase in the space temperature by about 9:00 am due to the sudden increase of internal latent loads in the building due to the start of the working hours. The internal loads include occupancy, equipment, and lighting shown in Figure 2.8, Figure 2.9, and Figure 2.10, respectively. Similarly, the cold liquid in the panels maintains a cold temperature overnight in the RCP system in Figure 4.2 (b) and no cooling is required overnight. The ambient temperature also drops sharply overnight which also slows the temperature rise inside the space even further and no cooling is required.

Figure 4.3 shows the variation of the space temperature on January 15 in Saskatoon. Saskatoon is characterized by a very cold winter as the ambient temperature reaches -36°C on the design day in the TMY-2 weather data. The all-air system in Figure 4.3 (a) is able to keep the space temperature very close to the set point temperature. However, the lag in response of the RCP and the effect of the low heating heat transfer coefficient of the ceiling panels is most obvious in Figure 4.3 (b) especially as the ambient temperature was falling in the morning (4:00 am to 12:00 pm). After that time and until the end of the working day, it can be claimed that the RCP performed better than the all-air system and kept the space temperature relatively close to the set point temperature. However, the lowest space temperature that is reached in the RCP system during the working hours in Figure 4.3 (b) is about 18.7°C which probably will not be accepted and will result in a high percentage dissatisfaction of the occupants. This can be

improved by using floor radiant panels, increasing the RCP area, or increasing the water temperature as will be discussed in CHAPTER 5.

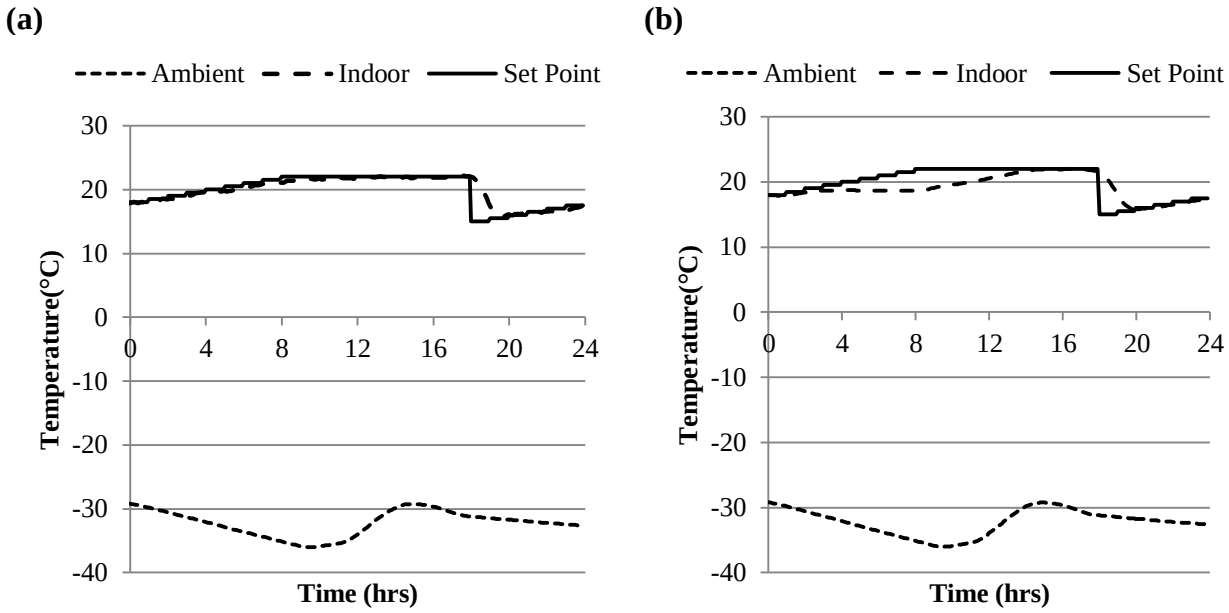

Figure 4.3: Heating space temperature variation with respect to set point temperature on the design heating day in Saskatoon: (a) All-air system and (b) RCP system.

Figure 4.4 shows the variation of the space temperature on August 19 in Saskatoon. The performance in Saskatoon in cooling is relatively better than Chicago. Slight overcooling takes place in the all-air system. However, the space temperature varies closely to the set point temperature in Figure 4.4 (a). The temperature in Figure 4.4 (b) varies closely to the set point

temperature. The RCP is capable of covering the cooling load most of the day. There is also no cooling required overnight in the RCP system.

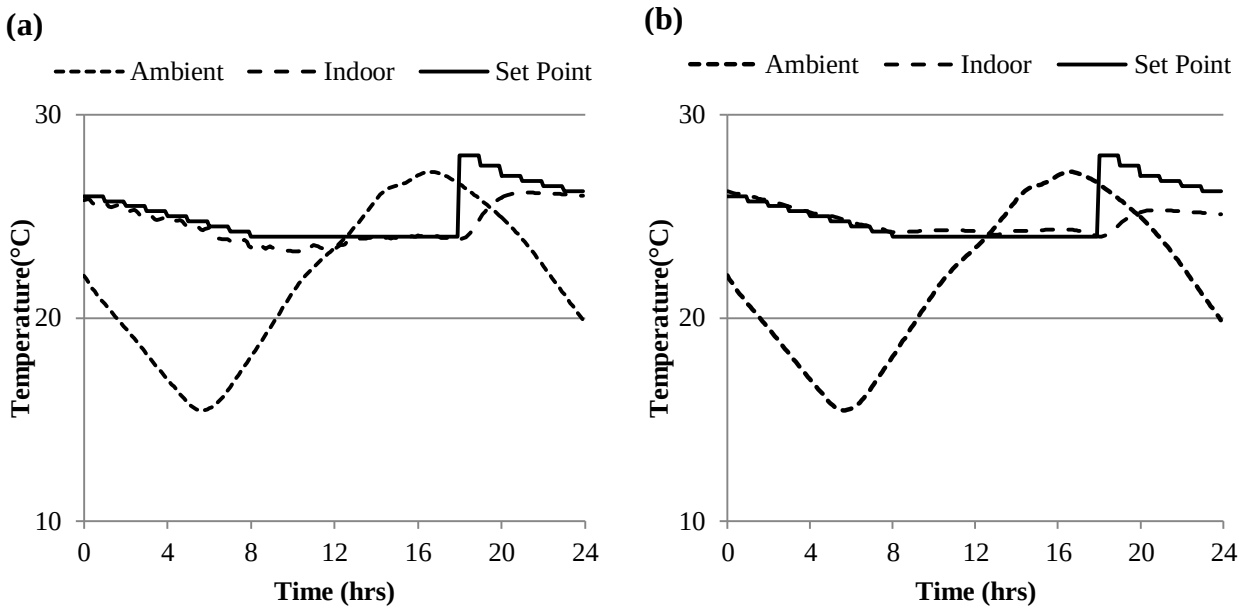

Figure 4.4: Cooling space temperature variation with respect to set point temperature on the design cooling day in Saskatoon: (a) All-air system and (b) RCP system.

Figure 4.5 shows the variation of the space temperature on January 1 in Miami. Miami is characterized by a very hot and humid summer and very mild winter. After simulating the office building under several control conditions in Miami's winter, it is decided to turn off the heating in Miami. The minimum space temperature reached under the no heating condition is 20°C which confirms that Miami does not need heating. No heating or cooling is done in both systems.

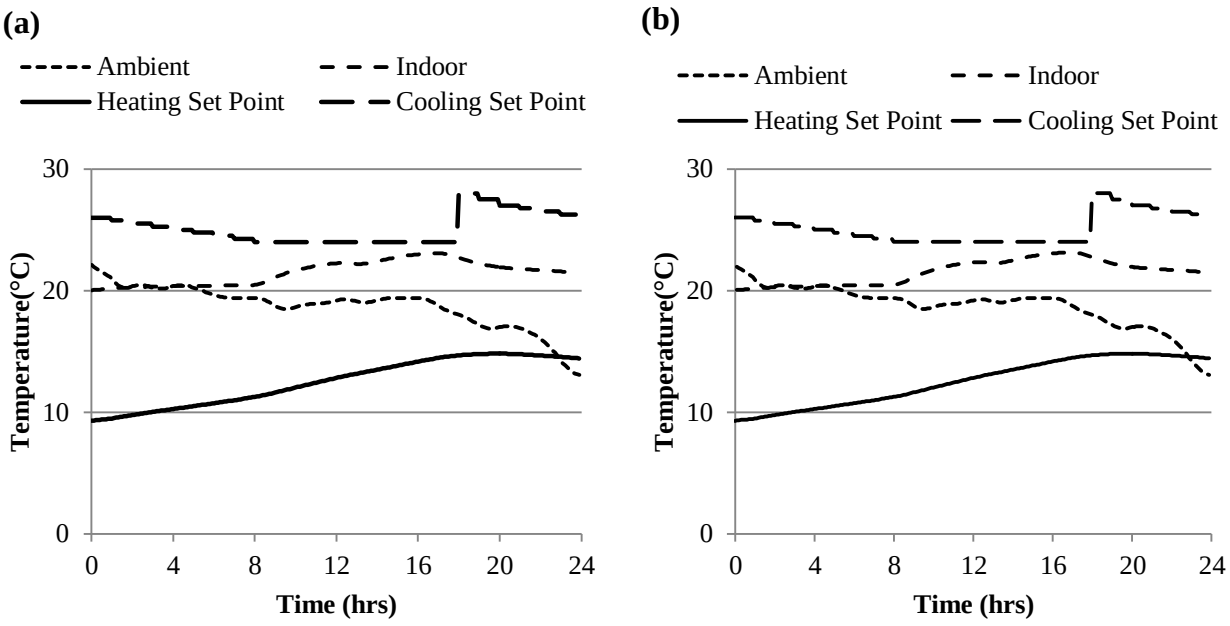

Figure 4.5: Space temperature variation in the heating season with respect to set point temperatures on the design heating day in Miami: (a) All-air system and (b) RCP system.

Figure 4.6 shows the variation of the space temperature on July 16 in Miami. The performance resembles that of Chicago and Saskatoon. The RCP system shows a good performance in cooling as the space temperature is close to the set point temperature. However, there is a very slight increase in the indoor temperature between 8:00 am and 10:00 am and between 3:00 pm and 5:00 pm in the space temperature due to the sudden increase of internal latent loads in the building and the increase in the ambient temperature. As discussed previously, the cold liquid remains in the RCP during night maintaining a cold temperature overnight in the

RCP system in Figure 4.6 (b). Although some cooling is required in the all-air system in Figure 4.6 (a), there is no cooling required in the space for the RCP system.

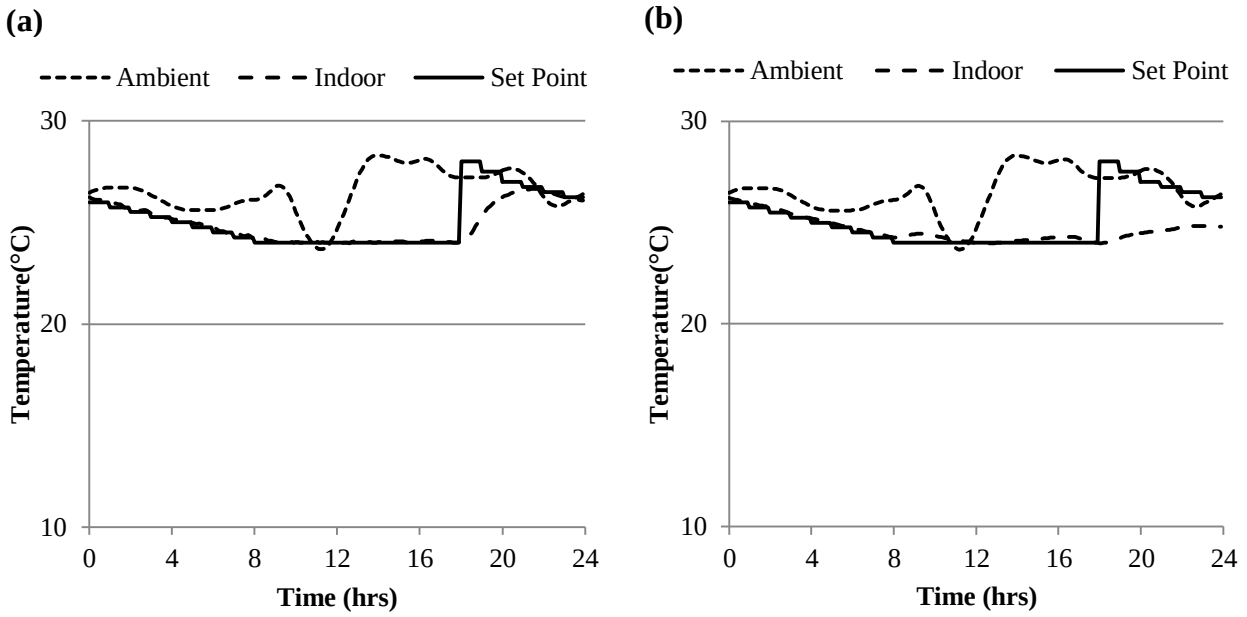

Figure 4.6: Space temperature variation in the cooling season with respect to set point temperatures on the design cooling day in Miami: (a) All-air system and (b) RCP system.

Figure 4.7 shows the variation of the space temperature on December 24 in Phoenix. In Phoenix, both heating and cooling may be required in winter. This is due to the mild winter that characterizes the city. However, no cooling is required in both systems because the indoor temperature does not exceed the cooling set point temperature as shown in Figure 4.7.

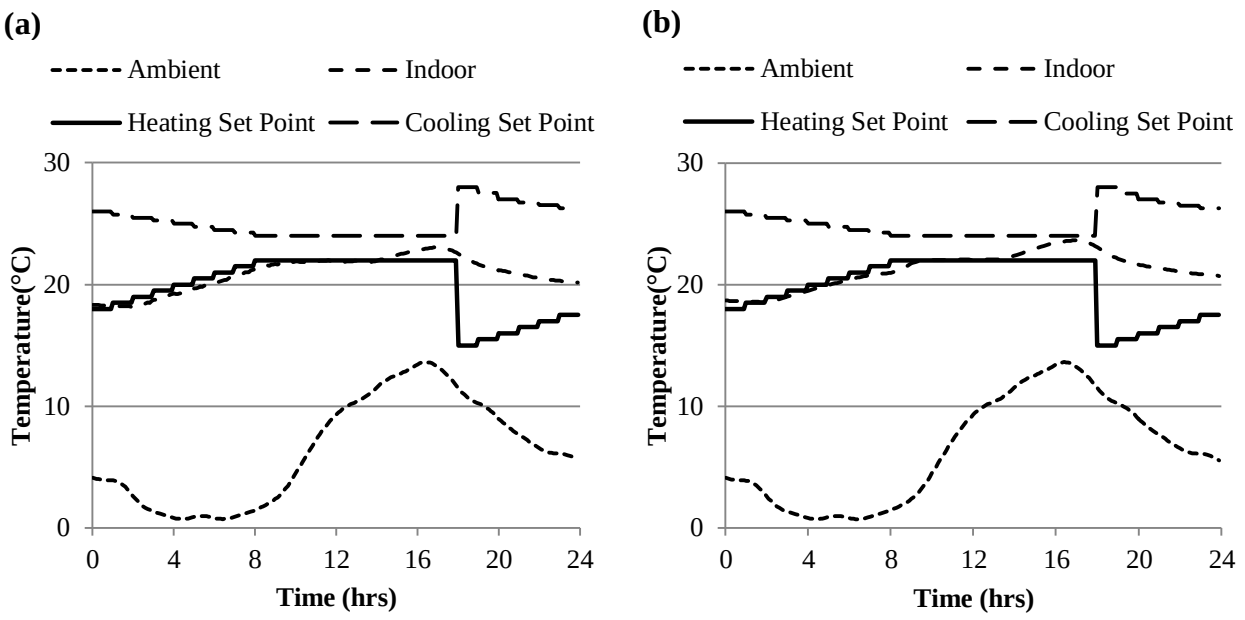

Figure 4.7: Space temperature variation in the heating season with respect to set point temperatures on the design heating day in Phoenix: (a) All-air system and (b) RCP system.

Figure 4.8(a) shows the design (theoretical) heating and cooling loads required in Phoenix on the December 24 together with the loads of both systems plotted using a running average. The running average is the averaged value of the energy transfer rate over the previous ten time steps and is calculated for every time step. Figure 4.8(b) presents the same results as in Figure 4.8(a) except that the energy transfer rates are averaged over a specific hour. Therefore, Figure 4.8(b) presents the average energy transfer rate for a specific hour and will be used in energy plots throughout this thesis. Cooling in both systems is zero showing that no cooling is required all day. This shows that Phoenix requires heating only on the beginning of the day due to the cold

ambient temperature. The figure also shows that theoretical cooling is required at the end of the day due to the increase of the ambient temperature and the internal loads. However, no heating or cooling is required at the end of the day in both systems. Both the all-air system and the RCP system keep the indoor temperature close to the set point temperature in heating throughout the day.

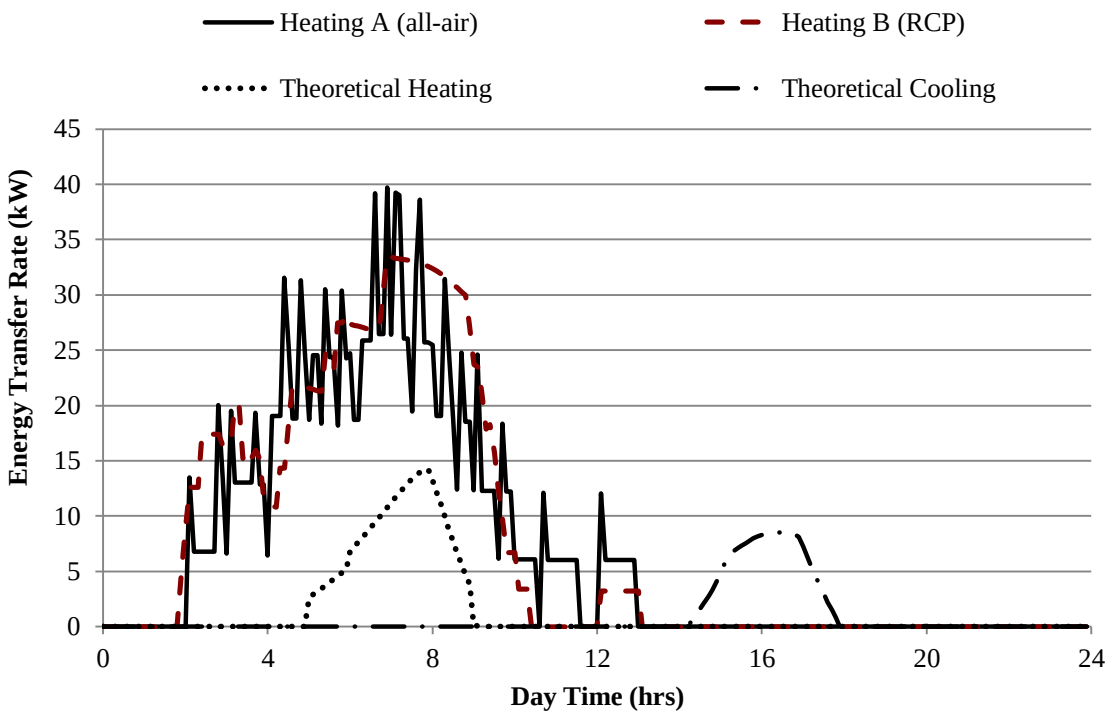

Figure 4.8(a): Energy transfer rate on December 24 (design heating day) in Phoenix of the two systems compared to the theoretical loads.

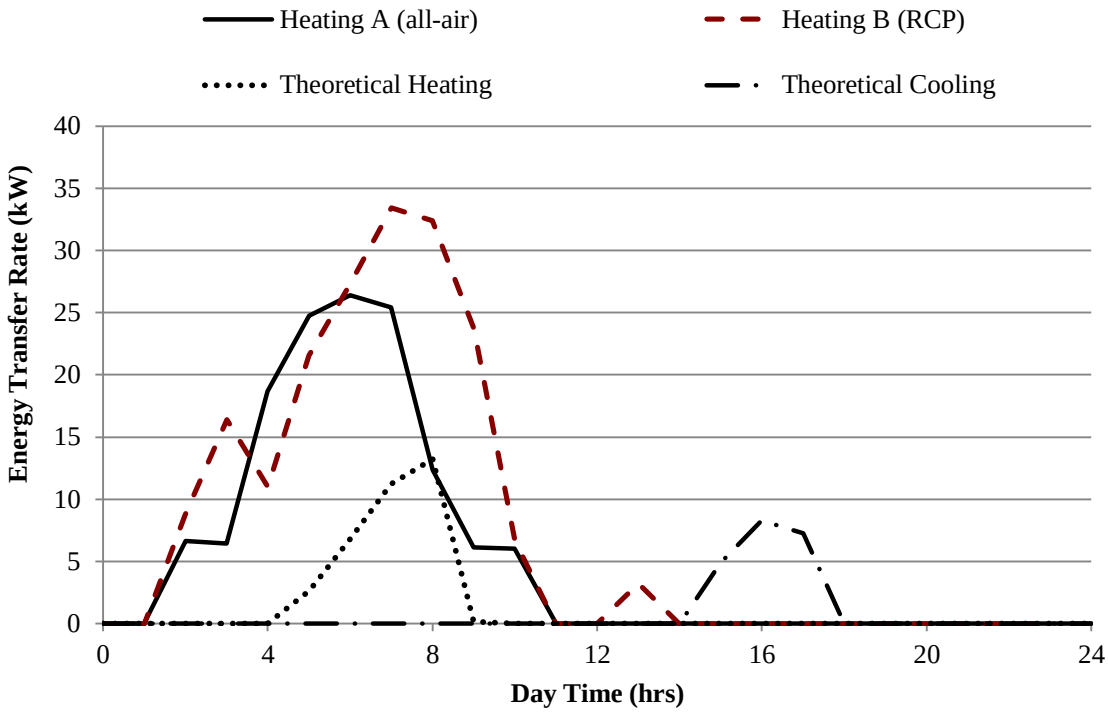

Figure 4.8(b): Hourly averaged energy transfer rate on December 24 in.

Figure 4.9 shows the variation of the space temperature on July 30 in Phoenix. The results are very similar to the results in Miami. There is no increase in space temperature with the increase of internal space loads except very slightly and there is no cooling required in the RCP system while some cooling is required in the all-air system during the night.

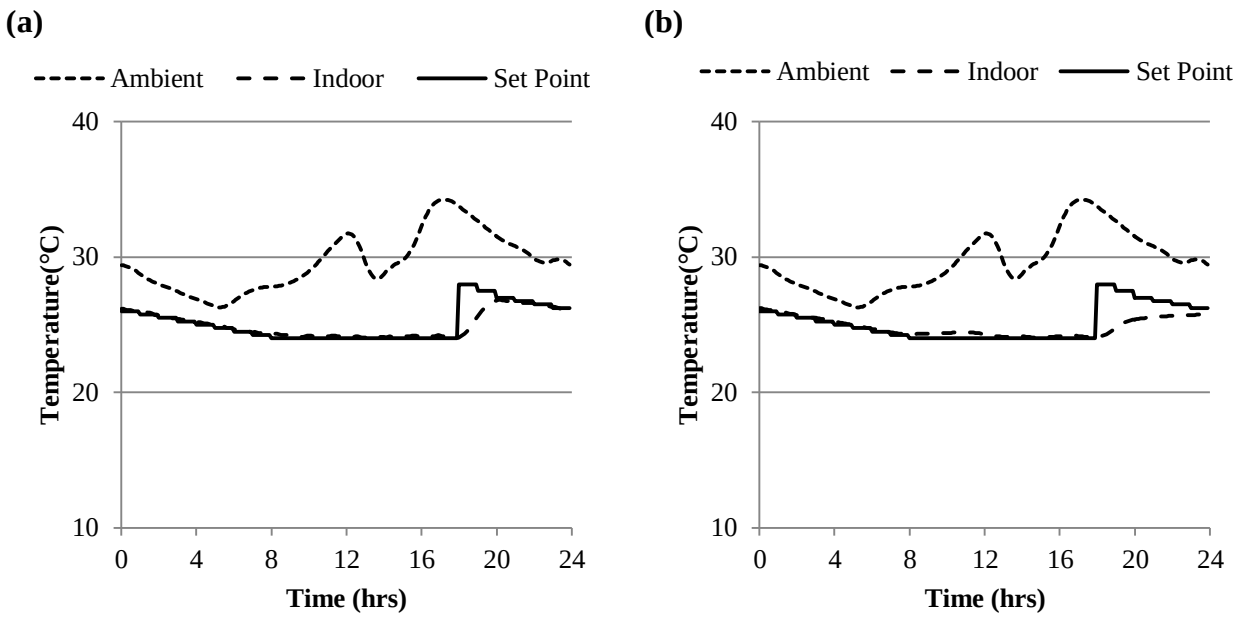

Figure 4.9: Space temperature variation in the cooling season with respect to set point temperatures on the design cooling day in Phoenix: (a) All-air system and (b) RCP system.

4.2 HOURLY ENERGY CONSUMPTION

After ensuring that the space temperature varies within the set point temperature limits, it is necessary to determine the energy consumption throughout the day and compare it to the theoretical energy consumption. Figure 4.8 shows an example of the energy consumption variation on a winter day in Phoenix. In this section, another two examples will be presented. The first is on the coldest winter day in Saskatoon, and the second in on the hottest summer day in Miami. Figure 4.10 shows the energy transfer rate on January 15 in Saskatoon in systems A, B, and D. System C is not presented in Figure 4.10 as it has the same pattern as system B.

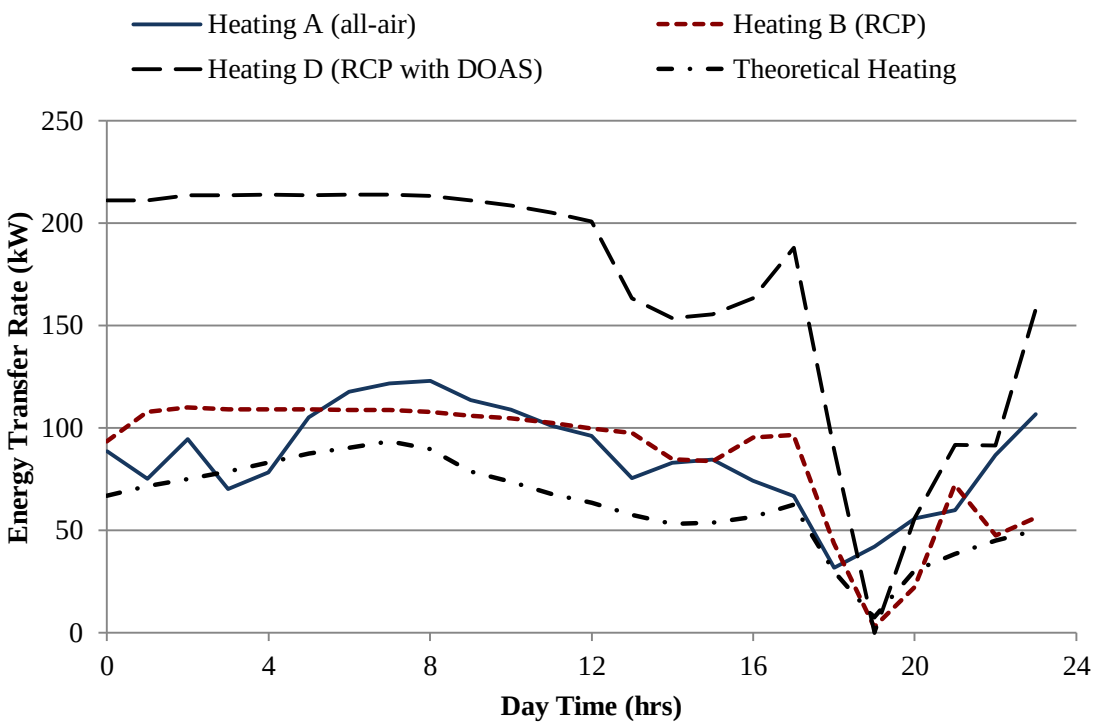

Figure 4.10: Hourly averaged building energy transfer rates on January 15 in Saskatoon.

The energy consumption depends on the inlet conditions of the OA and RA, the energy transferred by the energy wheel, and the outdoor air flow rate. The RCP shows a higher level of energy consumption than the theoretical load while it shows a similar level of energy consumption as the all-air system due to the low ambient temperature in Saskatoon. System D (RCP with DOAS) consumes even more energy due to the utilization of 100% OA with no RA which saves a great portion of energy in system A, while the flow rate of the OA used in system D is about 5-6 times greater than that used in system B. It should also be noted that 60% of the energy consumed in system D is due to the ventilation air while 40% of the energy is consumed

by the RCP. In general, the variation of the three systems shows a relatively good pattern relative to the theoretical energy consumption. However, the energy consumption of the all-air system (system A), the RCP system (system B), and the RCP with DOAS (system D) are 37%, 38, and 171% higher than the theoretical load on that day, respectively. Figure 4.11 shows the energy transfer rate on July 16 in Miami.

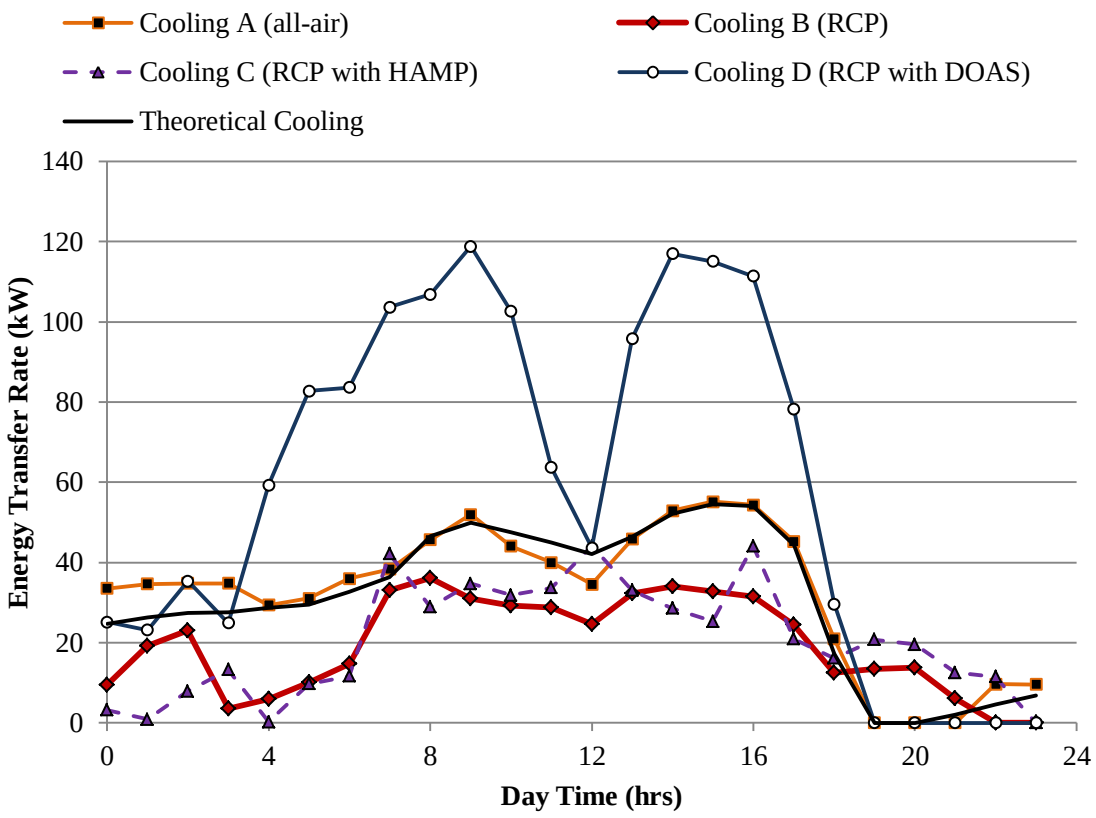

Figure 4.11: Hourly averaged building energy transfer rates on July 16 in Miami.

The pattern of the energy consumption in the all-air system resembles the theoretical energy transfer rate. The RCP system energy consumption also follows the pattern of the theoretical system during the working hours from 8:00 to 19:00 but consumes less energy. The RCP system provides direct cooling from the chilled water to the space instead of cooling the air by the chilled water in the chillers then using this air to cool the space as in system A. This has a great effect on the energy consumption. Also, the ceiling panels provide a high cooling convective coefficient due to the buoyancy effect allowing more cooling to take place. However, since no parallel system is used in system B to remove the latent load, the cooling energy might be less in system B because the latent load is not removed by the RCP. The energy consumption of system C is higher than that of system B due to the dehumidification energy consumed by the HAMP.

To further explain the effect of the absence of a parallel system, Figure 4.12 shows the hourly relative humidity during the working hours of the space air in Miami on July 16 in the four different systems while Figure 4.13 shows the hourly dew point temperature in systems B and C as compared to the RCP surface temperature of 14°C in Miami during the whole day. In Figure 4.12, the relative humidity in system B is higher than any other system showing that the latent load is not removed from the space. The relative humidity of the space air in system C, on the other hand, is around 60% all the time which shows that the probability of dehumidification taking place is high.

In Figure 4.13, the space dew point temperature in system B is around 20°C all day which is higher than the RCP surface temperature and thus, condensation will take place on the surface of

the RCP. On the other hand, the space dew point temperature in system C is around 13°C all day which is lower than the RCP surface temperature and condensation is not likely to take place. These results confirm that condensation takes place in system B. Although system B consumes less energy in cooling, there must be a parallel system to remove the latent load in the space to avoid condensation which may cause a number of health problems. The parallel system can be a DOAS as in system D or the HAMP as in system C.

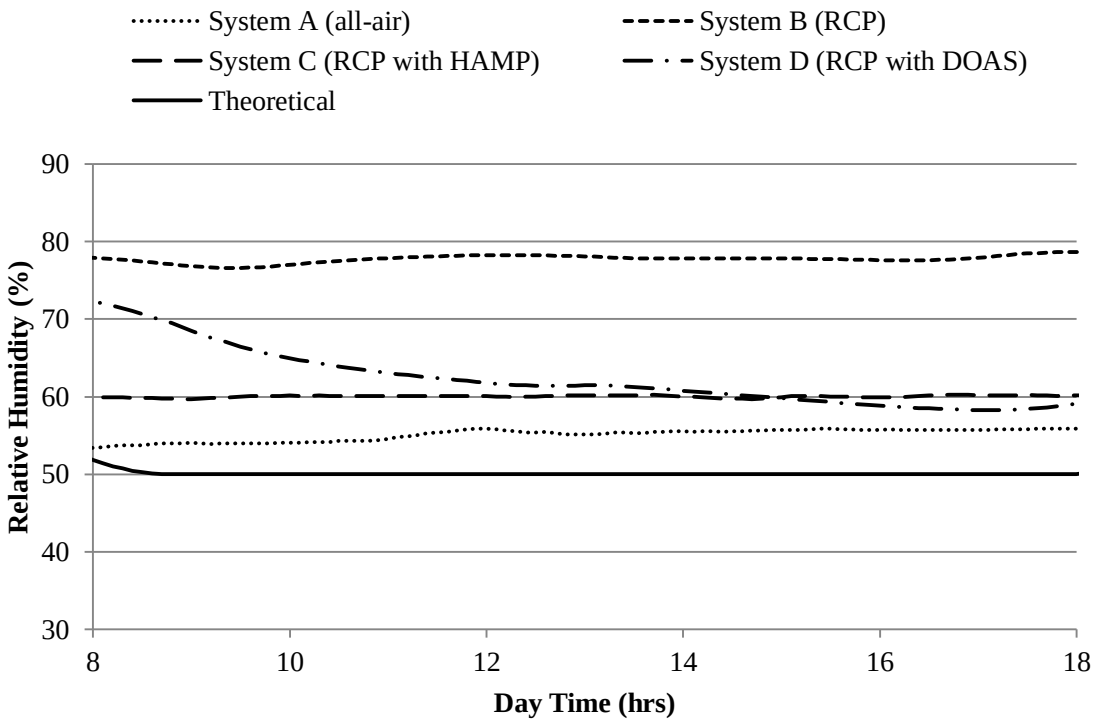

Figure 4.12: Hourly relative humidity in Miami on July 16.

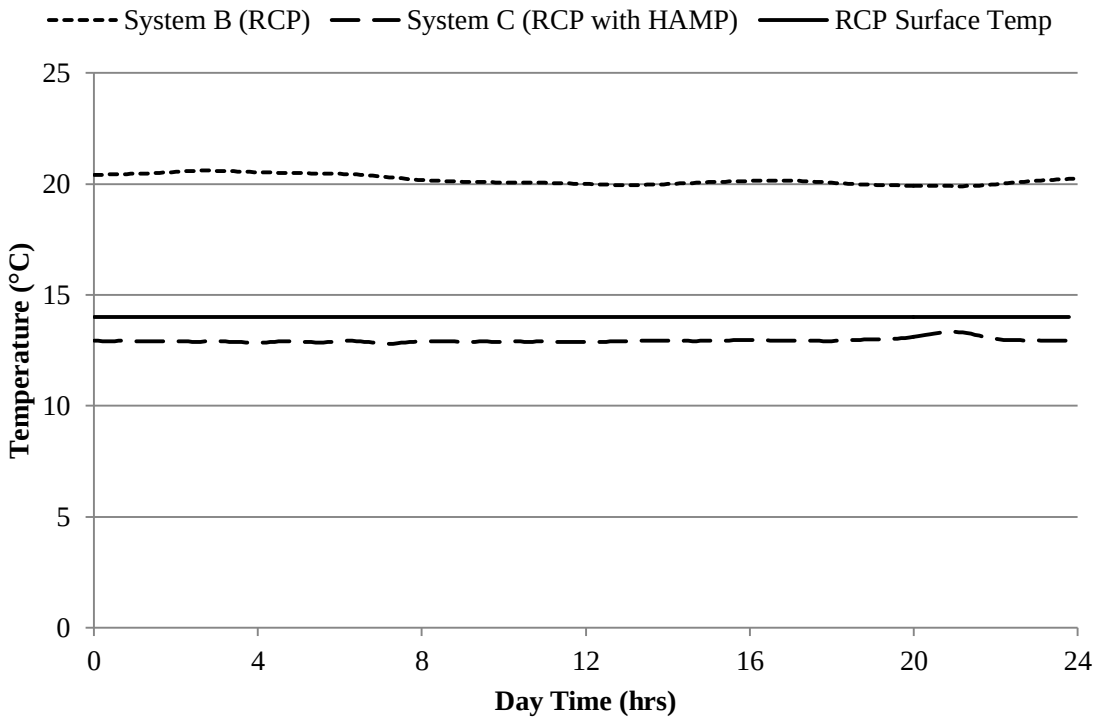

Figure 4.13: Space dew point temperature in Miami on July 16.

The energy consumption of system D, on the other hand, follows a similar pattern as the other systems but consumes more energy as it supplies enough outdoor ventilation air to remove the space latent load. System D, however, has some fluctuations during the morning hours and turns off completely at around 22:00. The energy consumption of system A is 5% higher than the theoretical, while the energy consumption of system B is 37% less than the theoretical, and the energy consumption of system D is 90% higher than the theoretical on that day. System B consumes 40% less energy than the system A on that day.

4.3 RELATIVE HUMIDITY

As suggested by ISO Standard 7730 (ISO Standard 7730, 1994), it is important to control the indoor relative humidity in buildings between 30% RH and 70% RH. In the all-air system, the supply air is dehumidified but not humidified. Less conditioning is done in system B as only the ventilation air is dehumidified to remove part of the latent load but also no humidification is done. In the third system, the HAMP is set to control the relative humidity inside the building space between 35% RH and 60% RH. Finally, in system D the whole latent load is removed by the DOAS.

Figure 4.14 shows the frequency of the resulting relative humidity in the building space in Chicago for the four systems during the working hours of the year. The all-air system is able to maintain the relative humidity between 3% RH and 65% RH. This shows that the all-air system studied in the thesis provides effective dehumidification and no humidification. In the RCP system (system B), the relative humidity is maintained between 3% RH and 78% RH. This is due to less dehumidification and no humidification. The relative humidity in system D is between about 15% RH and 56% RH which shows that some humidification and a lot of dehumidification are performed. Figure 4.14 shows that the HAMP is capable of maintaining the relative humidity between 26% RH and 62% RH during most of the time in Chicago. System C shows two peaks of relative humidity at 35% RH and 60% RH. The peak of 35% RH takes place 14% of the time, while the peak of 60% takes place 10% of the time. These are the control conditions set by the HAMP for humidification and dehumidification, respectively. If the relative humidity is below 35% RH less or no humidification takes place, while if the relative humidity is higher than 60%

RH no dehumidification takes place. This shows that both humidification and dehumidification take place significantly in Chicago. Humidification is mainly required in winter as the temperature goes lower than 0°C.

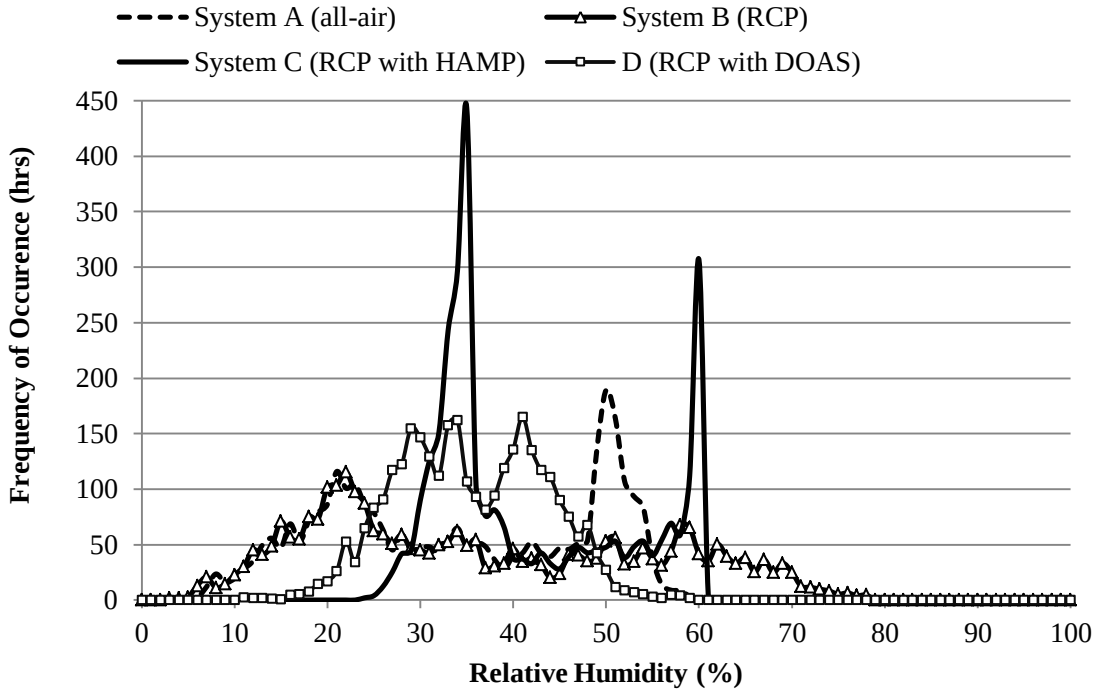

Figure 4.14: Frequency of relative humidity inside the building throughout the year in Chicago.

In Figure 4.14, system A shows a similar variation of the frequency of relative humidity as system B up to 50% RH where system A has a relatively higher frequency while system B has a lower frequency until 60% RH. This might be explained by the higher level of relative humidity in system B due to the absence of a parallel system to remove the space latent load as discussed

in Section 4.2. System D shows that some humidification and dehumidification takes places with smaller peaks at 33%RH, and 41% RH.

It should be noted that in all four cases, the supply air is supplied at 14°C and 84% RH for cooling and 30°C for heating. The supply heated air in system D is also humidified to 30% RH while the relative humidity of the heated ventilation air in the other systems depends on the air inlet condition to the heater which mainly depends on the ambient conditions and the energy wheel energy exchange. It also depends on the amount of RA mixed with the OA in system A.

Figure 4.15 shows the frequency of the resulting relative humidity in the building space in Saskatoon for the four systems during the working hours of the year. The all-air system is able to maintain the relative humidity between 1% RH and 55% RH. This shows that extensive dehumidification is done to the supply air while also no humidification takes place at all. In the RCP system, the relative humidity is kept between 1% RH and 61% RH. This is due to the very dry weather that characterizes Saskatoon especially in winter. System D maintained the relative humidity between about 14% RH and 47% RH which shows that some humidification and dehumidification were performed on the OA. Figure 4.15 shows that the HAMP is capable of maintaining the relative humidity between 24% RH and 57% RH. In Saskatoon, the relative humidity only peaks at 35% RH 13% of the time showing that humidification take place more significantly than dehumidification. However, dehumidification also takes place in Saskatoon by the HAMP. In Figure 4.15, system A follows the relative humidity of system B very closely as no humidification is performed in both systems and heating the air does not cause any extra

dehumidification. System D peaks at 32% RH, however, as some humidification is performed to the ventilation air.

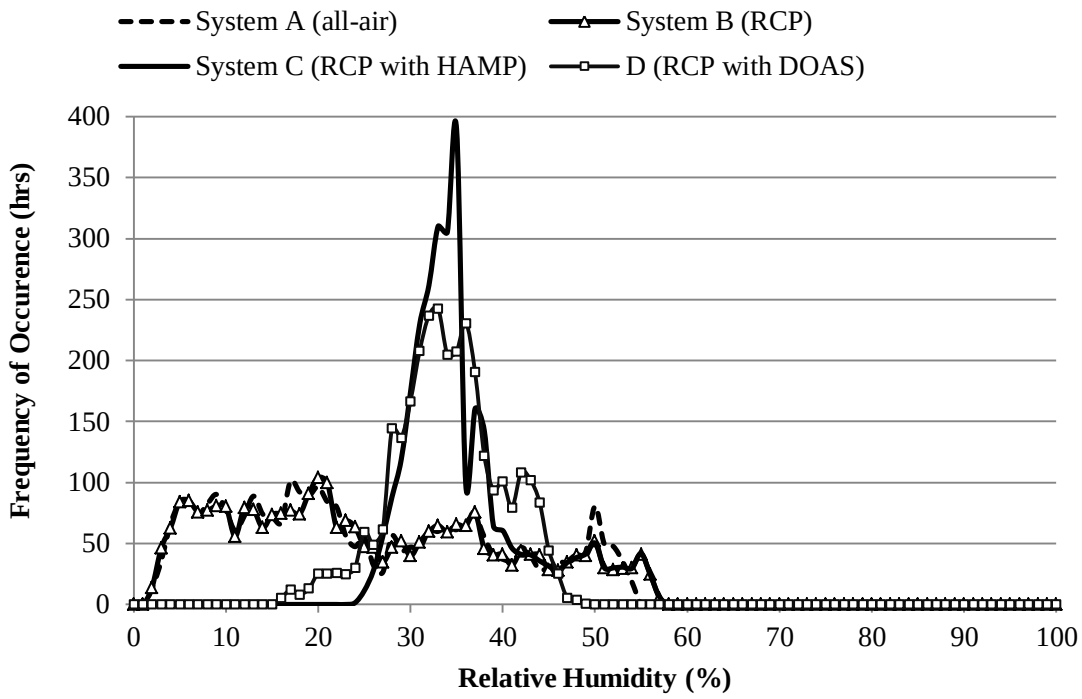

Figure 4.15: Frequency of relative humidity inside the building throughout the year in Saskatoon.

Figure 4.16 shows the frequency of the resulting relative humidity in the building space in Phoenix for the four systems during the working hours of the year.

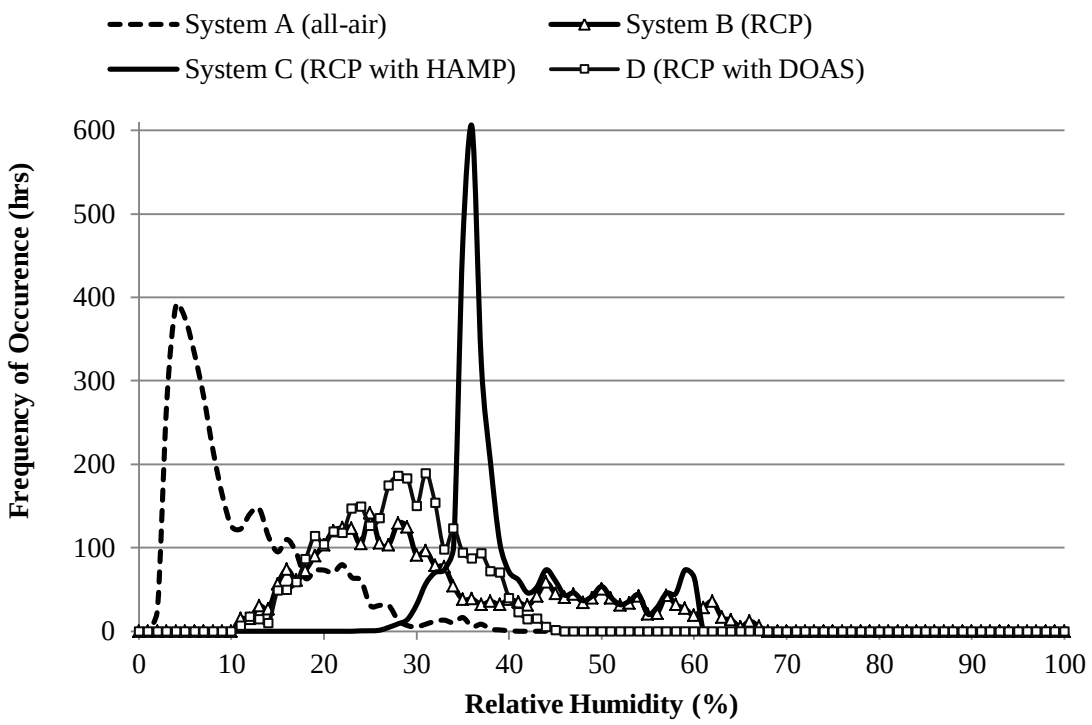

Figure 4.16: Frequency of relative humidity inside the building throughout the year in Phoenix.

In the all-air system the relative humidity is between 2% RH and 38% RH. This shows that Phoenix has a dry climate and no humidification takes place. However, the results of system A show lower values of space humidity ratio than outdoor humidity ratio values in Phoenix. This is not justified and shows that extra dehumidification takes place somewhere in the HVAC system and should be considered in future work. In the RCP system (system B), the relative humidity is kept between 11% RH and 67% RH. This is due to the very dry weather that characterizes Phoenix. System D maintains the relative humidity between about 13% RH and 47% RH which shows that humidification is performed on the OA but not sufficiently. Figure 4.16 shows that

the HAMP (system C) is capable of maintaining the relative humidity between 27% RH and 60% RH. In system C, the relative humidity peaks at 35% RH 20% of the time of the year showing that humidification take place more significantly all year. This shows that the HAMP helps in humidification. In Figure 4.16, the relative humidity peaks at 5% RH in system A while it slightly peaks at 31% RH in system D. This might be because the supply air which is cooled and further dehumidified in system A is much higher than that of systems B and D. Also the ventilation air is humidified in system D to 30% RH.

Figure 4.17 shows the frequency of the resulting relative humidity in the building space in Miami for the four systems during the working hours of the year. The all-air system is able to maintain the relative humidity between 24% RH and about 70% RH. The high level of space relative humidity is due to the humid weather that characterizes Miami. In the RCP system, the relative humidity is maintained between about 35% RH and about 83% RH. This is due to both the very humid weather and the insufficient dehumidification of the supply air. System D maintains the relative humidity between about 30% RH and 70% RH which shows that dehumidification is performed on the OA most of the time. In spite of the very humid weather of Miami, the HAMP (system C) is capable of maintaining the relative humidity between 40% RH and 62% RH most of the hours. The relative humidity peaks at 60% RH 55% of the time of the year showing that dehumidification takes place much more significantly in Miami.

System A peaks at 53% which is expected as the supply air flow rate is calculated such that it provides a space condition of 24°C and 50% RH. System B peaks somewhere around 74%

showing the inability of the RCP to remove the space latent load as previously explained. System D peaks at 51% which is expected as the ventilation rate is calculated such that it removes the space latent load.

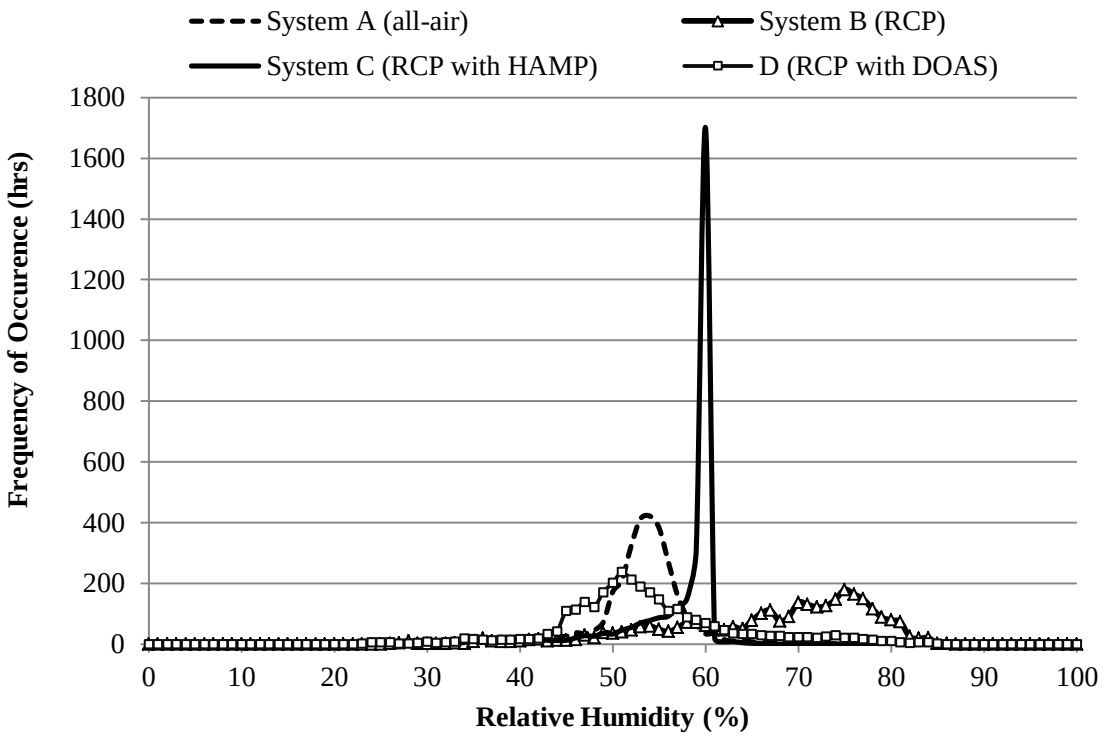

Figure 4.17: Frequency of relative humidity inside the building throughout the year in Miami.

4.4 ENERGY

Figure 4.18 shows the heating and cooling energy consumption in Chicago. System B consumes more heating energy than system A while it consumes less cooling energy. The

heating energy in B is higher by 9% than A while the cooling energy is reduced by 66%. This might be explained by Figure 4.1 as the space temperature of system B coincides with the set point temperature while the space temperature of system A is slightly lower than the heating set point temperature. This shows that more heating is done in system B than system A. The cooling energy is much less in B and C than A and D because free cooling of the RCP water takes place during the day and at night. This is done by the cooling tower described in Section 2.3.9 which uses indirect cooling. Also the cooling energy consumption in system B is low because the RCP system is unable to remove the space latent load which is considered high in Chicago as it is characterized by a dry winter and a humid summer as discussed in Section 4.2. Another reason discussed in Section 4.1 is that some cooling takes place in system A overnight while the space in system B takes more time to restore its temperature as the water takes more time to heat. The cooling energy is generally much lower in system B and C than that of A and D in all cities for these reasons. The total energy in B is less than system A by 29%.

System D consumes 36% heating energy more than system A and 24% more than system B. This is because system D uses 100% OA, the supply air flow rate is higher than systems B and C to be able to remove the space latent load, and no economizer is used as in system A. Also, some humidification takes place in system D while no humidification takes place in any of systems A or B. However, system D consumes less cooling energy than A by 9% as it uses a lower supply flow rate than that used in system A. This is because the supply air used in system D is required to handle the space design latent load only while the supply air in system A is required to handle the total design sensible and latent loads of the space. System C consumes more total heating and

humidification energy than system B by 4% as no humidification takes place in system B, and consumes more total cooling and dehumidification than system B by 22%. This is because system B does not remove the latent load as discussed before. The total cooling and dehumidification energy in system C is still less than the total cooling and dehumidification energy of system A. The total energy consumed by system C is 23% less than the total energy consumed by system A. this is because the RCP system consumes less energy than the all-air system as discussed before. However, the latent load is just an estimate of the regeneration energy required and it will possibly be greater than the theoretical value.

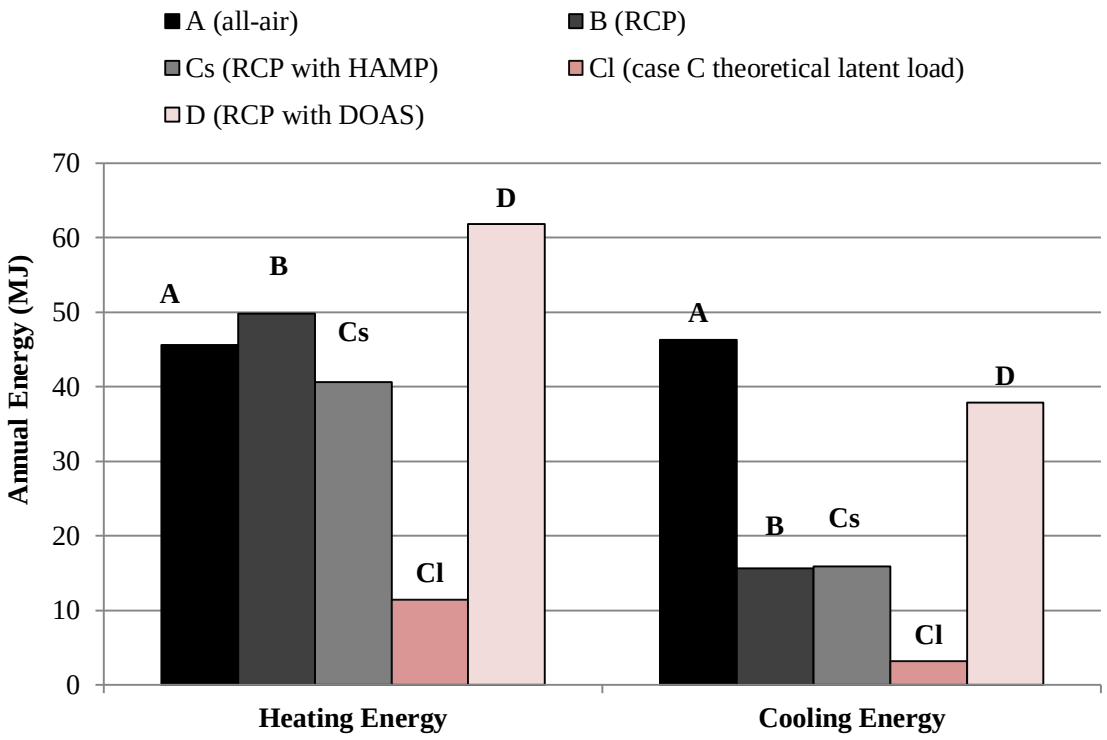

Figure 4.18: Building heating and cooling energy consumption in Chicago.

Figure 4.19 shows the total energy consumption in Saskatoon. The heating loads are generally much higher than the cooling loads due to the cold climate that characterizes Saskatoon. Also, Figure 4.3 shows that the space temperature in system B is lower than the space temperature showing that it does not provide enough heating. System B consumes less energy than system A in heating and cooling in Saskatoon. The heating energy in system B is reduced by 8% and the cooling energy is reduced by 80% compared to system A. System A consumes higher energy due to the high supply air flow rate used which is considered the highest of all cities. Also, the RCP water temperature used in system B is 50°C which is high compared to other cities. The total energy in system B is reduced by 18% compared to system A.

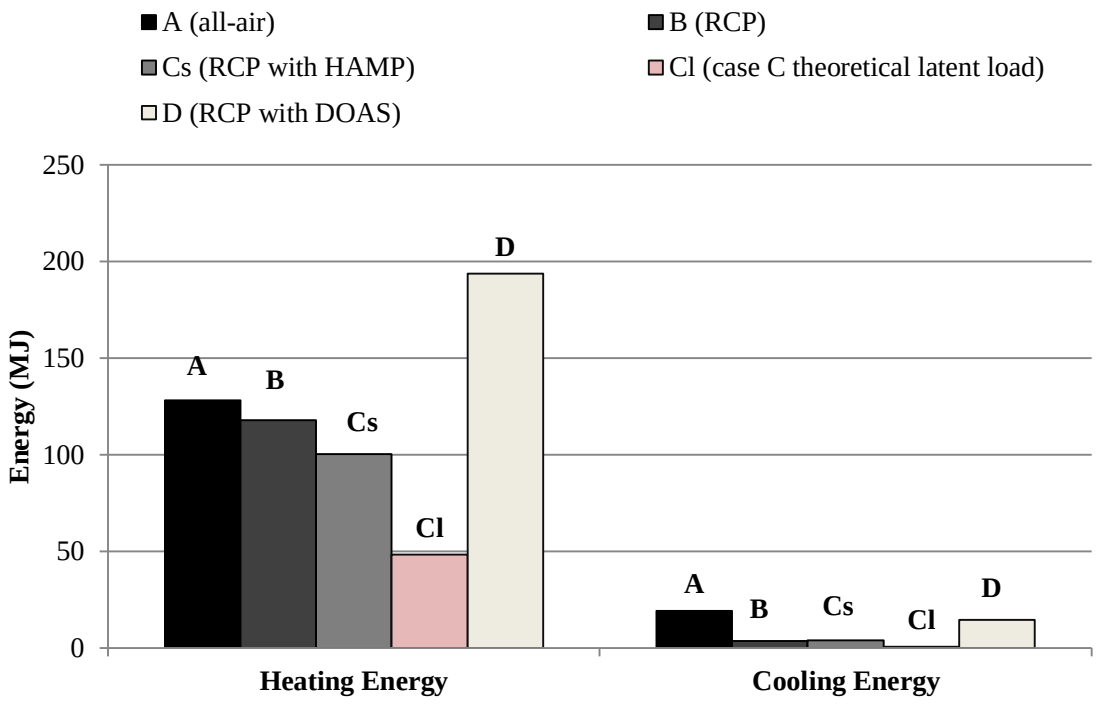

Figure 4.19: Building heating and cooling energy consumption in Saskatoon.

It should be noted that no humidification is done at all in systems A and B, such that the total heating and humidification in system C is expected to be higher than the heating energy of system A or B. It should be also noted that system D performs humidification and thus higher heating energy than system A and B. System D consumes higher heating energy than system C due to the higher supply air flow rate which is required to remove the space latent load. System C consumes more total heating and humidification energy than system B by 26%. System D consumes 51% more heating energy and 24% less cooling energy than system A. The total energy consumed by system C is 4% higher than the total energy consumed by system A.

Figure 4.20 shows the total energy consumption in Phoenix. The cooling loads are generally much higher than the heating loads due to the hot climate that characterizes Phoenix. System B consumes almost the same energy as that of system A in heating and less energy in cooling. The heating energy consumption in Phoenix is 0.65 MJ and 0.64 MJ in systems A and B, respectively, which is a very small amount compared to the cooling energy and heating energies in other cities. The cooling energy of system B is less than system A by 61%, while the cooling energy of system D is less than system A by 16%.

Figure 4.20 shows a great value of humidification energy used in system C compared to other systems. This is due to the fact than no humidification is done by systems A and B. This is also because humidification takes place in phoenix with cooling as well as with heating as Phoenix is characterized by a dry weather all year. However, the relative humidity might need to be more controlled to reduce the humidification energy consumption. The dehumidification

energy used in system C in Phoenix is too small relative to the cooling energy. The total energy consumed by system C is 54% less than the total energy consumed by system A.

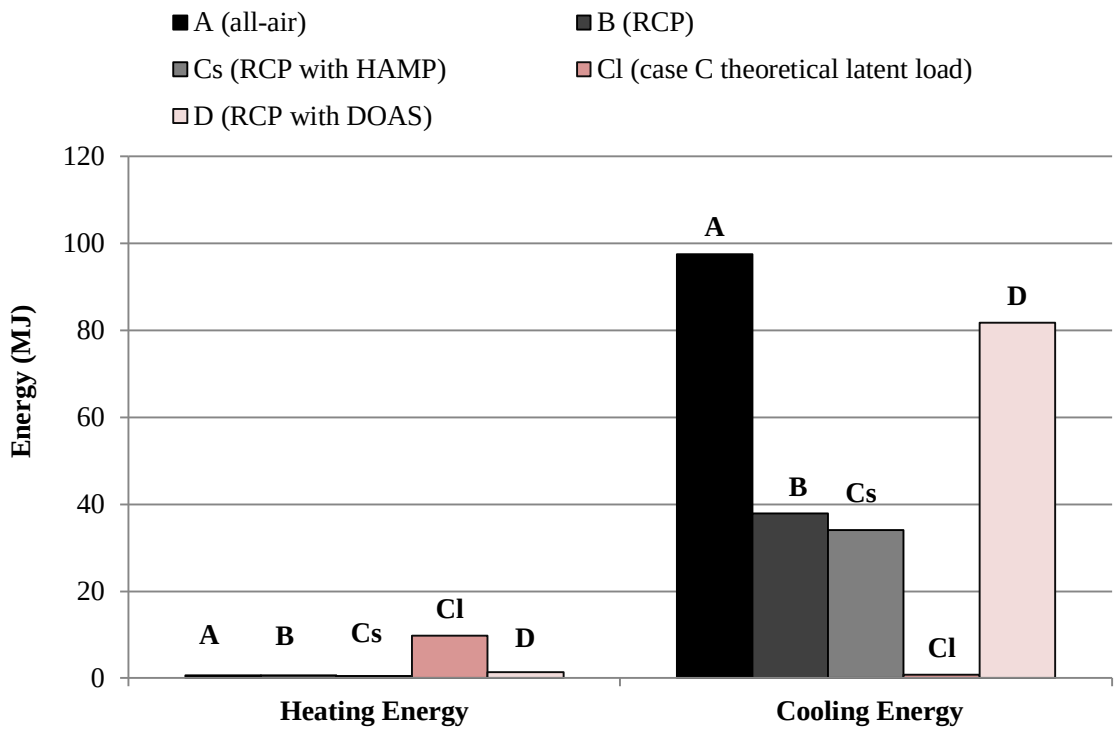

Figure 4.20: Building heating and cooling energy consumption in Phoenix.

Figure 4.21 shows the total cooling energy consumption in Miami. There is no heating energy in Miami as discussed in Section 4.1. Systems A, B, and C consume less cooling energy than the theoretical load while system D consumes the most cooling energy. System D consumes less cooling energy than system A by 9%, 24%, and 16% in Chicago, Saskatoon, and Phoenix, with the lowest saving in Chicago. This shows that system D uses higher supply air flow rates in more humid climates. This also shows that extensive dehumidification of the supply air takes

place in system D in the more humid climates. It should be also noted that system D uses 100% OA while system A uses an economizer which mixes RA with OA which saves a lot of energy.

It should be noted that the extensive dehumidification that is needed to be done in humid climates such as Chicago and Miami suggests potential high regeneration energy of the desiccant solution than the theoretical calculated latent loads. However, meanwhile the total cooling and dehumidification energy of system C is 18% higher than system B, 40% less than system A, and 66% less than system D. The theoretical dehumidification energy used by the HAMP is 19.2 MJ. System B consumes 49% less cooling energy than system A.

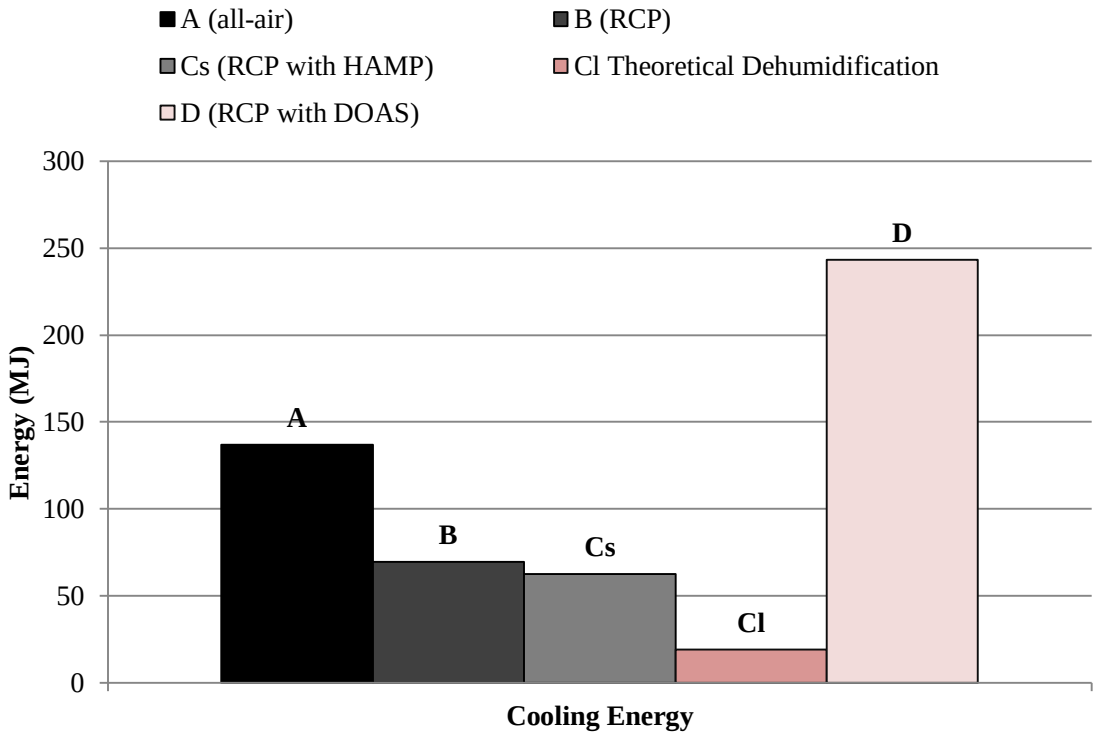

Figure 4.21: Building cooling energy consumption in Miami.

In Figure 4.21, system D consumes 78% more cooling energy than system A. The total energy consumed by system C is 40% less than the total energy consumed by system A.

Figure 4.22 shows the cooling energy of the four cities in the different systems. Miami shows the highest cooling energy consumption especially for system D, while Saskatoon shows the lowest cooling energy consumption. Miami has the highest total annual cooling energy due to the generally hot and humid climate all year round.

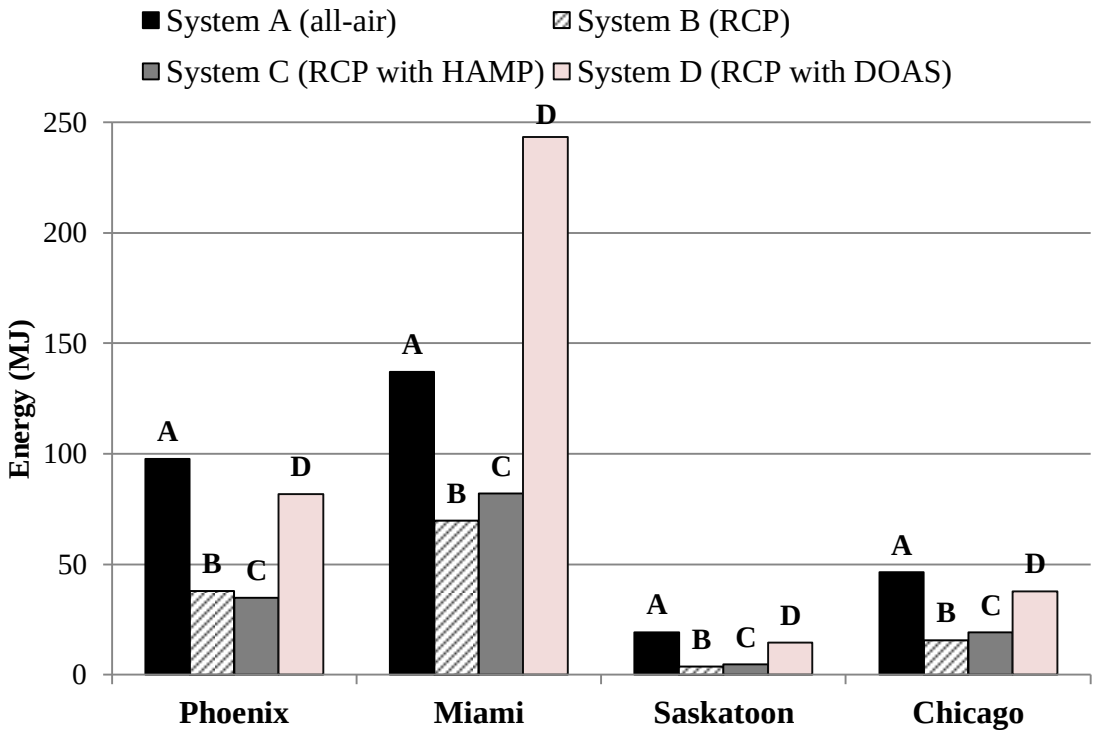

Figure 4.22: Building cooling energy consumption in the four cities.

Figure 4.23 shows the heating energy of the four cities in the different systems. Saskatoon shows the highest heating energy consumption especially for system D, while Phoenix shows the lowest heating energy consumption while there is no heating in Miami at all.

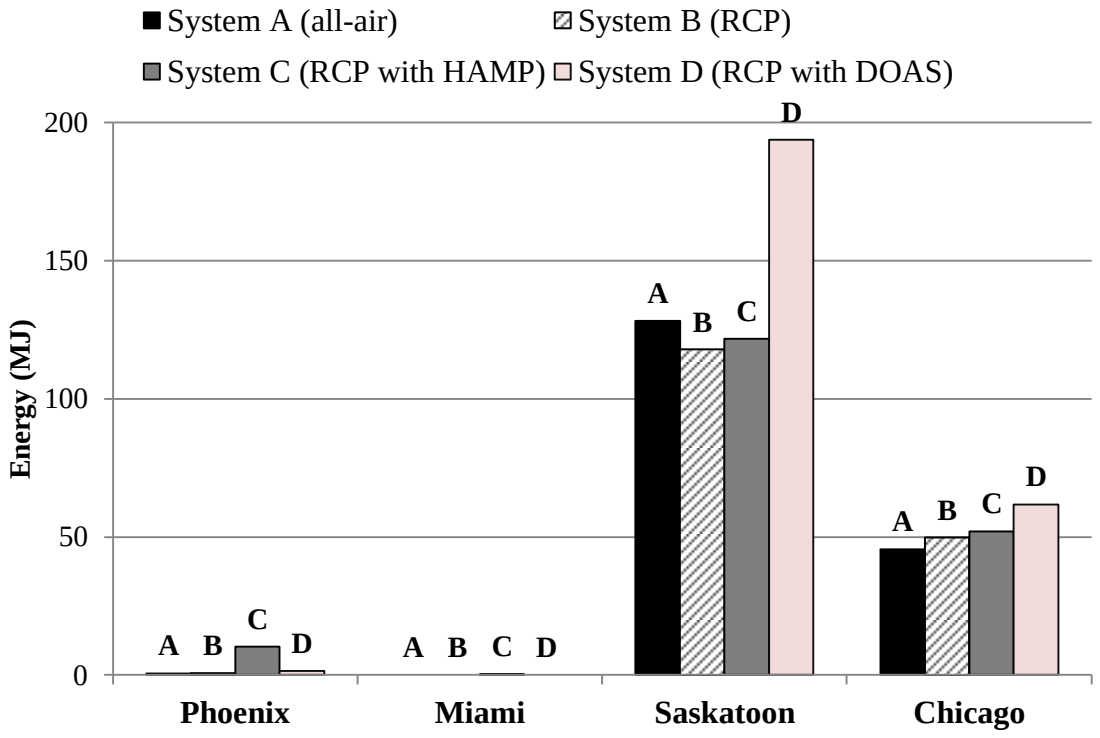

Figure 4.23: Building heating energy consumption in the four cities.

The maximum heating energy (Figure 4.23) is however lower than the maximum cooling energy (Figure 4.22). In general, the results show that radiant ceiling panels consume less energy than conventional all-air system in cooling, and in some cases in heating, which is shown in previous research and is expected. This is because, as discussed before, the RCP system heats or

cools the space air by heated or chilled water flowing in the panels directly while the all-air system uses heated or chilled water to heat the supply air and then supplies the air to the space.

CHAPTER 5 SENSITIVITY STUDY

This chapter investigates the effect of three different parameters on the performance of system C (RCP with HAMP and 100% OA mechanical ventilation). These parameters are the RCP relative area, the RCP water-air temperature difference, and the HAMP desiccant solution concentration.

5.1 SENSITIVITY OF THE RCP AREA

The RCP area used in systems B, C, and D is 60% of the ceiling area. Changing the RCP area will directly affect the space temperature and energy consumption, but will have a small effect on the space relative humidity. The RCP areas studied are 50%, 60%, 70%, and 90% of the ceiling area in system C. The HAMP area is maintained constant at 10% of the ceiling area.

5.1.1 Space Temperature

The effect of the RCP area on the space temperature is more significant in the heating season because the convective heat transfer coefficient of the RCP is lower during heating than during cooling. Figure 5.1 shows the variation of space temperature compared to the heating set point temperature on January 15 in Saskatoon with different RCP areas. The space temperature is closer to the set point temperature as the area of the RCP increases. When the RCP area is 50%, the space temperature is the farthest away from the set point temperature due to the high heating load in Saskatoon, the low convective heat transfer coefficient, and the decreased RCP area. The RCP area of 90%, on the other hand, has the closest space temperature variation to the set point

temperature. Figure 5.1 shows that a change to the RCP area by 10% has a significant impact on the space temperature.

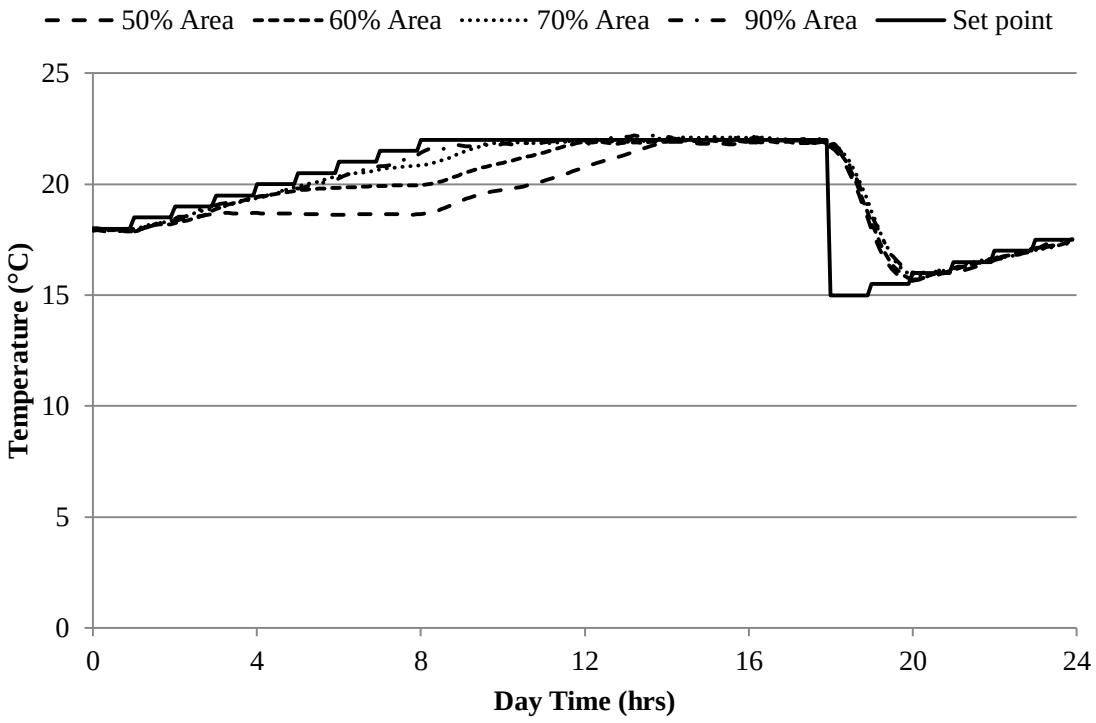

Figure 5.1: Space temperature compared to the set point temperature for different RCP areas on January 15 in Saskatoon.

Figure 5.2 shows the variation of space temperature compared to the heating set point temperature on December 31 in Chicago with different RCP areas. The heating load in Chicago is not as high as that of Saskatoon, and thus the variation in space temperature as the RCP area increases is not as great as in Saskatoon, especially when the RCP area is 60% of the ceiling area

or more. It should be noted, however, that even with the largest RCP area used, the space temperature does not exactly follow the set point temperature during heating.

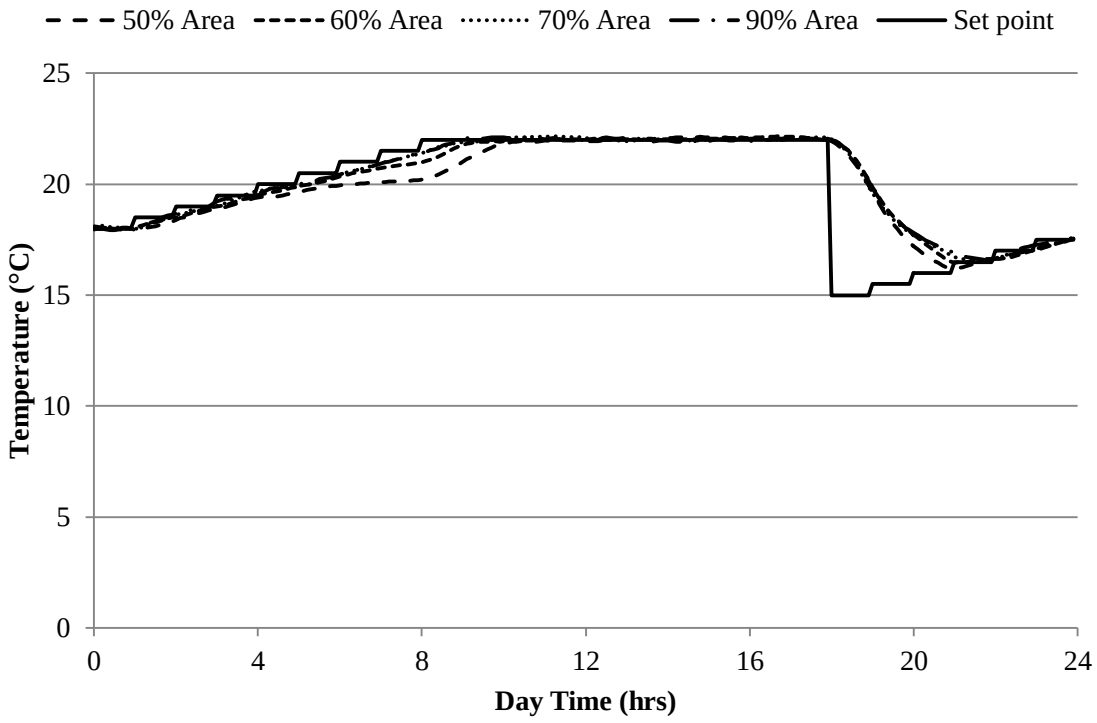

Figure 5.2: Space temperature compared to the set point temperature for different RCP areas on December 31 in Chicago.

In Figure 5.3, the variation of the space temperature compared to the cooling set point temperature on July 30 in Phoenix is presented. As shown in Figure 5.3, for an RCP area of 60% or higher the space temperature follows to the set point temperature closely. When the space loads increase between 8:00 and 12:00 and between 14:00 and18:00, there is a slight increase in the space temperature. This increase is most obvious with the RCP area of 50% and is less

obvious as the RCP area increases. The indoor air temperature is very similar for RCP area ratios of 60% or higher.

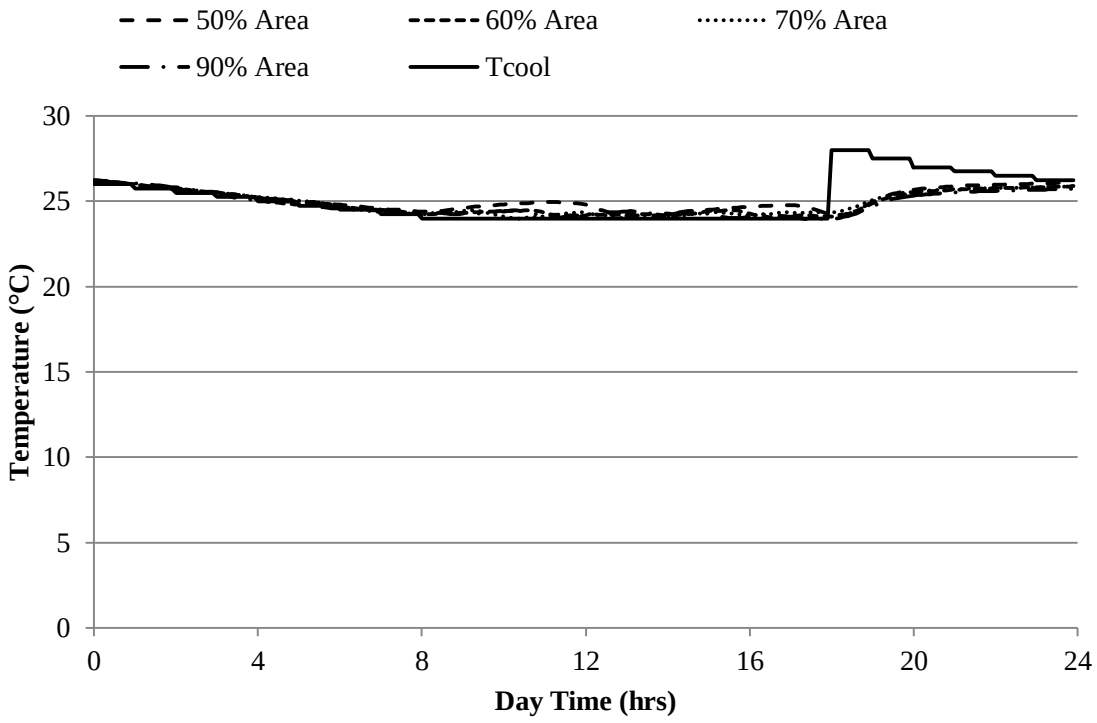

Figure 5.3: Space temperature compared to the set point temperature for different RCP areas on July 30 in Phoenix.

Figure 5.4 shows the variation of the space temperature compared to the cooling set point temperature on July 16 in Miami. The climate in Miami is humid and condensation takes place in system B as the RCP water temperature is lower than the space dew point temperature. However, the presence of the HAMP to remove the latent load prevents this condensation to take place. This is discussed in Section 4.2 in Figure 4.13.

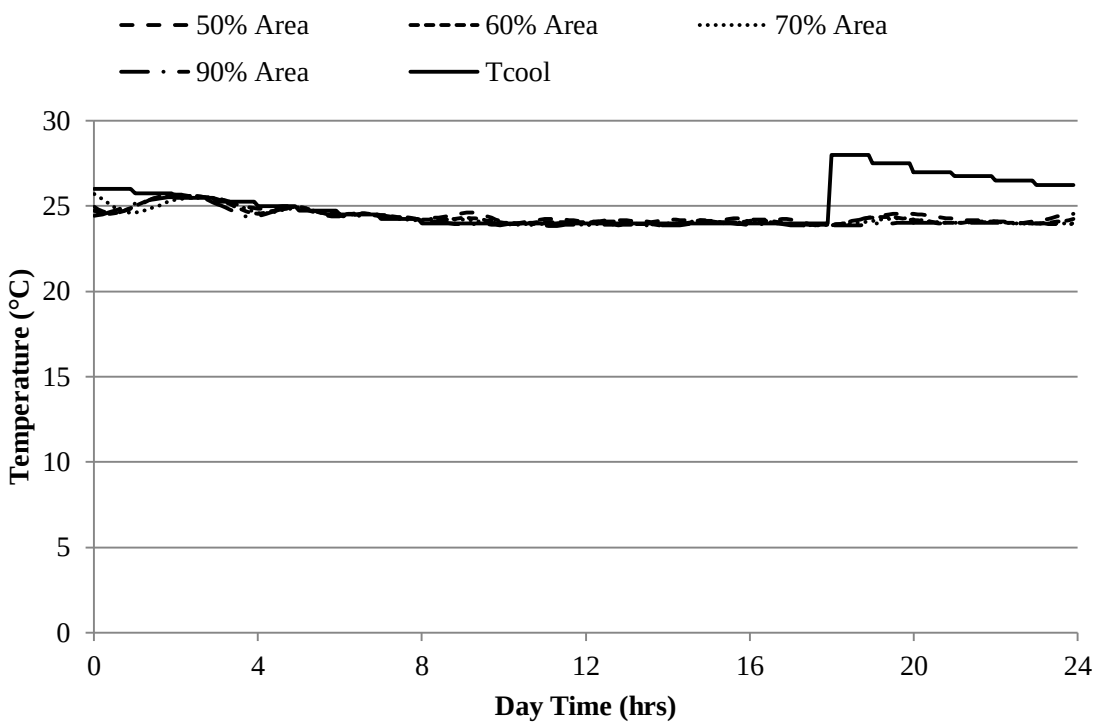

Figure 5.4: Space temperature compared to the set point temperature for different RCP areas on July 16 in Miami.

5.1.2 Relative Humidity

Changing the RCP area has no effect on the relative humidity in the space as seen in Figure 5.5 which presents the frequency of the indoor relative humidity in the building space in Miami. The lines of different RCP areas almost are nearly identical. The relative humidity in the other three cities is also the same with changing the RCP area.

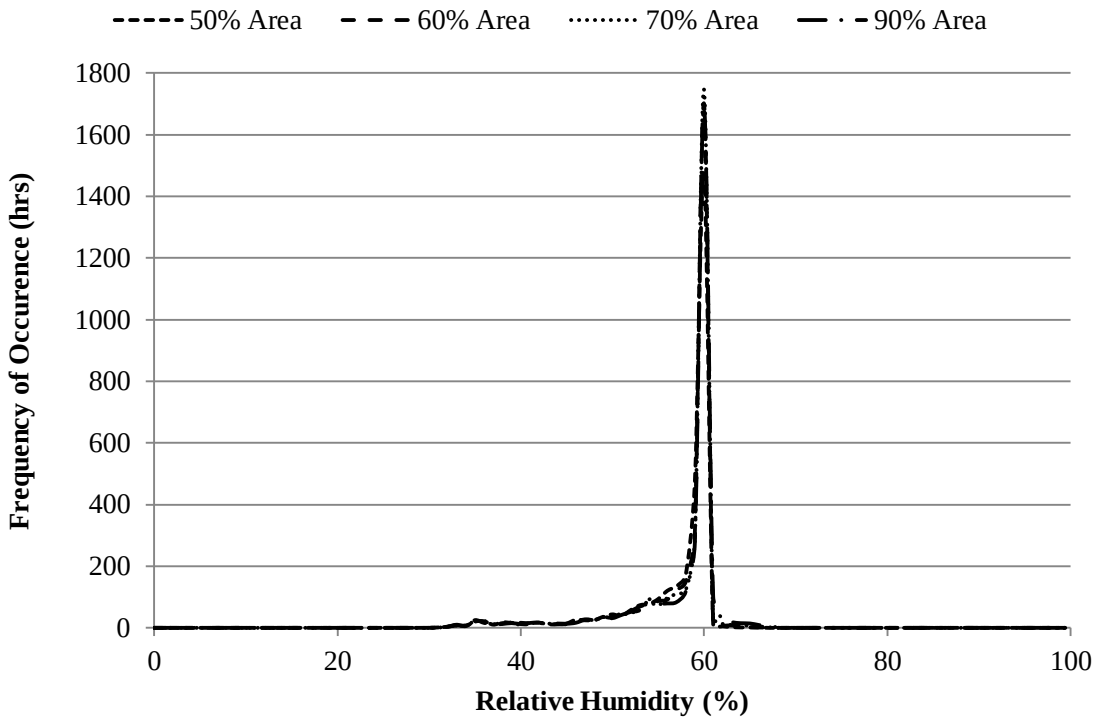

Figure 5.5: Frequency of relative humidity inside the building for different RCP areas throughout the year in Miami.

5.1.3 Energy Consumption

Generally, the energy consumption decreases as the RCP area fraction increases. This is valid for cooling but there are some exceptions in heating as will be shown in this section. Figure 5.6 shows the annual energy consumption in Chicago with different RCP area fractions. The heating energy decreases as the RCP area increases. However, the 50% area is the exception as the RCP is not able to meet the entire space load as evidenced by the space temperature variation shown in Figure 5.2.

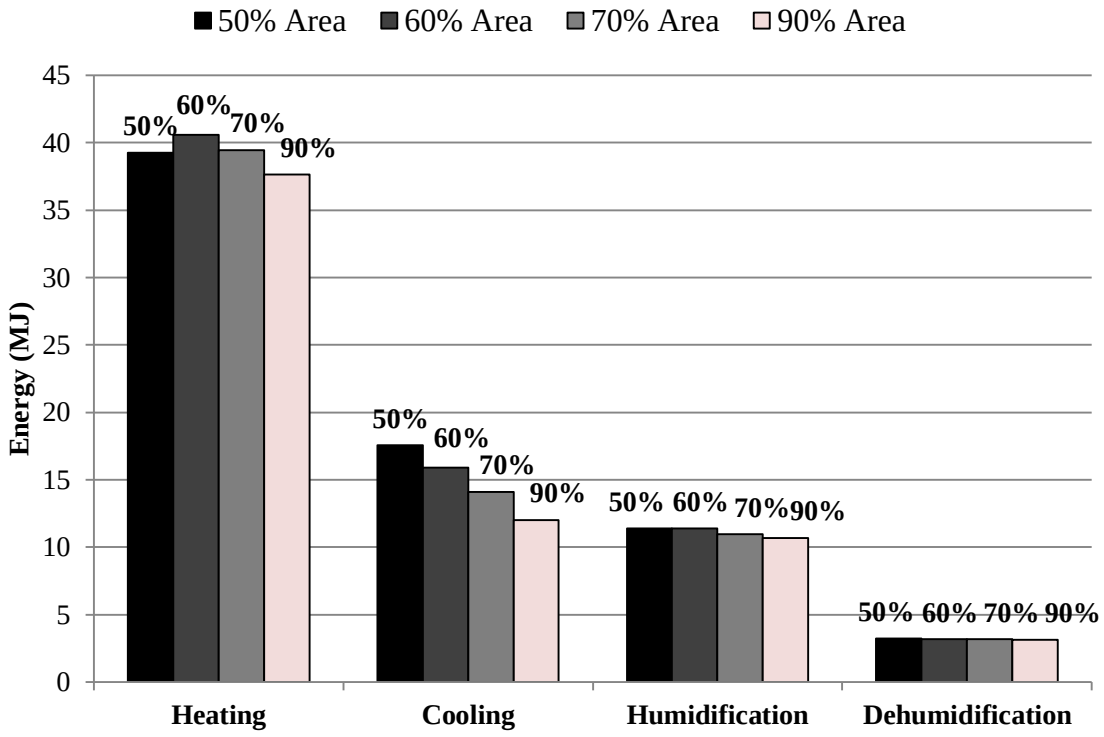

Figure 5.6: Annual energy consumption in Chicago for different RCP areas.

The cooling energy decreases as the RCP area increases. This is because more RCP exposed area contributes to the removal of the space load which will otherwise be removed by more cooling which consumes more energy. This is also shown in the general heat transfer equation (2.13) which indicates that the energy transfer rate is directly proportional to the RCP surface area. As the area increases, the energy transfer rate increases and the number of hours requiring cooling decreases. For example, on July 30 in Phoenix, the number of cooling hours is 18.9, 18.8, 18.7, and 18.6 hours using 50%, 60%, 70%, and 90% RCP area, respectively. However, the decrease in cooling times should be proportional to the increase in the energy transfer rate. Nevertheless, the fact that the cooling energy decreases with area may be due to changes in the

indoor conditions as the RCP area changes or due to enhanced free cooling with larger RCP area. The COP of the cooling unit varies through the day as presented in Appendix D which can also add another complexity to the simulations. The reason for this trend would require additional analysis and is left to future work. More cooling is carried out by operating the RCP for a longer time i.e. operating the auxiliary cooling for a longer time to perform more cooling. This might also be due more free energy taking place as the outlet water temperature from the space is higher as the RCP are increases allowing more free cooling potential. The RCP area of 90% consumes only 7% less heating energy than the RCP area of 60%. The RCP area of 90% consumes 32% less total energy than the RCP area of 50%. The humidification is only slightly decreased as the RCP area increases while the dehumidification load is almost unaffected.

Figure 5.7 shows the annual cooling and dehumidification energy consumptions in Miami with different RCP areas.

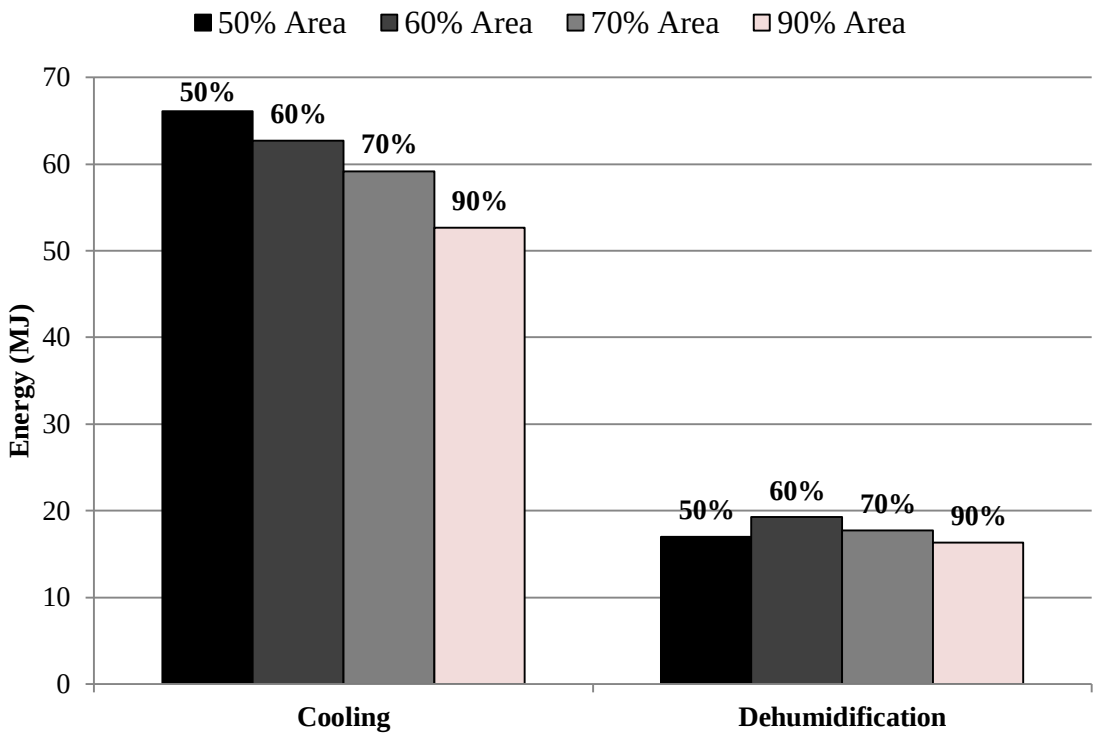

Figure 5.7: Annual energy consumption in Miami for different RCP areas.

The cooling energy decreases significantly as the RCP area increases similarly as discussed in Chicago. The RCP area ratio of 90% consumes 20% less energy than the RCP area of 50%. The dehumidification energy is quite constant regardless of the RCP area as expected.

Figure 5.8 shows the annual energy consumption in Saskatoon with different RCP areas.

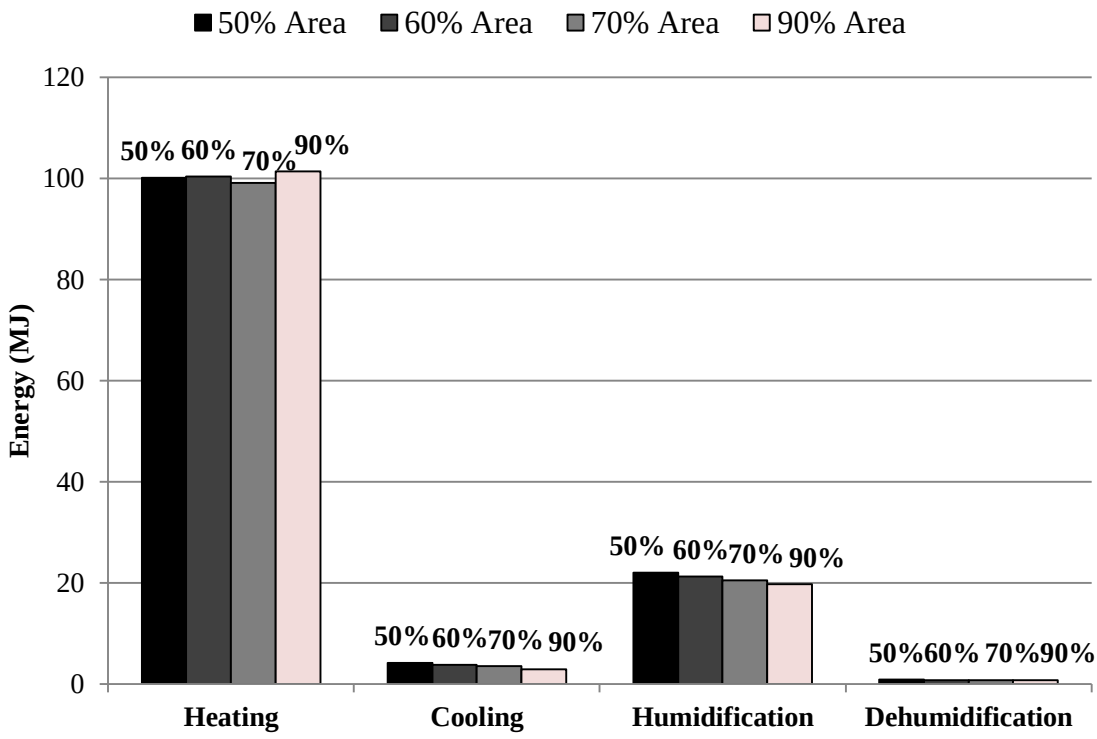

Figure 5.8: Annual energy consumption in Saskatoon for different RCP areas.

In Saskatoon, the heating energy varies differently due to the high heating load. The heating energy can increase or decrease slightly with the change of the RCP area. However, this change is just ±1.2% from the mean value which would be less than the uncertainty in the results because the energy consumption should be relatively independent of the RCP area provided the set point temperature is met. Thus, it could be concluded that the RCP area doesn't affect the heating energy in Saskatoon significantly. The cooling energy, humidification energy and dehumidification energy are also quite similar for all RCP areas.

Figure 5.9 shows the annual cooling and humidification energy consumptions in Phoenix. The cooling energy decreases significantly as the RCP area increases. The RCP area of 90% consumes 26% less energy than the RCP area of 50%. The humidification energy also decreases as the RCP area increases.

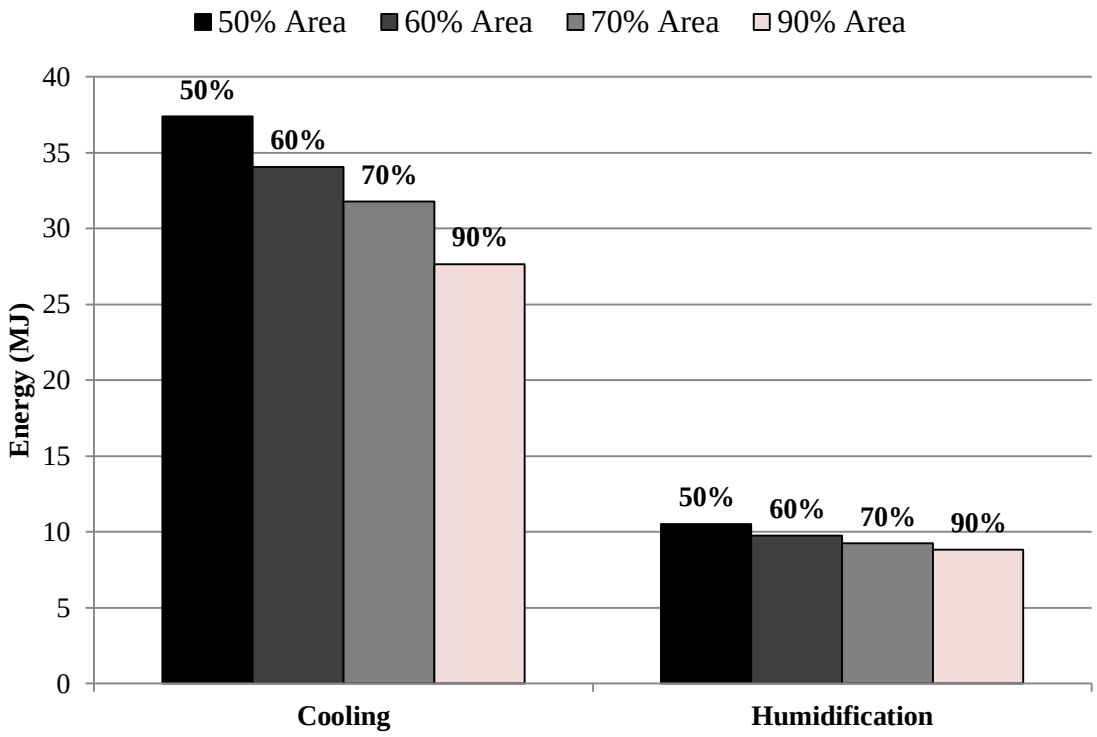

Figure 5.9: Annual energy consumption in Phoenix for different RCP areas.

5.2 SENSITIVITY OF THE RCP WATER TEMPERATURE

In this section, a sensitivity of the water temperature will be studied in the hottest and most humid climate in Miami and the coldest and most dry climate in Saskatoon to show how the water temperature affects the load removed from the space and consequently the space temperature.

Figure 5.10 shows the space temperature compared to the heating set point temperature on January 15 in Saskatoon using different RCP water temperatures. Although the recommended temperature for ceiling panels is about 27°C (Olesen 2008), the minimum temperature that can be used in Saskatoon for an acceptable level of space temperature is found to be 50°C by this sensitivity study. It should be noted that the recommended temperatures for heating are 35°C and 40°C for floor and wall panels, respectively (Olesen 2008). It is highly recommended to use floor and wall heating panels especially in cities with high heating loads such as Saskatoon and Chicago.

Although the space temperature is the closest to the heating set point temperature when the water temperature is 55°C, even 55°C water temperature does not result in a space temperature that follows the set point temperature as closely as the cooling case. This is seen previously and the reason is the low convective heat transfer coefficient for heating. The space temperature does not exceed 18°C all day when a water temperature of 35°C is used showing very poor heating and the inability of the RCP to meet the whole space heating load. The choice of the water

temperature of 50°C is based on a compromise between a relatively acceptable space temperature and the amount of energy required to provide this heating load.

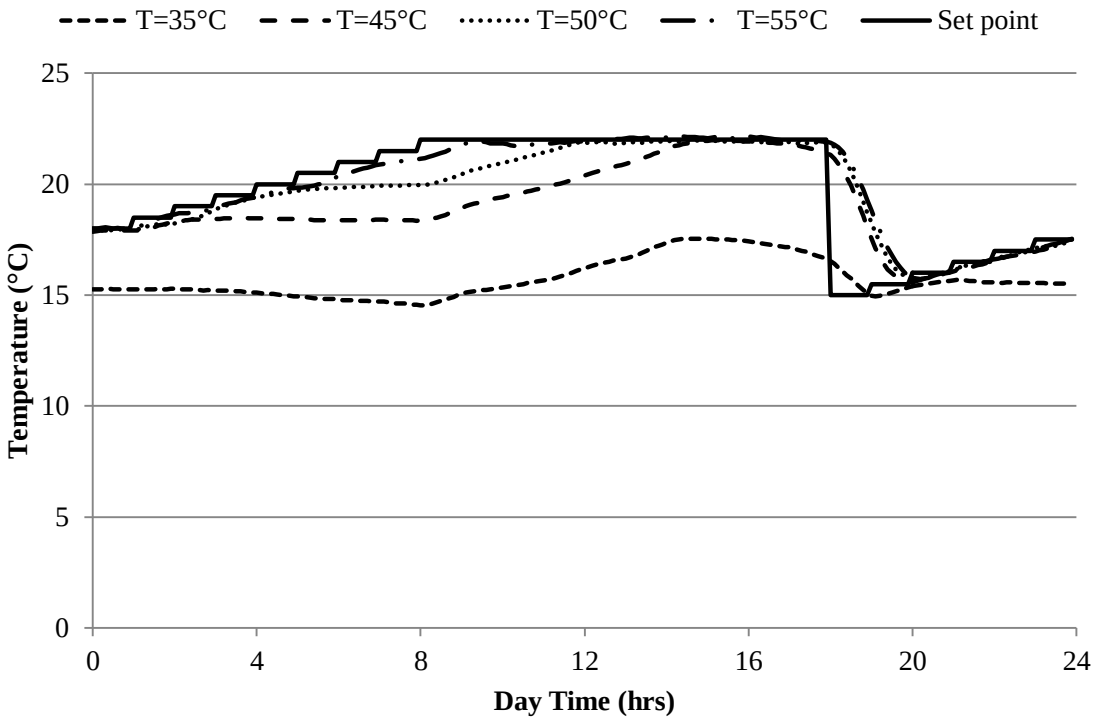

Figure 5.10: Space temperature compared to the set point temperature using different RCP water temperatures on January 15 in Saskatoon.

Figure 5.11 shows the frequency of the relative humidity in Saskatoon during the working hours of the year using different RCP water temperatures. The relative humidity frequency is the same for the temperatures of 45°C, 50°C, and 55°C, while it is narrower for the water temperature of 35°C. On the other hand, Figure 5.12 shows the variation of humidity ratio on January 15 in Saskatoon using different RCP water temperature. As the water temperature

increases, the heat transfer coefficient calculated from equation (2.9) increases and consequently the mass transfer coefficient calculated using equations (2.15) to (2.23) also increases and thus more moisture will be transferred to the space calculated from equation (2.24) which would expect to result in a higher humidity ratio in the space. Figure 5.11 shows that the relative humidity is the highest when the RCP temperature is 35°C due to a lower indoor temperature. Figure 5.12 also shows that the humidity ratio during the design day is the lowest when RCP temperature is 35°C.

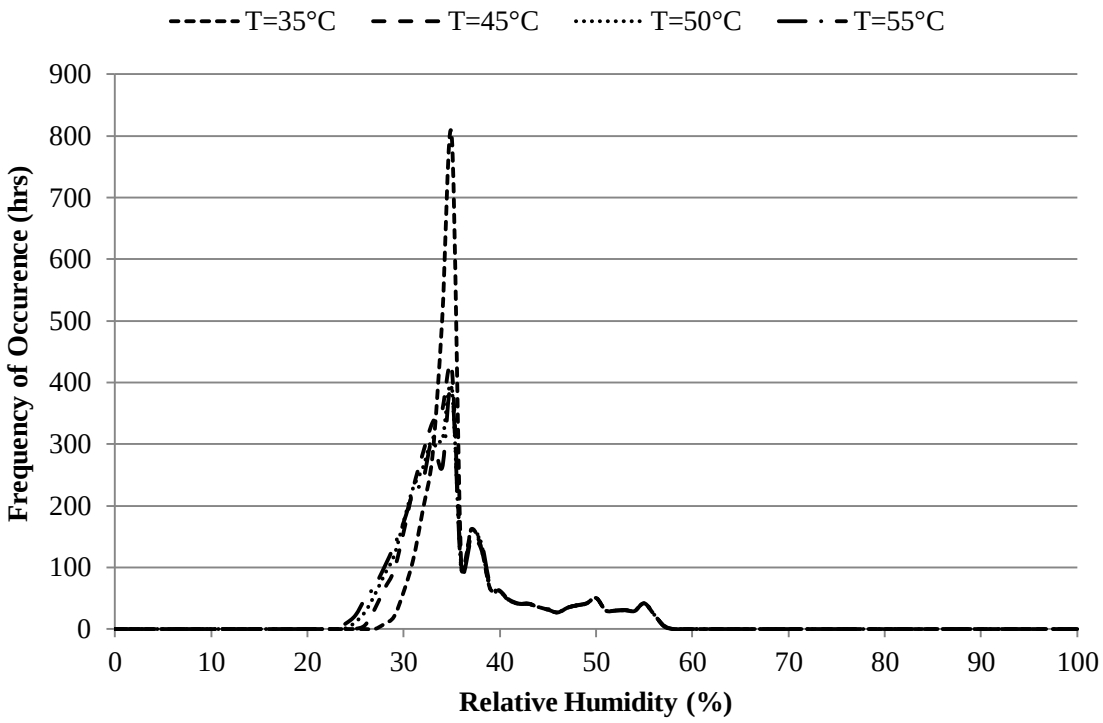

Figure 5.11: Frequency of relative humidity inside the building using different RCP water temperatures throughout the year in Saskatoon.

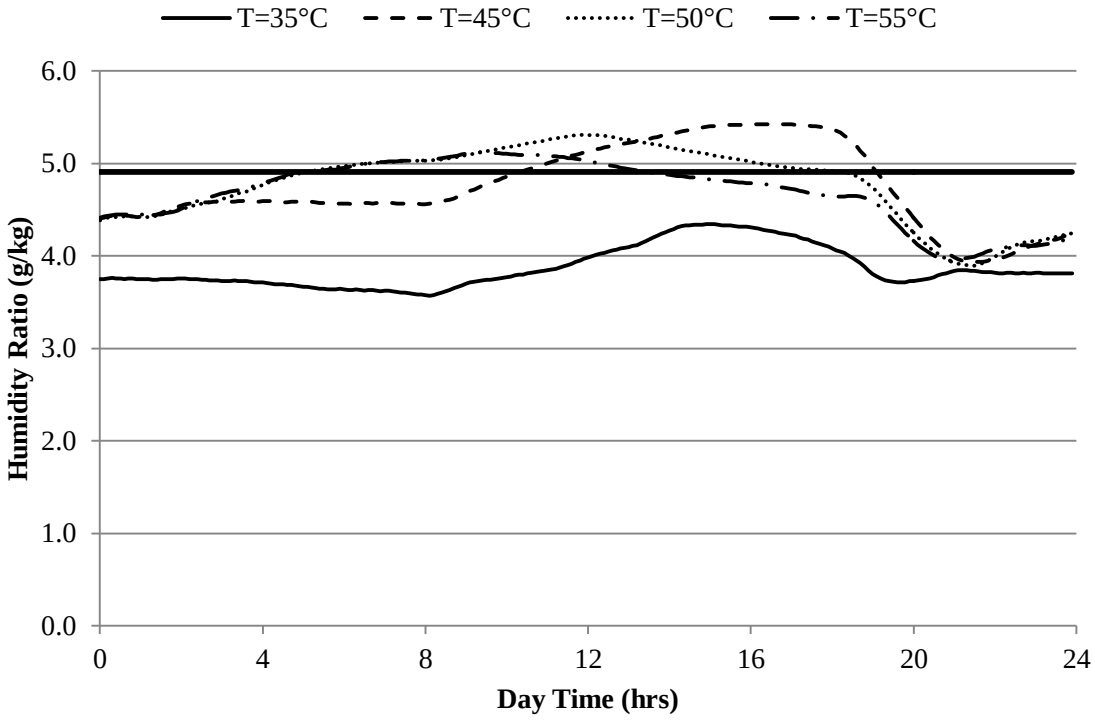

Figure 5.12: Indoor humidity ratio using different RCP water temperatures on January 15 in Saskatoon.

Figure 5.13 shows the annual energy consumption in Saskatoon using different RCP water temperatures. The cooling and dehumidification energies are unaffected as the cooling water temperature is kept constant. The heating energy increases as the water temperature increases as more energy is required to keep the space temperature closer to the set point temperature. The energy required at 55°C water temperature is 10%, 4%, and 1% higher than the energy required at 35°C, 45°, and 50°C, respectively. On the other hand, the humidification energy slightly decreases as more sensible heating is provided by the RCP

and less latent heating is required. However, the humidification energy is only decreased at 55°C by 4% than at 45°C.

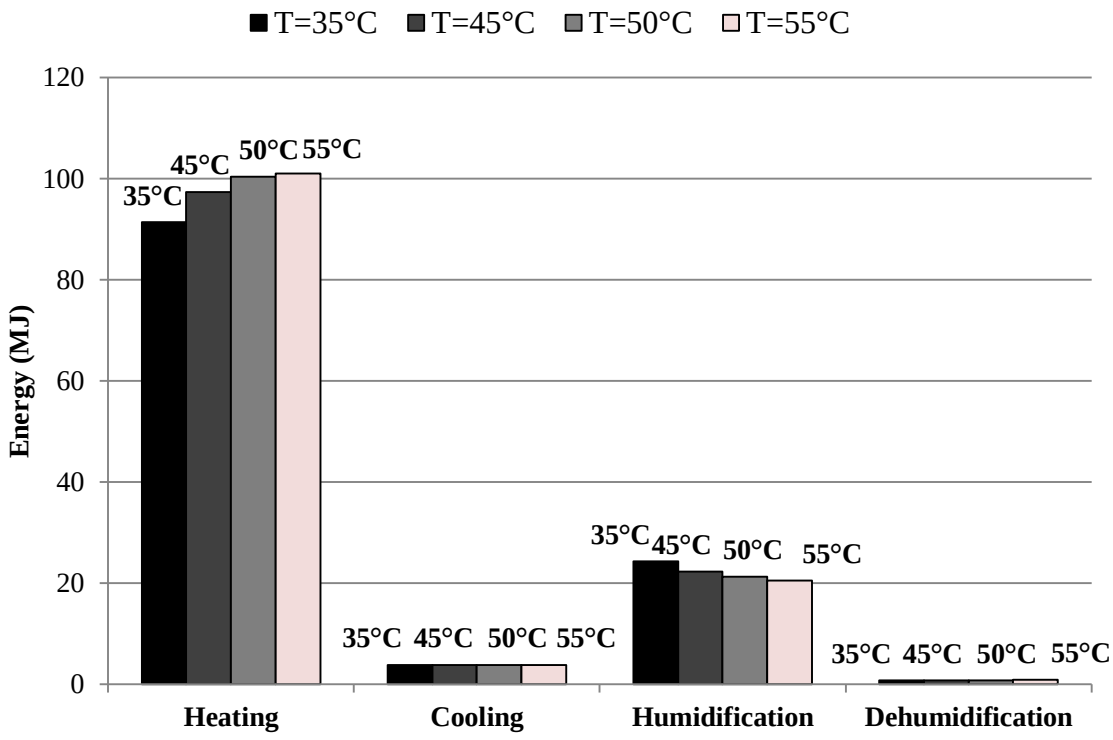

Figure 5.13: Annual energy consumption in Saskatoon using different RCP water temperature.

Figure 5.14 shows the space temperature compared to the cooling set point temperature on July 16 in Miami using different RCP water temperatures. As the water temperature decreases, the space temperature follows the cooling set point temperature more closely. A compromise is made in Miami between the space temperature performance and the energy consumption and thus the temperature of 14°C is selected.

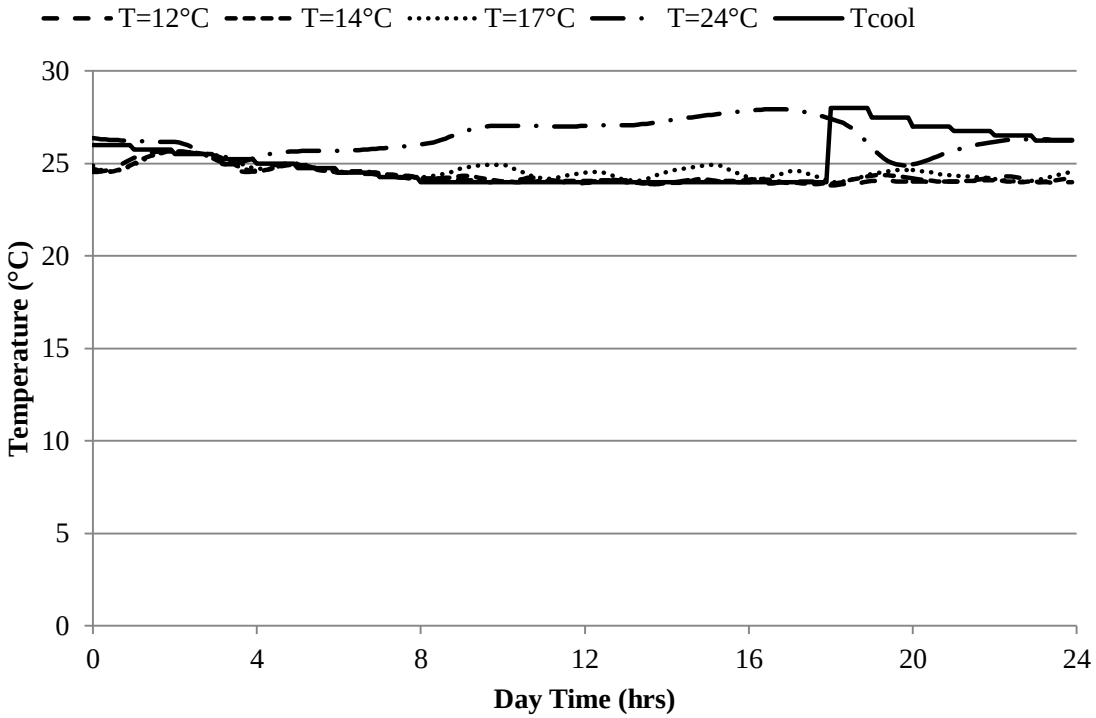

Figure 5.14: Space temperature compared to the set point temperature using different RCP water temperatures on July 16 in Miami.

Figure 5.15 shows the frequency of the relative humidity in Miami during the working hours of the year using different RCP water temperatures. As the temperature increases and the humidity ratio is constant, the relative humidity decreases. This is shown in Figure 5.15 by narrower frequency lines at higher RCP water temperatures.

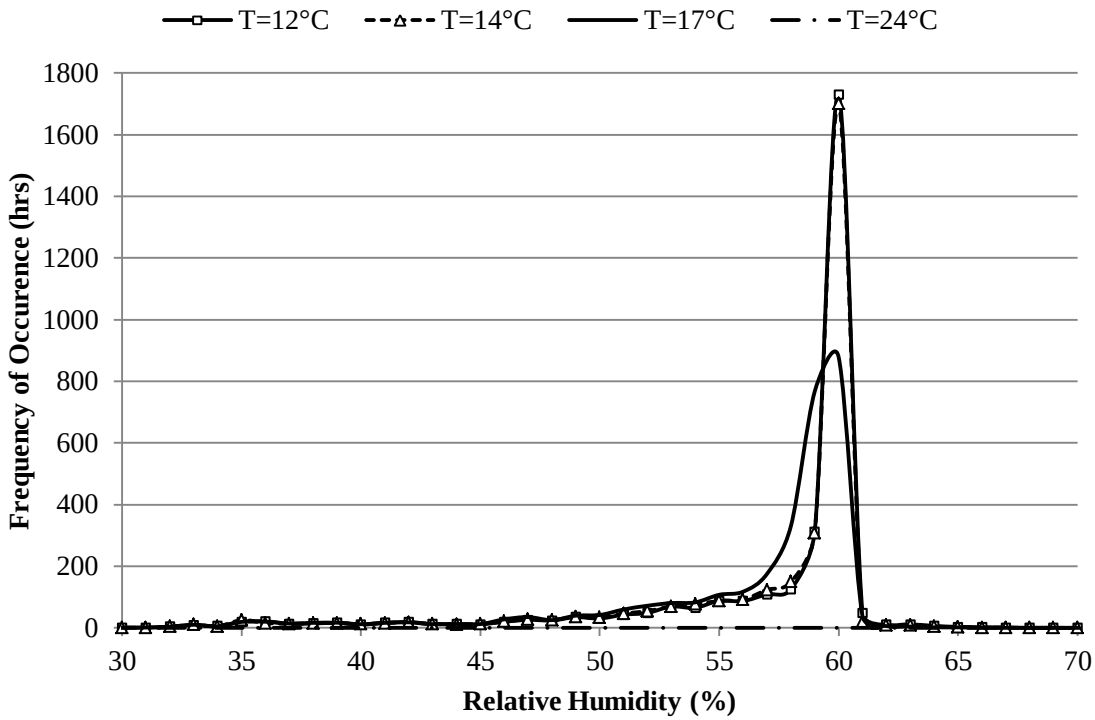

Figure 5.15: Frequency of relative humidity inside the building using different RCP water temperatures throughout the year in Miami.

Figure 5.16 shows the annual energy consumption in Miami using different cooling temperatures. The cooling energy increases as the temperature decreases as the space is maintained at a lower indoor temperature as the RCP water temperature is decreased. The cooling energy consumed using the water temperature of 12°C is 2%, 13%, and 35% higher than that consumed by the water temperature of 14°C, 17°C, and 24°C, respectively. The highest dehumidification energy consumed is at a water temperature of 14°C and it then decreases as the temperature increases. Figure 4.13 in Section 4.2 shows that the dew point temperature in Miami is around 13°C. This shows that condensation is likely to take place at a water temperature of

12°C which is another reason the water temperature of 14°C is used. This is probably the reason the temperature of 12°C has a lower dehumidification energy.

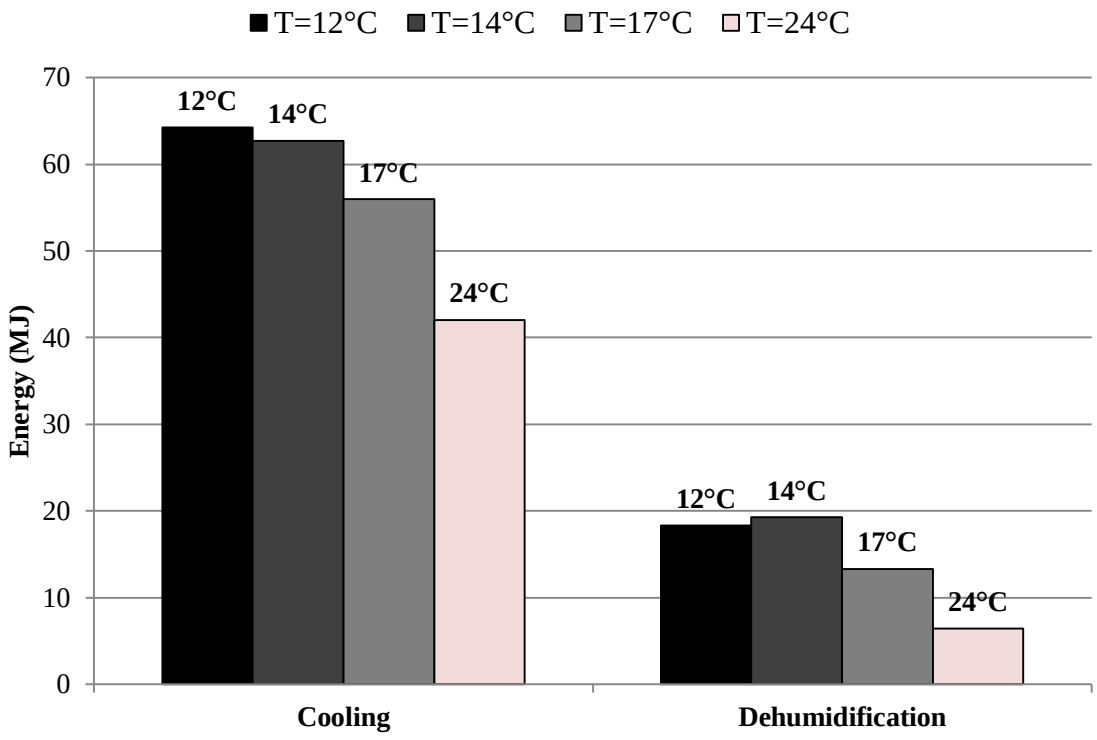

Figure 5.16: Annual energy consumption in Miami using different RCP water temperatures.

5.3 SENSITIVITY OF HAMP DESICCANT SOLUTION CONCENTRATION

In this section, the sensitivity of the desiccant solution concentration is studied through the humidification process in Saskatoon and the dehumidification process in Miami representing dry and humid climates respectively. The moisture transfer between the surface of the HAMP and the space air takes place through a humidity ratio gradient as discussed in Section 2.3.11. Thus, the desiccant solution concentration in the HAMP will directly affect the rate of moisture transfer between the HAMP surface and the space air. Table 5.1 gives the temperature, desiccant concentration, and the resulting HAMP surface humidity ratio used in the simulations for different mass and heat transfer processes for the base case of system C.

Table 5.1: Desiccant solution concentration

Process	Temperature (°C)	Concentration (%)	W_s (g/kg)
Heating and humidification	40	38	12.048
Cooling and dehumidification	16	32	4.2830

Figure 5.17 shows the variation of humidity ratio on January 15 in Saskatoon for different LiCl concentrations. The humidity ratio is varied using desiccant concentrations of 38%, 40%, 44%, and 46% giving a humidity ratio difference between the HAMP surface and the set point humidification humidity ratio (4.91 g/kg at 22°C) of 7.14, 5.32, 2.37, and 1.23 g/kg, respectively. The desiccant concentration of 38% is the only concentration that is able to maintain the humidity ratio higher than the humidification limit of 4.91 g/kg and thus maintaining a good level of space humidity to avoid low relative humidity values.

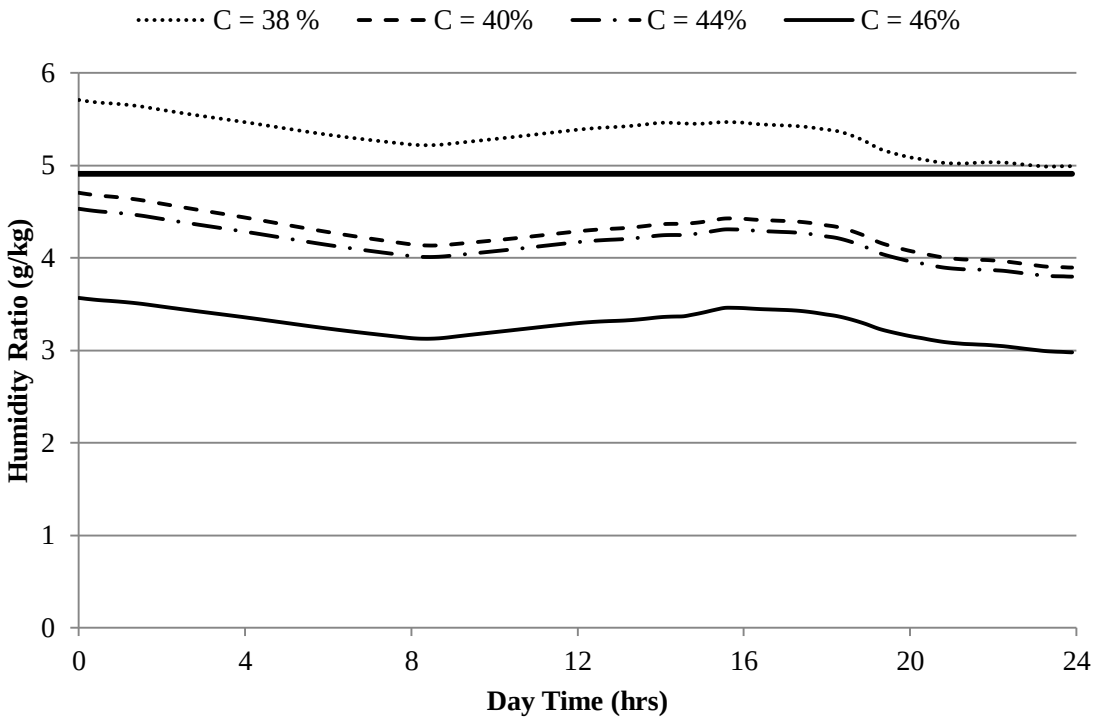

Figure 5.17: Indoor humidity ratio with different desiccant solution concentrations on January 15 in Saskatoon.

Figure 5.18 shows the variation of relative humidity in Saskatoon on January 15. The indoor relative humidity is between 30% and 50% all the time when the desiccant concentration is 38%. This gives a good level of space humidity in the building. The desiccant solution concentrations of 40% and 44% keep the relative humidity level between 25% and 40% which also can be considered a good range of relative humidity but will give a drier environment than the concentration of 38%. The desiccant concentration of 46% as shown from both Figure 5.17 and Figure 5.18 gives the lowest space humidity level. The desiccant solution can be regenerated for

humidification by adding water to the solution in an amount that make up for the water vapor added to the space.

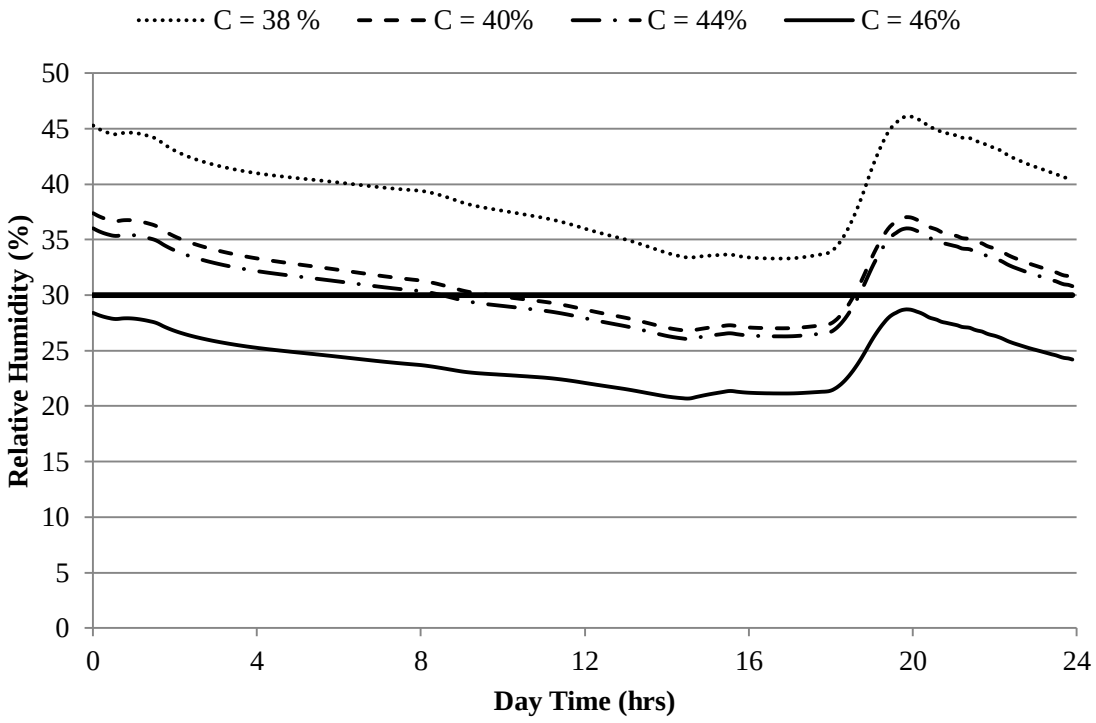

Figure 5.18: Indoor relative humidity with different desiccant solution concentrations on January 15 in Saskatoon.

Figure 5.19 shows the variation of humidity ratio on July 16 in Miami. The humidity ratio is varied using desiccant concentrations of 32%, 28%, 24%, 20% and 16% giving a humidity ratio difference between the HAMP surface and the set point dehumidification humidity ratio (9.30 g/kg at 24°C) of 5.02, 3.80, 2.55, 1.35, and 0.27 g/kg, respectively. The concentrations of 32%, 28%, 24%, and 20% show a close variation to the set point humidity ratio during the working

hours, while there is humidity ratio increase in the night hours probably due to the shutdown of the ventilation system. The concentration of 16% however is unable to dehumidify sufficiently due to the small mass transfer potential.

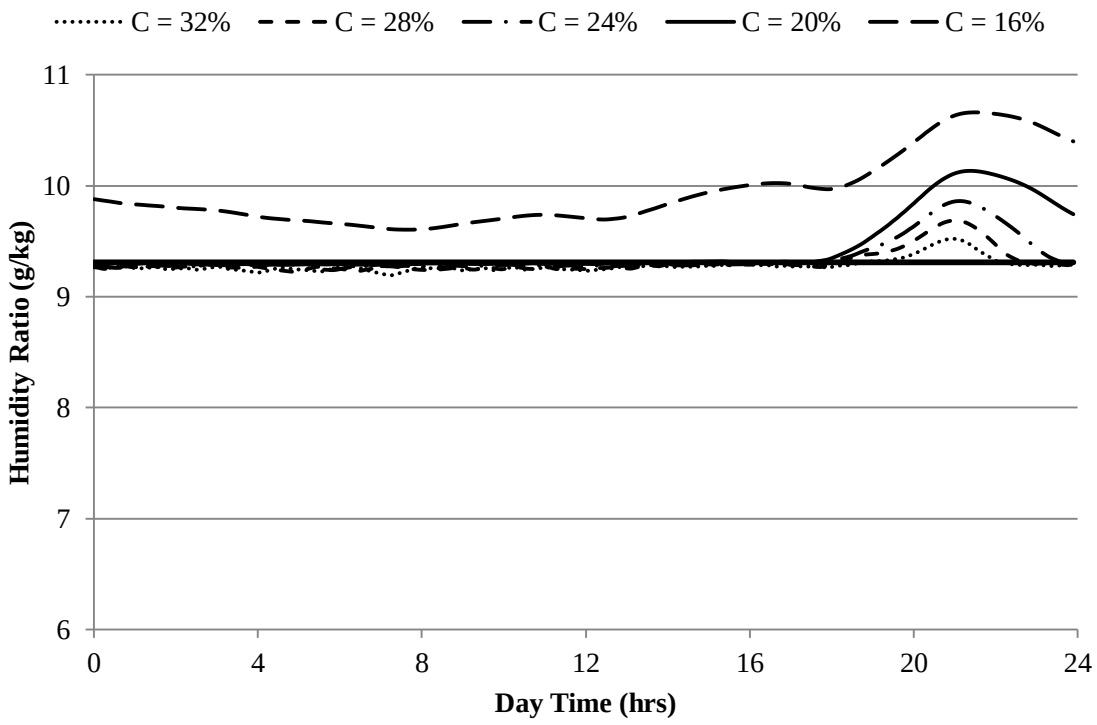

Figure 5.19: Humidity ratio variation with different desiccant solution concentrations on July 16 in Miami.

Figure 5.20 shows the variation of relative humidity in Miami on July 16. The relative humidity of all the desiccant concentrations vary in the required range with the concentration of 32% having the lowest relative humidity and the concentration of 16% having the highest relative humidity. The desiccant solution can be regenerated for dehumidification by adding LiCl

to the solution in an amount that maintains the required desiccant concentration. The regeneration analysis is generally left for future work.

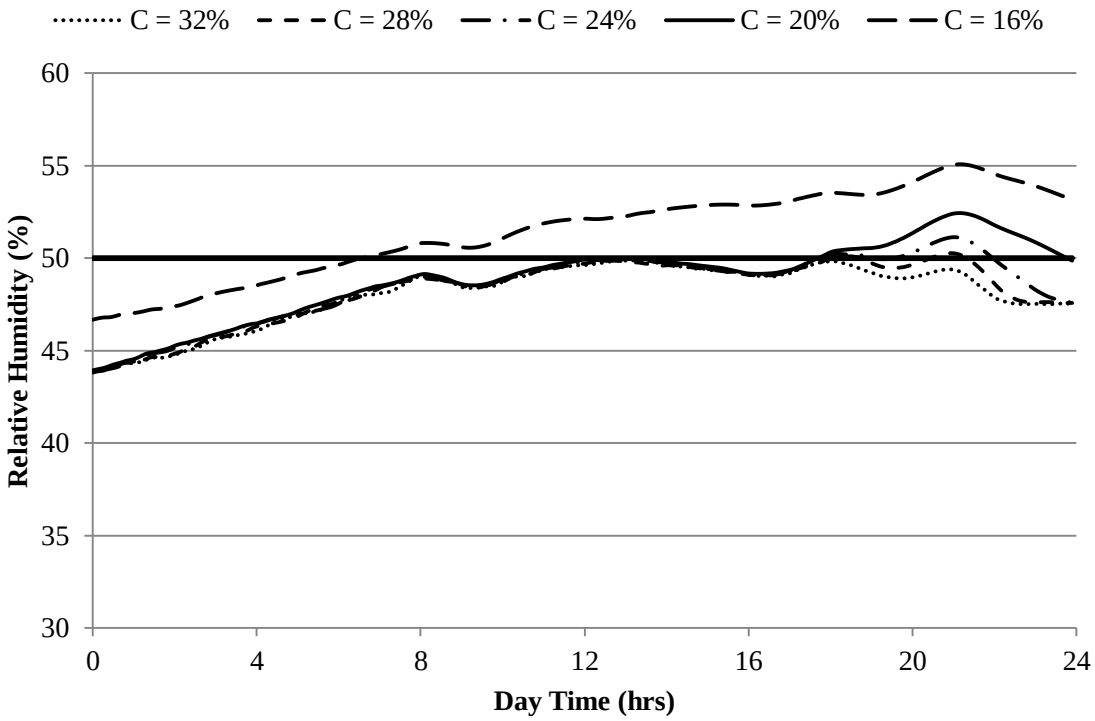

Figure 5.20: Relative humidity variation with different desiccant solution concentrations on July 16 in Miami.

Generally, as the desiccant concentration increases, the humidity ratio difference between the HAMP surface and the space air decreases and mass transfer decreases.

CHAPTER 6 CONCLUSIONS

In this thesis, the TRNSYS computer program was used to perform simulations on an office building in four different cities. The simulations were done on four different HVAC systems: a conventional all-air system (system A), RCP system with mechanical ventilation (system B), RCP system with DOAS (system D), and RCP with HAMP and mechanical ventilation (system C).

6.1 CONCLUSIONS

In this thesis, a one-storey office building located in El Paso, Texas, is selected to be studied with the TRNSYS computer simulation program to test the applicability of a novel heat and moisture transfer panel (HAMP). This thesis focuses on the moisture transfer of the HAMP although experiments carried out on the HAMP in the heat and mass transfer lab in the University of Saskatchewan show that the HAMP is also able to transfer heat as well as moisture. The office building construction is modified to meet ASHRAE Standard 90.1 (2010) requirements. Ventilation, infiltration, and internal loads of the building are calculated and/or selected according to ASHRAE Handbook (2012), Standards 62.1 (2010), and 90.1 (2010). The equipment used in the simulations are selected according to the availability of different components in TRNSYS simulation program.

The simulations are run in four different cities representing four major climate conditions. The results show the ability of the RCP system in cooling to maintain the space temperature

variation throughout the working day close to the cooling set point temperature. However, the response of the RCP in heating is slower and in more cold climates, such as Saskatoon and Chicago, the space temperature takes more time to reach the designed heating set point temperature. It is thus recommended to use hydronic baseboard heating or floor radiant panels instead of ceiling panels for heating especially in cities with heating loads higher than 42 W/m^2.

The HAMP proves to be able to control the space relative humidity in all cities within or close to the required limits of 30% RH to 70% RH. The HAMP is able to keep the relative humidity in the dry climates of Saskatoon and Phoenix between around 25% RH and 60% RH, and in the humid climates of Chicago and Miami between 26%-40% RH and 62% RH, respectively.

The RCP system in systems B and C consumes less cooling energy than the all-air system in all cities, and consumes less heating energy than the all-air system in Saskatoon and Phoenix. This is because the heat transfer in the RCP system is done directly from the heated or chilled water to the space objects. The cooling energy is also less due to the use of the cooling tower in systems B and C which provides free cooling of the RCP water during the day and at night. This is in addition to the fact that in system B, the RCP is unable to remove the space latent load. No heating is done in any of the four systems in Miami. The RCP system consumes more heating energy in Chicago than the all-air system due to the low heat transfer coefficient of the RCP in heating and the low RCP heating water temperature used. However, the total energy (heating and cooling energies) consumed by system B is lower than the total energy consumed by the all-air

system in all cities. Generally, system C consumes less total energy than the conventional all-air system in the hot climates by 40% and 54% in Miami and Phoenix respectively, and in the cold climates by 14% and 23% in Saskatoon and Chicago, respectively.

Three sensitivity studies are performed to show the effect of three different parameters on the performance of system C. The first sensitivity study shows the effect of the RCP area on the performance of system C. The results of the study show that (in all cities) as the RCP area increases, the space temperature is closer to the set point temperature showing higher heat transfer rates. This is most obvious in the cold climates. The relative humidity levels are completely unaffected by changing the RCP area. The heating energy decreases, but generally the change is not very significant, while the cooling energy is significantly decreased as the RCP area is increased. This is because more RCP exposed area contributes to the removal of the space load which will otherwise be removed by cooling for a longer time consuming more energy.

The second sensitivity study shows the effect of the RCP water temperature on the heat transfer between the RCP and the space air. The results in the cold climate of Saskatoon show that the space temperature is closer to the set point temperature as the water temperature increases which causes the energy consumption to increase as the water temperature increases. The humidification energy however decreases as the water temperature increases. This because more sensible heating is done by the RCP and less latent heating energy is needed. The relative humidity is unaffected by the increase in water temperature. The results of the study in the hot climate of Miami show that the space temperature is closer to the set point temperature as the

water temperature decreases and, as a result, the energy consumption increases as the water temperature decreases.

The third sensitivity study shows the effect of the HAMP desiccant concentration on the performance of the HAMP in system C. The results of the study show that as the desiccant concentration increases, the humidity ratio difference between the HAMP surface and the space air decreases and thus the mass transfer decreases. The desiccant concentration and temperature recommended for dry climates in winter is 38% and 40°C, while the desiccant concentration and temperature recommended for humid climates in summer is 32% and 16°C.

6.2 RECOMMENDATIONS FOR FUTURE WORK

It is highly recommended to study the different ways that can be used to regenerate the HAMP desiccant solution. It is required to find a way that consumes reasonable levels of energy in order to produce a system combining the RCP and the HAMP or just the HAMP that consumes less energy than the all-air system and capable of removing the space latent loads. It is also recommended for future work to test the HAMP in a real room to validate the simulations and be able to deal with the challenges of the commissioning of the HAMP. For future work it will be valuable to do additional sensitivity studies on the effects of the ventilation supply temperature and humidity ratio, different latent loads in other cities, and the thermal conductivity of the HAMP membrane.

It is also highly recommended to apply the sensitivity studies in Appendix C to the entire thesis. Of particular importance is a study to determine the temperature and concentration of the salt solution that are required to adequately humidity and dehumidify the building when realistic membranes are used in the HAMP (including thermal and moisture resistances) as identified in Appendix C.

Other future work might include studying the effect of changing the desiccant solution temperature and concentration on the HAMP channels in order to avoid crystallization and maintain the HAMP for a good lifetime that will produce a good payback period to be able to put this system in a the competition with the different HVAC systems that are currently used.

REFERENCES

Afshin, M., 2010. Selection of a liquid desiccant in a run-around membrane energy exchanger, M.Sc. thesis, University of Saskatchewan, Canada.

AHRI Standard 340/360, 2007. Standard for Performance Rating of Commercial and Industrial Unitary Air-Conditioning and Heat Pump Equipment, Air-Conditioning Heating, and Refrigeration Institute, Arlington, VA, USA.

ASHRAE, 2012. ASHRAE Handbook – HVAC Systems and Equipment, SI ed., Atlanta, Georgia, USA: American Society of Heating, Refrigerating and Air-Conditioning Engineers, Inc., Atlanta, GA, Chapter 6.

ASHRAE Standard 62.1, 2010. Ventilation for Acceptable Indoor Air Quality (IAQ), SI ed., American Society of Heating, Refrigerating and Air-Conditioning Engineers, Inc., Atlanta, GA.

ASHRAE Standard 90.1, 2010. Energy Standard for building except low-rise residential buildings, SI ed., American Society of Heating, Refrigerating and Air-Conditioning Engineers, Inc., Atlanta, GA.

ASHRAE, 2009. ASHRAE Handbook of Fundamentals, SI ed., American Society of Heating, Refrigerating and Air-Conditioning Engineers, Inc., Atlanta, GA.

Beckman, W.A., L. Broman, A. Fiksel, S.A. Klein, E. Lindberg, M. Schuler, J. Thornton, 1994. TRNSYS, the most complete solar energy system modeling and simulation software, *Renewable Energy*, **5**, 486–488.

Bornehag, C.G., G. Blomquist, F. Gyntelberg, B. Jarvholm, P. Malmberg, L. Nordvall, A. Nielsen, G. Pershagen, J. Sundell, 2001. Dampness in Buildings and Health - Nordic Interdisciplinary Review of the Scientific Evidence on Associations between Exposure to "Dampness" in Buildings and Health Effects, *Indoor Air*, **11**, 72-86.

Briggs, R., D. Crawley, D. Belzer, 1987. Analysis and categorization of the office building stock. Pacific Northwest Laboratory, for Gas Research Institute.

Briggs, R.S., R.G. Lucas, T.Z. Todd, 2003. Climate classification for building energy codes and standards, Part 2, Zone definitions, maps, and comparisons, *ASHRAE Transactions*, **109**(1), 122–130.

Burns, P.R., J.W. Mitchell, W.A. Beckman, 1985. Hybrid desiccant cooling systems in supermarket applications. *ASHRAE Transactions*, **91**(1B).

Busweiler, U., 1993. Air conditioning with a combination of radiant cooling, displacement ventilation, and desiccant cooling, *ASHRAE Transactions*, **99**(2), 503-510.

Conroy, C.L., S.A. Mumma, 2001. Ceiling radiant cooling panels as a viable distributed parallel sensible cooling technology integrated with dedicated outdoor air systems, *ASHRAE Transactions*, **107**(1), 578-585.

Energy Information Administration, 1986. Nonresidential Building Energy Consumption Survey (CBECS), U.S. Department of Energy, USA.

Fauchoux, M.T., 2012. Design and performance testing of a novel ceiling panel for simultaneous heat and mass transfer to moderate indoor temperature and relative humidity, Ph.D. thesis, University of Saskatchewan, Canada.

Fauchoux, M.T., 2006. Review of energy building simulation tools that include moisture storage in buildings materials and HVAC systems, M.Sc. thesis, University of Saskatchewan, Canada.

Fauchoux, M.T., M. Bansal, P. Talukdar, C.J. Simonson, D.A. Torvi, 2010. Testing and modelling of a novel ceiling panel for maintaining space relative humidity by moisture transfer, *International Journal of Heat and Mass Transfer*, **53**, 3961–3968.

Fauchoux, M.T., C.J. Simonson, D.A. Torvi, 2009. Tests of a Novel Ceiling Panel for Maintaining Space Relative Humidity by Moisture Transfer from an Aqueous Salt Solution, *Journal of ASTM International*, **6**(4).

Fauchoux, M.T., C.J. Simonson, D.A. Torvi, 2008. Investigation of a novel ceiling panel for heat and moisture control in buildings, *Proceedings of the 8th Symposium on Building Physics in the Nordic Countries*, Danish Society of Engineers, Copenhagen, Denmark, 1269–1276.

Hukka, A., H.A. Viitanen, 1999, A mathematical model of mould growth on wooden material, *Wood Science and Technology*, **33**, 475-485.

Imanari, T., T. Omori, K. Bogaki, 1999. Thermal comfort and energy consumption of the radiant ceiling panel system. Comparison with the conventional all-air system, *Energy and Buildings*, **30**, 167-175.

Incropera, F.P. and D.P. DeWitt, 2002. *Fundamentals of Heat and Mass transfer*, 5th ed., John Wiley and Sons, Inc., Toronto, ON.

ISO Standard 7730, 1994. Moderate thermal environments – determination of the PMV and PPD indices and specification of the conditions for thermal comfort, International Standards Organization, Geneva, Switzerland.

Klein, S.A., 2000. TRNSYS—A Transient System Simulation Program, Engineering Experiment Station Report 38-13, Solar Energy Laboratory, University of Wisconsin Madison, USA.

Kosonen, R., and F. Tan, 2004. Assessment of productivity loss in air-conditioned buildings using PMV index, *Energy and Buildings*, **36**, 987-993.

Kulpmann, R.W., 1993. Thermal comfort and air quality in rooms with cooled ceilings-Results of scientific investigations, *ASHRAE Transactions*, **99**(2), 488-502.

Miriel, J., L. Serres, S. Trombe, 2002. Radiant ceiling panel heating-cooling systems: experimental and simulated study of the performances, thermal comfort and energy consumptions, *Applied Thermal Engineering*, **22**, 1861-1873.

Mumma, S.A., 2001a. Ceiling Panel Cooling Systems, *ASHRAE Journal*, **43**(11), 28-32.

Mumma, S.A., 2001b. Dedicated outdoor air-dual wheel system control requirements, *ASHRAE Transactions*, **107**(1), 147-155.

National Building Code, 1995. National Building Code of Canada, issued by the Canadian Commission on Building and Fire Codes, National Research Council of Canada, Ottawa.

National Renewable Energy Laboratory (NREL), 2009. TMY2 weather data file.

Olesen, B.W., 2008. Radiant heating and cooling by embedded water-based systems, Technical University of Denmark, International Centre for Indoor Environment and Energy, Department of Civil Engineering, Denmark: http//www.ie.dtu.dk.

Rasouli, M., 2010. Building energy simulation of a run-around membrane energy exchanger (RAMEE) , M.Sc. thesis, University of Saskatchewan, Canada.

Rasouli, M., C.J. Simonson, R.W. Besant, 2010. Applicability and optimum control strategy of energy recovery ventilators in different climatic conditions, *Energy and Buildings*, **42**, 1376-1385.

Simmonds, P., 1997. Radiant systems offer users greater comfort control, *Energy Users News*, **3**, 34-35.

Simonson, C.J., W. Shang, R.W. Besant, 2000a. Part-load performance of energy wheels: Part I - Wheel speed control, *ASHRAE Transactions*, **106**(1), 286-300.

Simonson, C.J., W. Shang, R.W. Besant, 2000b. Part-load performance of energy wheels: Part II – Bypass control and correlations, *ASHRAE Transactions*, **106**(1), 301-310.

Sodec, F., 1999. Economic viability of cooling ceiling systems, *Energy and Buildings*, **30**, 195-201.

Vangtook, P. and S. Chirarattananon, 2007. Application of radiant cooling as a passive cooling option in hot humid climate, *Building and Environment*, **42**, 543-556.

Vangtook, P. and S. Chirarattananon, 2006. An experimental investigation of application of radiant cooling in hot humid climate, *Energy and Buildings*, **38**, 273-285.

Viitanen, H., 1996. Factors affecting the development of mould and brown rot decay in wooden material and wooden structures, Effect of humidity, temperature and exposure time, The Swedish University of Agricultural Sciences, Uppsala, Sweden.

Wyon, D.P., L. Fang, L. Lagercrantz, P.O. Fanger, 2006. Experimental determination of the limiting criteria for human exposure to low winter humidity indoors, *HVAC&R Research*, **12**(2), 201-213.

APPENDIX A SUPPLY AIR CALCULATIONS

A.1 System A SA calculation

The supply air in system A is calculated such that it handles the whole sensible and latent design loads of the space. This is done by first calculating the design heating and cooling design loads in each city. The heating and cooling design loads are given in Table 3.3 for each city and will be used here directly. The air is supplied at 14°C and 84% RH (h = 34.9 kJ/kg) to cool the space to 24°C and 50% RH (h = 47.7 kJ/kg) while for heating it is supplied at 30°C and an assumed relative humidity of 22% RH (h = 44.6kJ/kg) (the supply air is not humidified in system A) to heat the space to 22°C and 30% RH (h = 34.5 kJ/kg). Figure A.1 shows a simple schematic of the cooling process. SA is the supply air, $\dot{m}_{SA}$ is the supply air mass flow rate, and Q is the heat loss from the space.

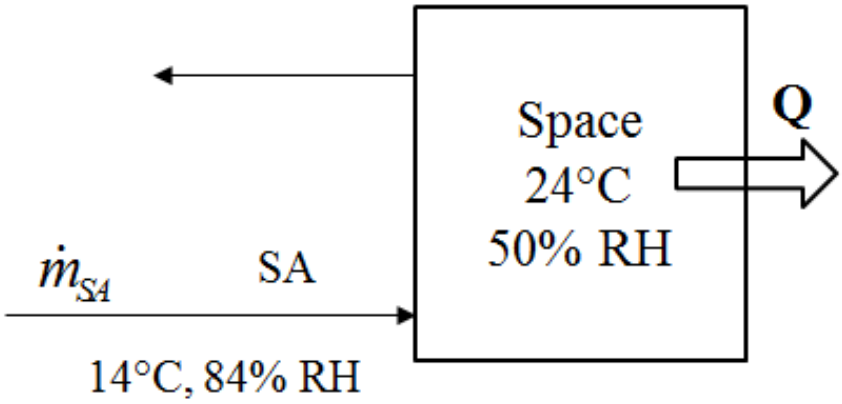

Figure A.1: Schematic of the cooling process

1. Chicago

The cooling design load, Q_c, in Chicago is 61 kW while the heating design load, Q_h, is 74 kW. The SA flow rate will be calculated for cooling and heating and the larger value will be used in system A as a constant supply. The cooling SA flow rate is calculated using the following equations:

$$Q_c = \dot{m}_{SA}(h_{out} - h_{in}) = \dot{m}_{SA}(47.7-34.9) = \dot{m}_{SA}(12.8\ kJ/kg) = 61\ kW \quad (A.1)$$

$$\therefore \dot{m}_{SA} = 4.77\ kg/s = 17{,}156\ kg/hr \quad (A.2)$$

where h_{out} is the enthalpy of the air flowing out of the space, and h_{in} is the enthalpy of the air flowing into the space. The heating SA flow rate is calculated using the following equations:

$$Q_h = \dot{m}_{SA}(h_{in} - h_{out}) = \dot{m}_{SA}(44.6-34.5) = \dot{m}_{SA}(10.1\ kJ/kg) = 74\ kW \quad (A.3)$$

$$\therefore \dot{m}_{SA} = 7.33\ kg/s = 26{,}376\ kg/hr \quad (A.4)$$

The supply air in Chicago is thus taken as the heating supply air which is the maximum of both calculations. The minimum ventilation calculated using ASHRAE Standard 90.1 (2010) is 13659 kg/hr. The SA and the minimum ventilation ($\dot{m}_{min}$) are used to calculated the maximum fraction of RA used by the economizer, X_{max}, using the following equation,

$$X_{max} = 1 - \frac{\dot{m}_{min}}{\dot{m}_{SA}} = 1 - \frac{1358.6}{31{,}651.44} = 0.957 \quad \text{(A.5)}$$

2. Miami

There is no heating required in Miami, and thus the SA flow rate of cooling is only calculated. The design cooling load in Miami is 66 kW. The SA flow rate and the maximum fraction of RA are calculated using the following equations,

$$Q_c = \dot{m}_{SA}(12.8 \text{ kJ/kg}) = 66 \text{ kW} \quad \text{(A.6)}$$

$$\therefore \dot{m}_{SA} = 5.156 \text{ kg/s} = 18{,}562 \text{ kg/hr} \quad \text{(A.7)}$$

$$X_{max} = 1 - \frac{1358.6}{18{,}562.5} = 0.927 \quad \text{(A.8)}$$

3. Saskatoon

The design heating load in Saskatoon is 102 kW while the design cooling load is only 47 kW. Therefore, the heating SA flow rate is higher than the cooling SA flow rate. The SA flow rate and maximum fraction of RA are calculated using the following equations,

$$Q_h = \dot{m}_{SA}(10.1 \text{ kJ/kg}) = 102 \text{ kW} \quad \text{(A.9)}$$

$$\therefore \dot{m}_{SA} = 10.1 \text{ kg/s} = 36{,}356 \text{ kg/hr} \quad \text{(A.10)}$$

$$X_{max} = 1 - \frac{1358.6}{36{,}356.4} = 0.962 \quad \text{(A.11)}$$

4. Phoenix

The design cooling load in Phoenix is 56 kW while the design heating load is only 34 kW. Therefore, the cooling SA flow rate is higher than the heating SA flow rate. The SA flow rate and maximum fraction of RA are calculated using the following equations,

$$Q_c = \dot{m}_{SA}(12.8 \text{ kJ/kg}) = 56 \text{ kW} \quad \text{(A.12)}$$

$$\dot{m}_{SA} = 4.375 \text{ kg/s} = 15{,}750 \text{ kg/hr} \quad \text{(A.13)}$$

$$X_{max} = 1 - \frac{1358.6}{15{,}750} = 0.914 \quad \text{(A.14)}$$

A.2 System D SA calculation:

The SA is system D is calculated such that it removes the design latent load. In the theoretical case, the humidification is turned off and thus, the latent load represented here is necessarily dehumidification load only. However, the heater is set to heat the supply air to 30°C and 30% RH. This means that the SA will be calculated based on the design dehumidification load only. Since the energy wheel removes part of the ventilation latent load, the SA is required to remove the rest of the ventilation latent load as well as the space latent load. The percentage of latent load removed by the SA from the total latent load is different from one city to the other. However, the latent load that is used in the calculations will certainly cover the full space latent load. Table A.1 shows the design latent load of each city.

Table A.1: Design latent load

City	Design latent load (kW)
Saskatoon, Saskatchewan	30
Miami, Florida	40
Phoenix, Arizona	27
Chicago, Illinois	38

1. Chicago

The latent load removed by the energy wheel in Chicago at the design conditions is 65% of the design load. The SA removes 35% of the design load which is 13.3 kW. The SA in Chicago is supplied at a humidity ratio of 7 g/kg. The SA flow rate is calculated using

$$Q_{lat} = \dot{m}_{SA}(W_{out} - W_{in})h_{fg} \quad \text{(A.15)}$$

The humidity ratio of the air exiting the building is assumed to be at the cooling design condition of 24°C and 50% RH. The value of this humidity ratio is 9.299 g/kg. Thus,

$$13.3\ \text{kW} = \dot{m}_{SA}(9.299-7)\times10^{-3}\times2257 \quad \text{(A.16)}$$

$$\therefore \dot{m}_{SA} = 2.563\ \text{kg/s} = 9227\ \text{kg/hr} = 2.1\ \text{m}^3/\text{s} \quad \text{(A.17)}$$

2. Miami

The latent load removed by the energy wheel in Miami is only about 15% at the design condition. Thus,

$$Q_{lat} = 0.85\times40 = 34\ \text{kW} \quad \text{(A.18)}$$

The SA in Miami is dehumidified to 7 g/kg, and thus,

$$34\ \text{kW} = \dot{m}_{SA}(9.299-7)\times10^{-3}\times2257 \quad \text{(A.19)}$$

$$\therefore \dot{m}_{SA} = 6.553\ \text{kg/s} = 23589\ \text{kg/hr} = 5.5\ \text{m}^3/\text{s} \quad \text{(A.20)}$$

3. Saskatoon

The latent load removed by the energy wheel in Saskatoon is about 47% at the design condition. Thus,

$$Q_{lat} = 0.53 \times 30 = 15.9 \text{ kW} \tag{A.21}$$

The SA in Saskatoon is dehumidified to 7 g/kg, and thus,

$$15.9 \text{ kW} = \dot{m}_{SA}(9.299\text{-}7) \times 10^{-3} \times 2257 \tag{A.22}$$

$$\therefore \dot{m}_{SA} = 3.06 \text{ kg/s} = 11031 \text{ kg/hr} = 2.6 \text{ m}^3/\text{s} \tag{A.23}$$

4. Phoenix

The latent load removed by the energy wheel in Phoenix is about 62% at the design condition. Thus,

$$Q_{lat} = 0.38 \times 27 = 10.26 \text{ kW} \tag{A.24}$$

The SA in Phoenix is dehumidified to 7 g/kg, and thus,

$$10.26\ \text{kW} = \dot{m}_{SA}\,(9.299\text{-}7)\times 10^{-3}\times 2257 \qquad \text{(A.25)}$$

$$\therefore \dot{m}_{SA} = 1.977\ \text{kg/s} = 7118\ \text{kg/hr} = 1.6\ \text{m}^3/\text{s} \qquad \text{(A.26)}$$

APPENDIX B MATLAB CODE

HAMP MatLab code:

```
mFileErrorCode = 100;    % Beginning of the m-file

% input-1: TAIR_INT --? air temperature of airnode
% input-2: RELHUM_INT -? relative humidity of airnode
% input-3: ABSHUM_INT -? absolute humidity of airnode
% input-4: TALM_S3 -? node temperature of active layer
% input-5: hc -? convection heat transfer coefficient of active layer

% output-1: HUM -? humidity gain through which moisture will be added or
removed


% --- Process Inputs ------------------------------------------------------

%Setting Inputs

tz=trnInputs(1); %Space Temperature
RHz=trnInputs(2); %Space Relative Humidity
Winf=trnInputs(3); %Space Humidity Ratio
thamp=trnInputs(4); %HAMP surface temperature taken as an average of input
and output liquid temperature
hc=trnInputs(5); %convection htc in kJ/hr.m2K

hc1=hc*1000/3600; % convection htc in W/m2K

mFileErrorCode = 120;     % After processing inputs

%Setting Parameters

Ac=729.96; %Zone cross sectional area in m2
P=124; %Zone perimeter in m
P1=0.1*P; %10% of the perimeter
As=0.1*Ac; % 10% of the space area (the surface area of the HAMP)
L=4*As/P1; %Characteristic length of space
V=2258.72; %Volume of zone in meter cube
R=8314.31/28.97; %Air gas constant J/kg.K
hth=0.2*10^-3; %HAMP thickness between the air layer and liquid layer in m
Kth=0.334; %HAMP material conductivity in W/mK
Patm=101325; %atmospheric pressure in Pascals

mFileErrorCode = 110;     % After setting parameters

if RHz<35 %Dehumidification condition
    dconc=10; %desiccant solution concentration
    tliq=42;  %inlet desiccant solution temperature to HAMP

    mFileErrorCode = 101;

elseif RHz>60 %Humidification condition
```

```
    dconc=35;
    tliq=12;
    mFileErrorCode = 102;
else % Minimum moisture transfer condition
    dconc=20;
    tliq=20;
    mFileErrorCode = 103;
end

mFileErrorCode = 104;

% Calculation of Parameters

conc=[2 4 6 8 10 12 14 16 18 24 26 28 30 32 34 36 38 40];
SPHCOSavg=[4074.888889 3976.888889 3885.222222 3789.111111 3694.888889
3604.222222 3517.444444 3424 3341 3094 3017 2939.888889 2863.888889 2790 2719
2643 2576.111111 2508]/1000; %SPHCOS averaged over temperature
SPHCOS=interp1(conc,SPHCOSavg,dconc); %Specific heat coefficient of desiccant
solution kJ/kgK
%dconc is the desiccant concentration to be calculated later

mFileErrorCode = 106; %To check for errors
U=1/(hth/Kth+1/hc1); %Total heat transfer coefficient in W/m2K
tzone=[250 300 350]; %Temperature in Kelvins
tzk=tz+273.15; %Space temperature in Kelvins
thampk=thamp+273.15; %HAMP surface temperature in Kelvins

Kf1=[0.0223 0.0263 0.03]; %Conductivity at 250, 300, and 250K
Pr1=[0.72 0.707 0.700]; %Prndtl number at 250, 300, and 350 Kelvins
Neu1=[11.44*10^-6 15.89*10^-6 20.92*10^-6]; %Viscosity at 250, 300, and 350K

Kf=interp1(tzone,Kf1,tzk); % Space air conductivity
Pr=interp1(tzone,Pr1,tzk); % Space air Prandtl number
Neu=interp1(tzone,Neu1,tzk); %Space air viscosity

%Mass Transfer Coefficient Calculation

Nu=U*L/Kf; %Nusselt number

conc1=[0 2 4 6 8 10 12 14 16 18 20 24 26 28 30 32 34 36 38 40];
DABC=[2.453E-09 2.316E-09 2.203E-09 2.083E-09   1.957E-09 1.827E-09 1.701E-09
1.575E-09   1.449E-09   1.323E-09   1.203E-09   1.093E-09   9.94E-10
8.98E-10    8.03E-10    7.08E-10    6.13E-10    5.18E-10    4.23E-10
3.28E-10];

DAB=interp1(conc1,DABC,dconc); %The diffusivity of moisture into air

Sc=Neu/DAB; %Schmidt number
Sh=Nu*(Sc/Pr)^(1/3); %Sherwood number by heat/mass analogy

MTC=Sh*DAB/L*1000; %Mass transfer coefficient
```

```
tliqk=tliq+273.15; %Desiccant temp in Kelvins

% This part is to calculate the surface relative humidity of the HAMP, for
more information refer to excel file "RH forlithium chloride"
xsol=100/(dconc)-1; %kgw/kgs
mi=1000/(xsol*42.394); %mol/kg
l=1/2*mi*2; %mol/kg
A=-0.021302+3.60591*10^-4*l+18/2303;
B=-5.390915+1.382982*l-0.031185*(l^2);
C=7.192959-3.99334*10^-3*l-1.11614*10^-4*l^2+18*l*(1-2)/2303;
D=1730.2857-0.138481*l+0.027511*l^2-1.79277*10^-3*l^3;

K=0.72567;
Es=39.53;
logpv=K*l*(A-B/(tliqk-Es))+(C-D/(tliqk-Es));
pv=10^logpv; %Vapou pressur in kPa


Pvsat=exp(-5674.5359/(tz+273.15)+6.3925247-
0.009677843*(tz+273.15)+6.22116*10^-7*(tz+273.15)^2+2.07478*10^-
9*(tz+273.15)^3+-9.48402*10^-13*(tz+273.15)^4+4.1635019*log(tz+273.15));
Ws=0.62198*(pv/(Patm/1000-pv)); % HAMP surface humidity ratio from "RH for
lithium chloride" excel kg/kg

Pw=(Ws/621.98*Patm)/(1+Ws/621.98); %in Pascals
RHs=100*Pw/Pvsat; %HAMP surface relative humidity

Pa=RHz/100*0.6219*Pvsat/Winf; %Space air partial pressure
rowdryair=Pa*V/R/tzk/1000; %Dry air density

% Moistyure added or removed from space
% The value is positive for humidification and negative for dehumidification

HUM=MTC*As*(Ws-Winf)*rowdryair*3600; %output-5 in kg/hr

% --- Set outputs ---

% trnOutputs(1)=hr;
trnOutputs(1)=HUM;

mFileErrorCode = 0; % Tell TRNSYS that we reached the end of the m-file
without errors
return
```

APPENDIX C SENSITIVITY OF DIFFERENT PARAMETERS

C.1 Atmospheric Pressure

It was assumed in the simulations that the atmospheric pressure is constant at 1 atm (101,325 Pa) as presented in the Matlab code in Appendix B. However, it should be noted that in some cities the atmospheric pressure can be lower or higher than this value depending on the elevation of the city from the sea level. In this section, the effect of the atmospheric pressure on the moisture transfer of the HAMP is presented. Figure C.1 presents the space humidity ratio in Saskatoon on January 15 using the actual atmospheric pressure given by the TMY2 weather file which is 94,152 Pa compared to the standard atmospheric pressure of 1 atm in system C (RCP and HAMP).

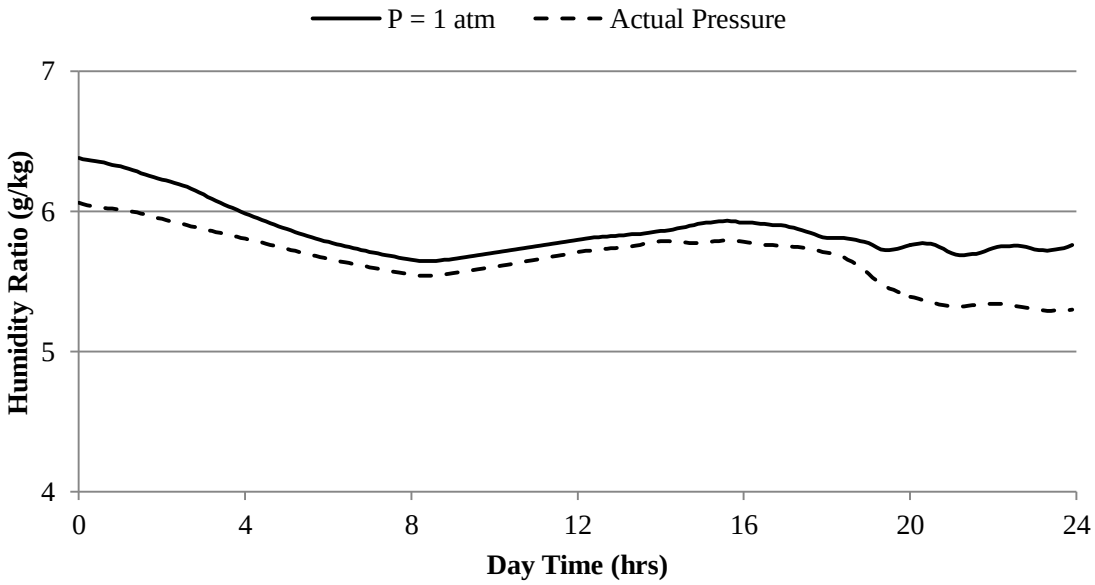

Figure C.1: Space humidity ratio on January 15 in Saskatoon using different atmospheric pressure levels for system C (RCP+HAMP).

The space humidity ratio level using the actual atmospheric pressure is slightly lower than the space relative humidity ratio using a pressure of 1 atm in the simulation. However, both humidity levels are higher than the required humidification level of 4.91 g/kg. Figure C.2 presents the frequency of the relative humidity during the working hours in the building throughout the year in Saskatoon. The figure shows higher levels of relative humidity inside the space when the actual pressure is used.

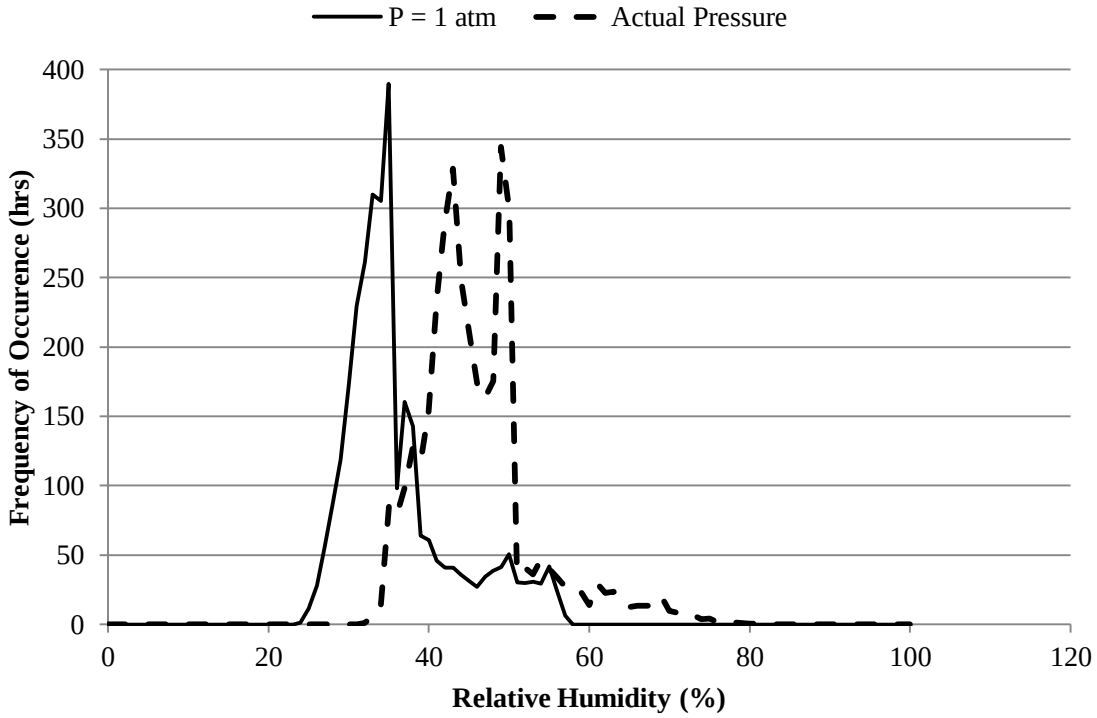

Figure C.2: Frequency of relative humidity inside the building throughout the year in Saskatoon using different atmospheric pressure levels system C (RCP+HAMP).

Figure C.3 presents the annual humidification and sensible energies of system C in Saskatoon over the whole year using the actual atmospheric pressure given by the TMY2 weather file compared to the atmospheric pressure of 1 atm. The humidification energy consumption is lower by 20% while the sensible energy only 3% less when the actual atmospheric pressure in Saskatoon is used rather than 1 atm. It is shown that the atmospheric pressure directly affects the surface humidity ratio of the HAMP and thus affects moisture transfer while it has minor effect on heat transfer..

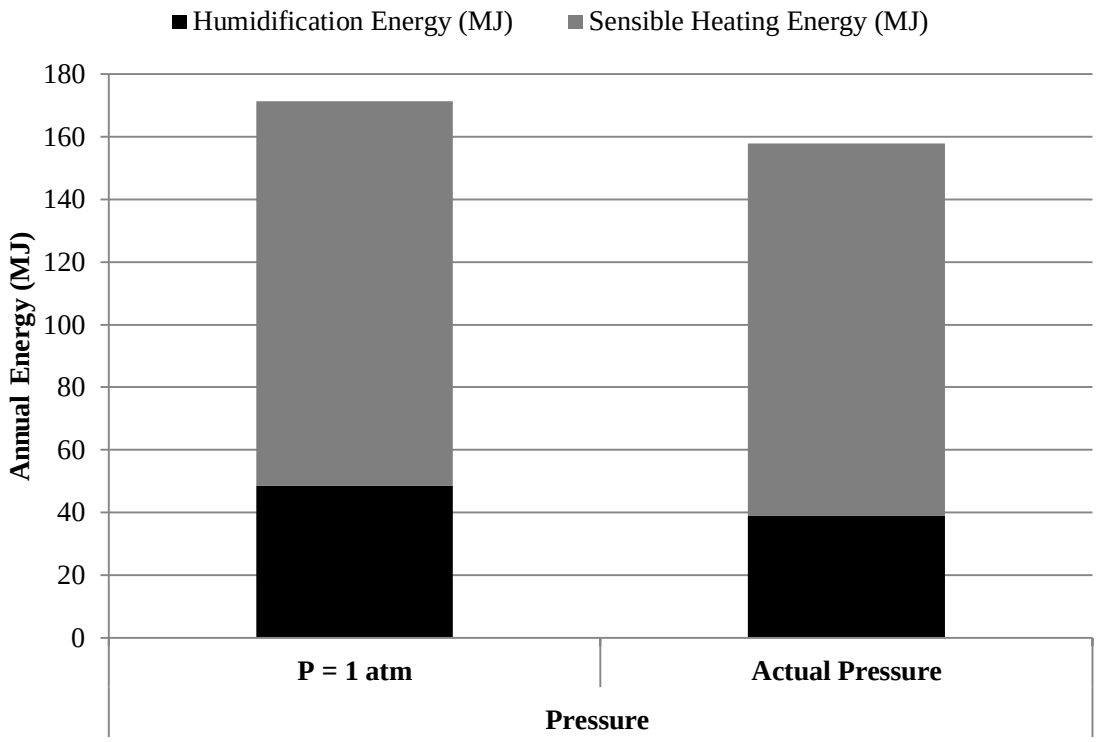

Figure C.3: Annual Humidification energy consumption in Saskatoon using different atmospheric pressure levels system C (RCP+HAMP).

C.2 Energy Wheel Latent Effectiveness

The sensible and latent effectiveness of the energy wheel used in this study were assumed to be constant and equal to 75%. This section presents some results using a latent effectiveness of 60% (and a sensible effectiveness of 75%). Figure C.4 presents the space humidity ratio in Miami on July 16 using system A when a latent effectiveness of 60% compared to the latent effectiveness of 75% is used in the simulations.

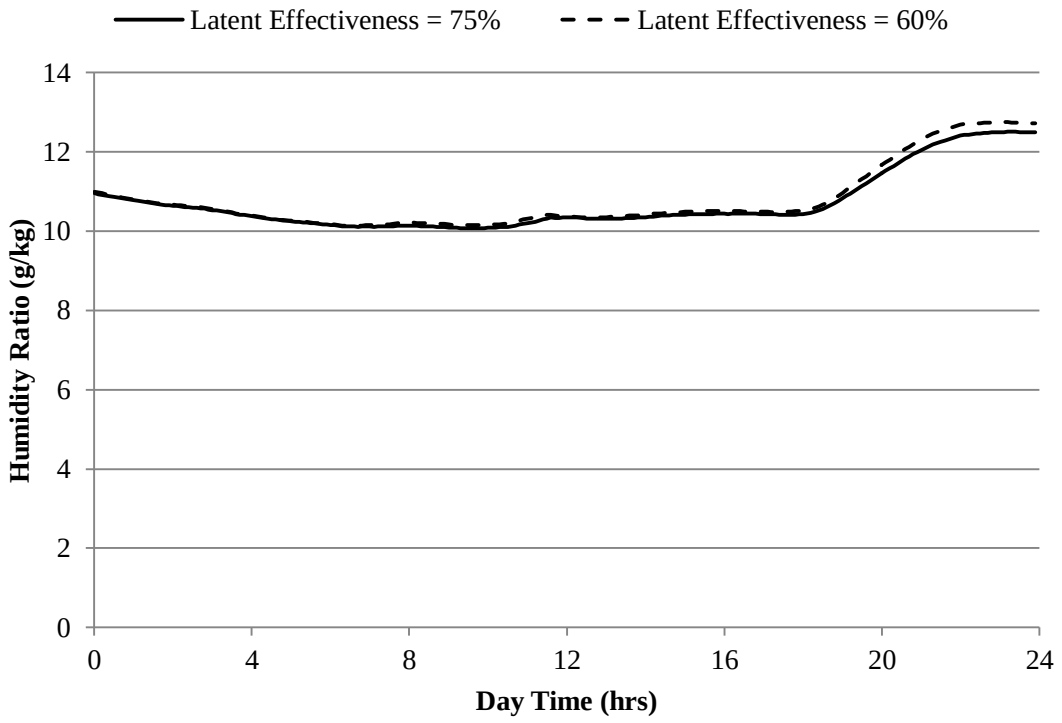

Figure C.4: Space humidity ratio on July 16 in Miami using different energy wheel latent effectiveness values for system A (all-air).

As shown in the figure, there almost no difference in the space humidity level during the working hours showing that the energy wheel latent effectiveness has a small effect on the space humidity level. Figure C.5 presents the annual cooling energy of system A in Miami over the whole year using a latent effectiveness of 60% compared to the latent effectiveness of 75% used in the simulations. The cooling energy only increased by 2% showing that the latent effectiveness of the energy wheel in Miami has a small effect on the cooling energy consumption.

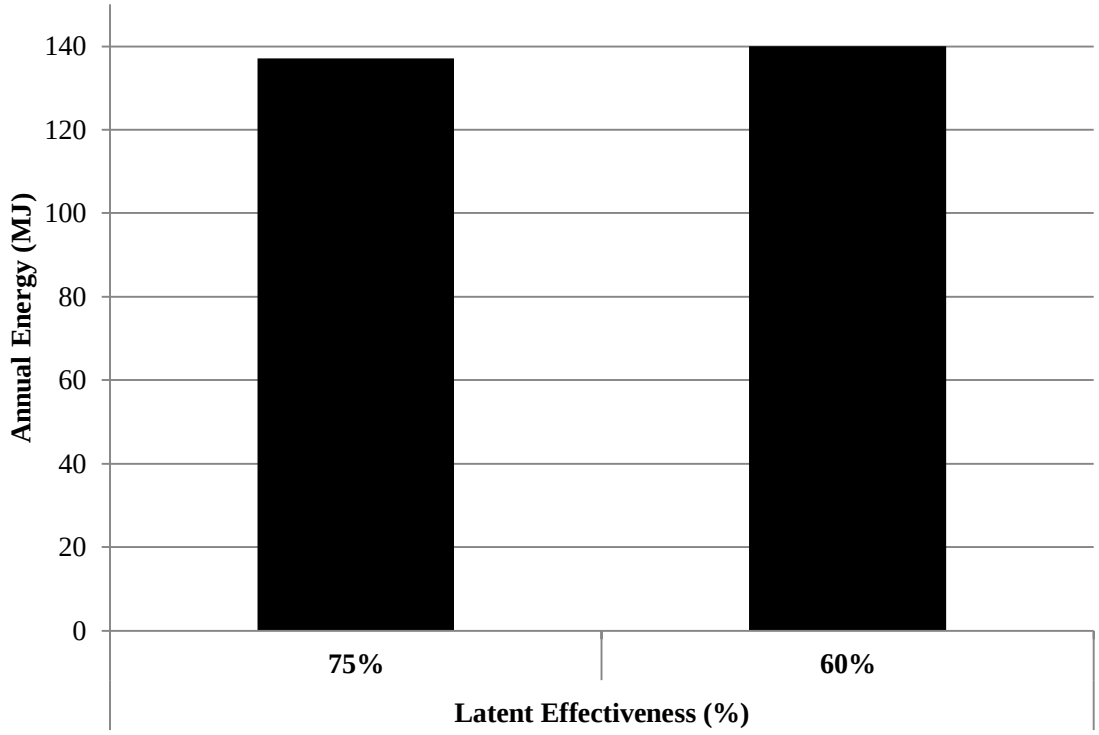

Figure C.5: Annual cooling energy consumption in Miami using different energy wheel latent effectiveness values system A (all-air).

C.3 HAMP Sensible Heat Transfer

The energy consumption of system C included the energy consumed by the auxiliary heater and auxiliary cooler in addition to the latent load transferred by the HAMP; however, sensible heat transfer between the HAMP and the space was neglected as was stated in Sections 2.3.11.2 and 2.3.11.3. However, the HAMP is able to transfer sensible energy by radiation and convection as well. Equations (2.8) to (2.12) are used to calculate the sensible energy transferred by the HAMP using the HAMP surface area, and the desiccant solution temperature. In this section, the sensible energy of the HAMP is added to the energy consumption of system C.

Figure C.6 presents the space temperature in Miami on July 16 after adding the sensible load of the HAMP to the space compared to the simulation result. Figure C.6 shows that the space temperature follows the set point temperature closer and with less fluctuation when sensible heat transfer of the HAMP is included in the simulation.

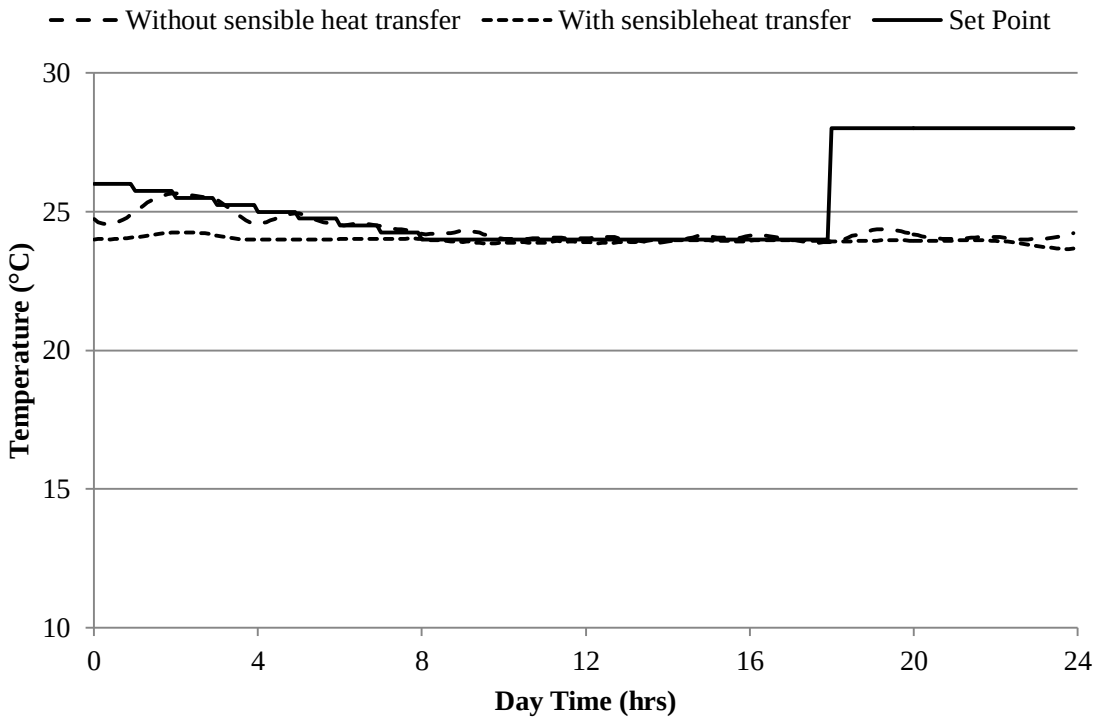

Figure C.6: Space temperature on July 16 in Miami before and after including the sensible heat transfer of the HAMP in system C (RCP+HAMP).

Figure C.7 presents the cooling energy consumption of system C in Miami over the whole year after adding the sensible heat transfer of the HAMP to the space compared to the simulation result. The sensible cooling energy is 27% higher and the dehumidification energy is 53% higher. The total cooling energy (sensible and latent) increased by 33%.

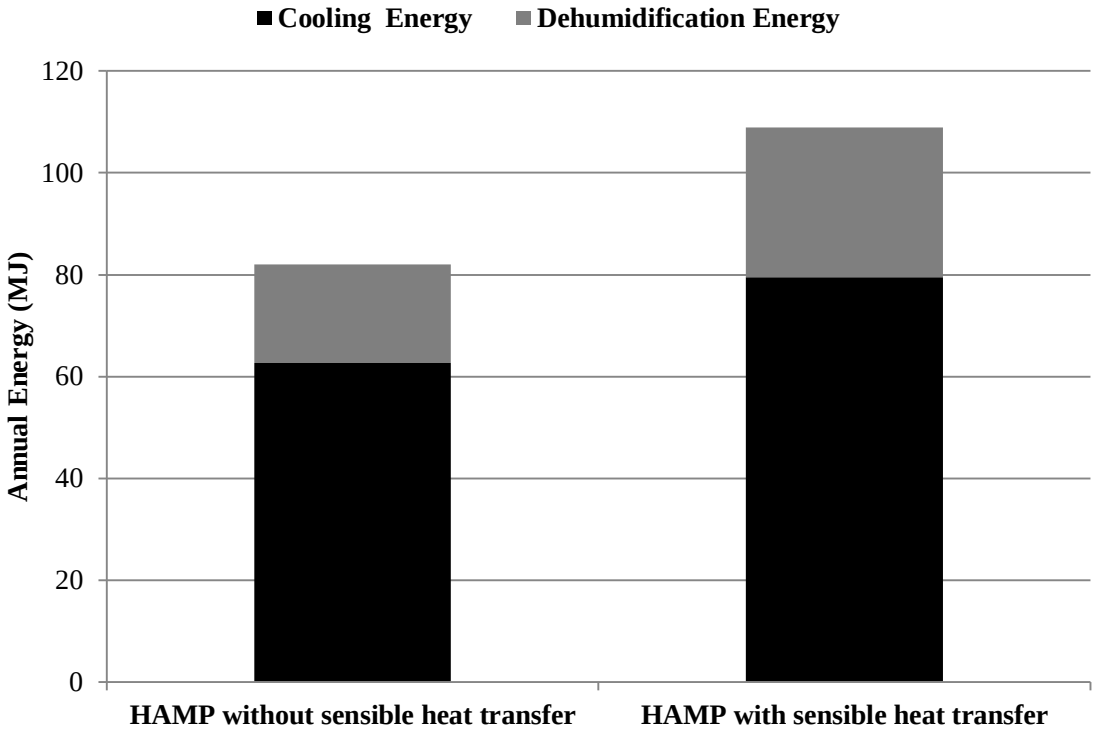

Figure C.7: Annual Cooling and Dehumidification energy consumption in Miami before and after including the sensible heat transfer of the HAMP in system C (RCP+HAMP).

The increase in the sensible heat transfer is due to the addition of the HAMP sensible heat transfer which may be surprising because the loads of the building should not change by including the heat transfer from the HAMP provided the indoor conditions do not change. Therefore, one plausible explanation for this change could be that the space temperature decreases (due to control or other difficulties in the TRNSYS simulation) when the sensible heat transfer between the space and the HAMP is included in the simulation. To justify this idea, one would plot the indoor temperature and humidity ratio for the design day and the frequency

distributions of temperature and humidity ratio for the entire year. Also the variation the cooling unit COP presented in Appendix D may add another complexity to the system. This is left for future work.

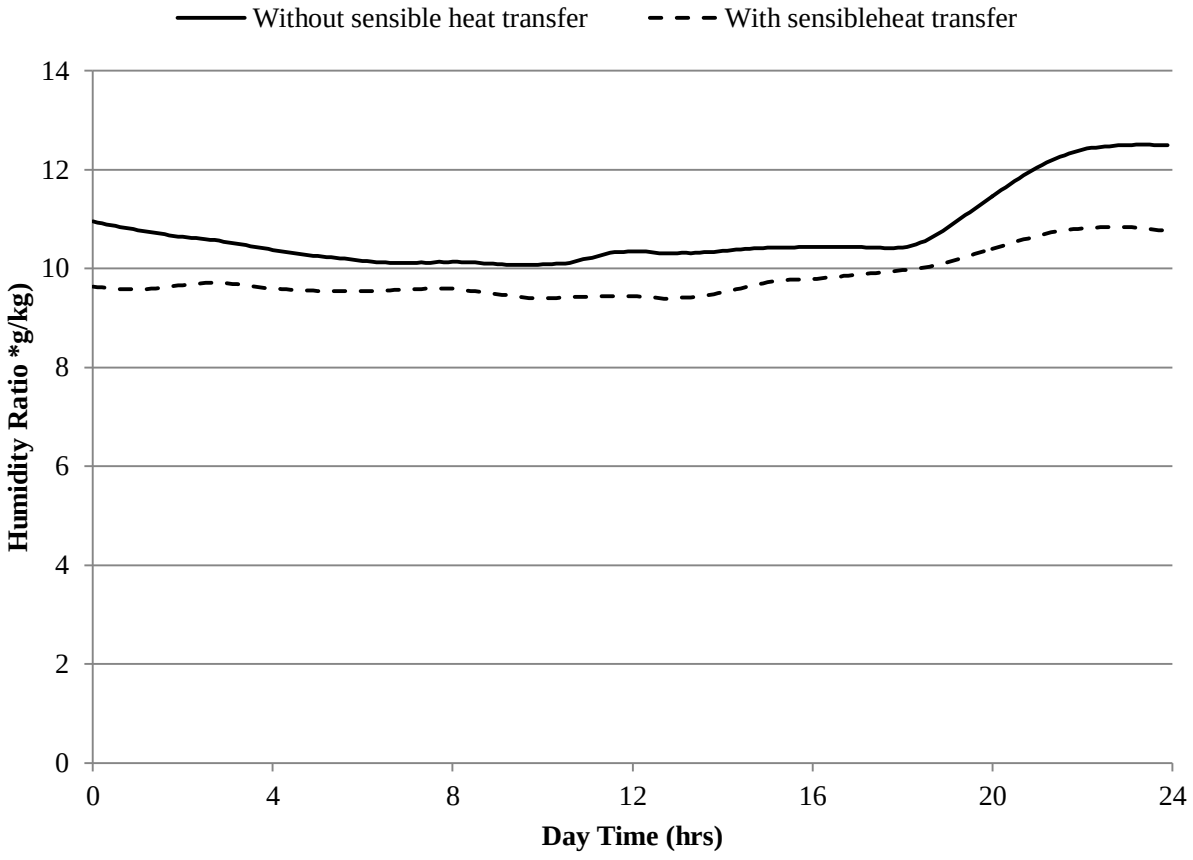

Figure C.8: Space humidity ratio on July 16 in Miami before and after including the sensible heat transfer of the HAMP in system C (RCP+HAMP).

The increase in the latent load is due to lower humidity ratios in the space when the sensible heat transfer is included, which is shown in Figure C.8 for Miami on July 16 and indicates that

more extensive dehumidification is done which leads to a lower level of space humidity ratio. This is also again proven by Figure C.9 which shows lower levels of space relative humidity when the sensible heat transfer is added.

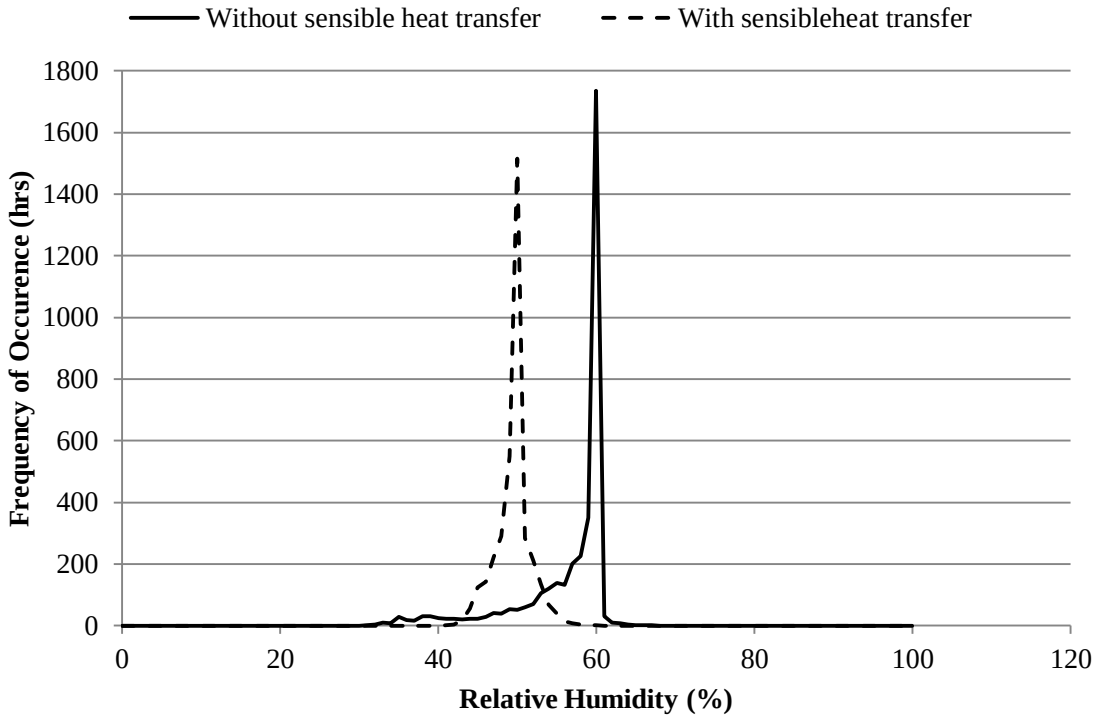

Figure C.9: Frequency of relative humidity inside the building throughout the year in Miami before and after including the sensible heat transfer of the HAMP in system C (RCP+HAMP).

C.4 HAMP Mass Transfer Coefficient

The mass transfer coefficient of the HAMP was calculated using heat-mass transfer analogy in Section 2.3.11.2. The analogy used Nu to calculate Sh which was used to calculate the mass transfer coefficient. Nu was calculated using the overall heat transfer coefficient of the HAMP calculated using Equation (2.16). However, in order to obtain correct values of the mass transfer coefficient from the heat-mass transfer analogy, the calculated Nu should be based only on the convection heat transfer coefficient, h_{c1}, rather than the overall heat transfer coefficient. This section will present some results obtained using the Nu based on h_{c1}. The new equation for calculation Nu is

$$Nu_{new} = \frac{h_{c1} L}{k_f} \tag{C.1}$$

Using the same sequence of equation as in Section 2.3.11.2, the convection mass transfer coefficient [m/s] in the air will be

$$h_{m,air} = \frac{Sh\, D_{AB}}{L} \tag{C.2}$$

The overall mass transfer coefficient [kg/(m^2·s)] is calculated using Equation (C.3)

$$U_{m,new} = \frac{1}{\frac{1}{h_{m,air} \times \rho_{air}} + \frac{R_{membrane}}{\rho_{air}} + \frac{1}{h_{m,air}}} \quad \text{(C.3)}$$

where $R_{membrane}$ is the resistance to vapour diffusion of the semi-permeable membrane of the HAMP [s/m], $h_{m,air}$ is the convection mass transfer coefficient in the liquid desiccant [kg/(m^2·s)], and ρ_{air} is the density of the air [kg/m^3]. $R_{membrane}$ of Propore^{TM} (125 s/m) is used in this study and $h_{m,air}$ is neglected (Fauchoux 2012). The resulting space humidity ratio in Miami on July 16 is shown in Figure C.10, and the relative humidity frequency distribution is shown in Figure C.7.

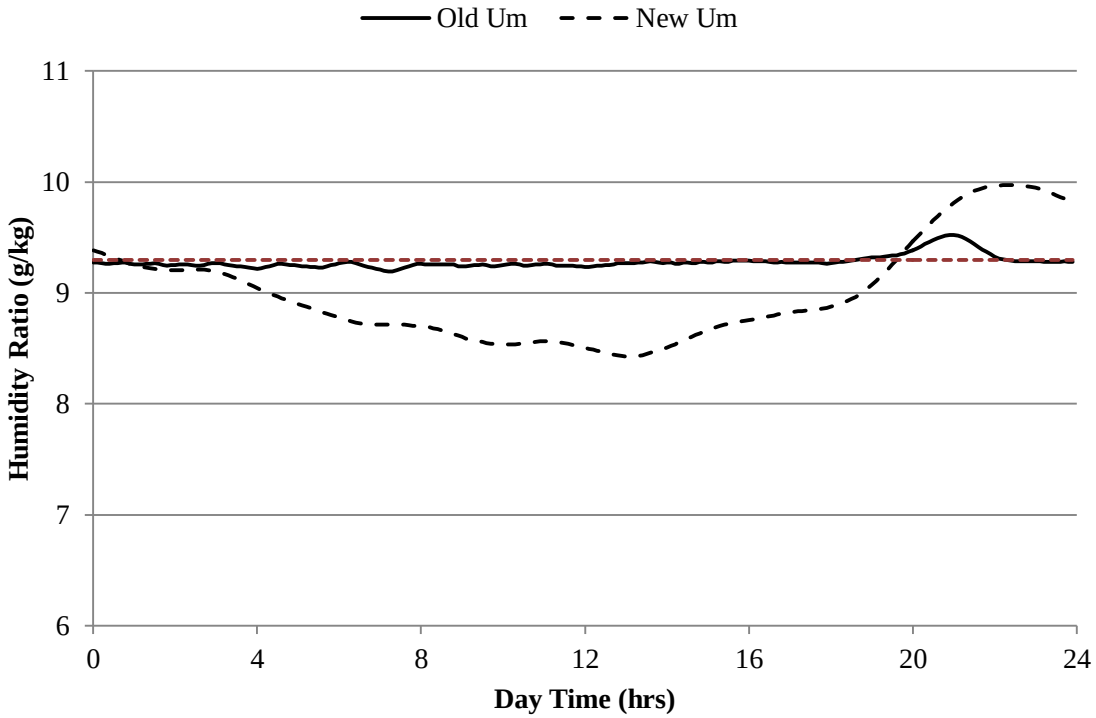

Figure C.10: Space humidity ratio on July 16 in Miami using the old and the new values of the mass transfer coefficient U_m in system C (RCP+HAMP).

Both figures show lower levels of space humidity and the ability of the HAMP to remove more than the entire required latent load. This major factors that affect moisture transfer are the $R_{membrane}$ and the surface humidity ratio used. A proper choice of the membrane resistance to vapour diffusion and surface humidity is required in order for the HAMP to be able to just meet the entire latent load.

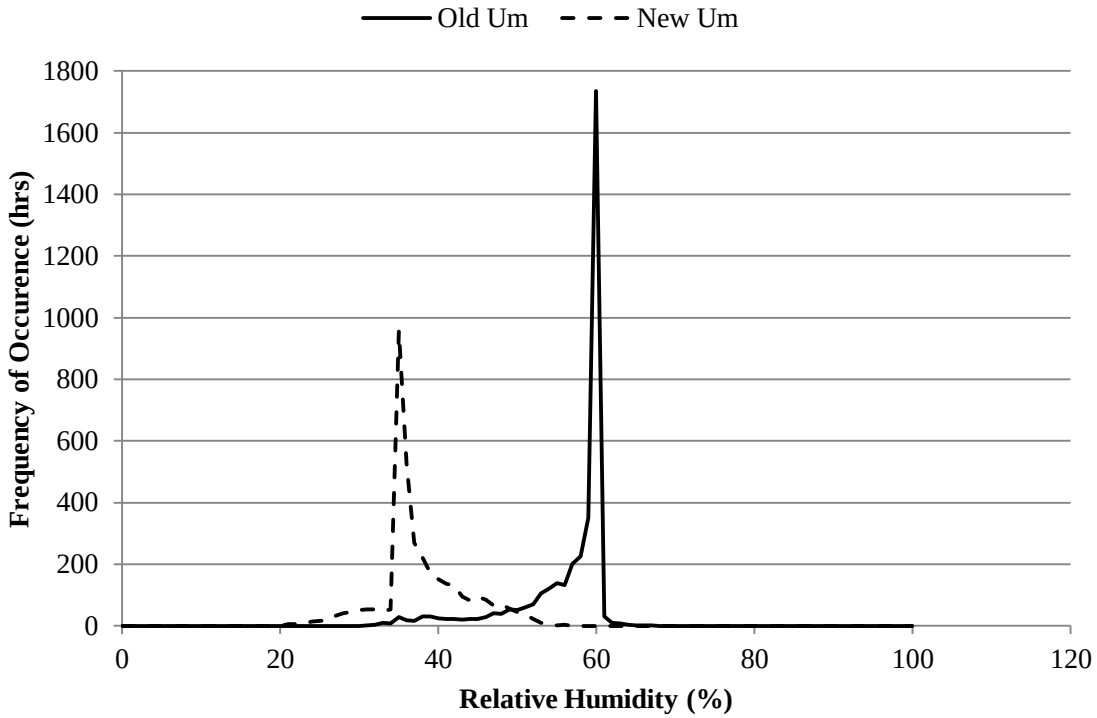

Figure C.11: Frequency of relative humidity inside the building throughout the year in Miami using the old and the new values of the mass transfer coefficient U_m in system C (RCP+HAMP).

APPENDIX D COOLING AND HEATING UNITS PERFORMANCE

D.1 Cooling unit

Figure D.1 shows the variation of the unit cooler COP on June 12 in Phoenix in case A. It also shows the inlet and outlet air temperatures variation on the same day.

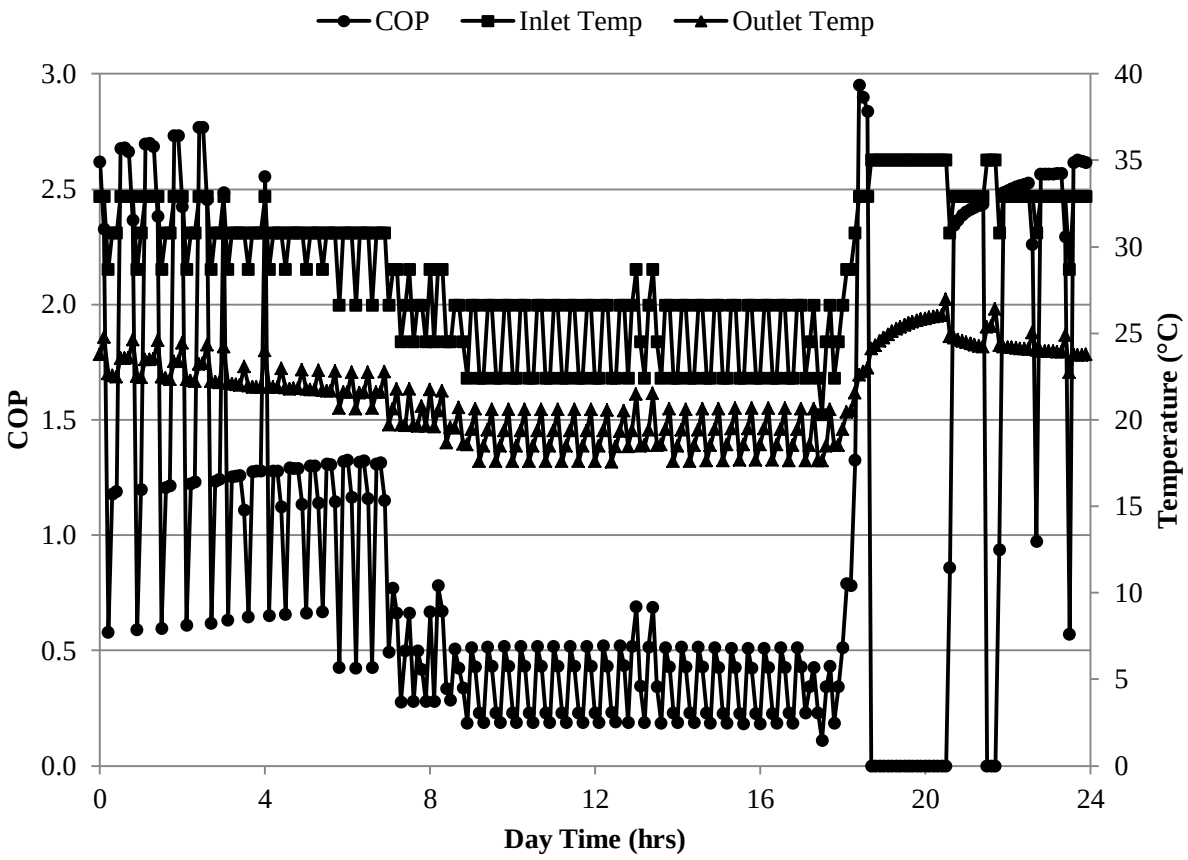

Figure D.1: The unit cooler COP and the inlet and out air temperature in Phoenix on June 12 (case A).

D.2 Heating unit

Figure D.2 shows the variation of the unit heater efficiency on November 4 in Saskatoon. It also shows the inlet and outlet air temperatures variation on the same day.

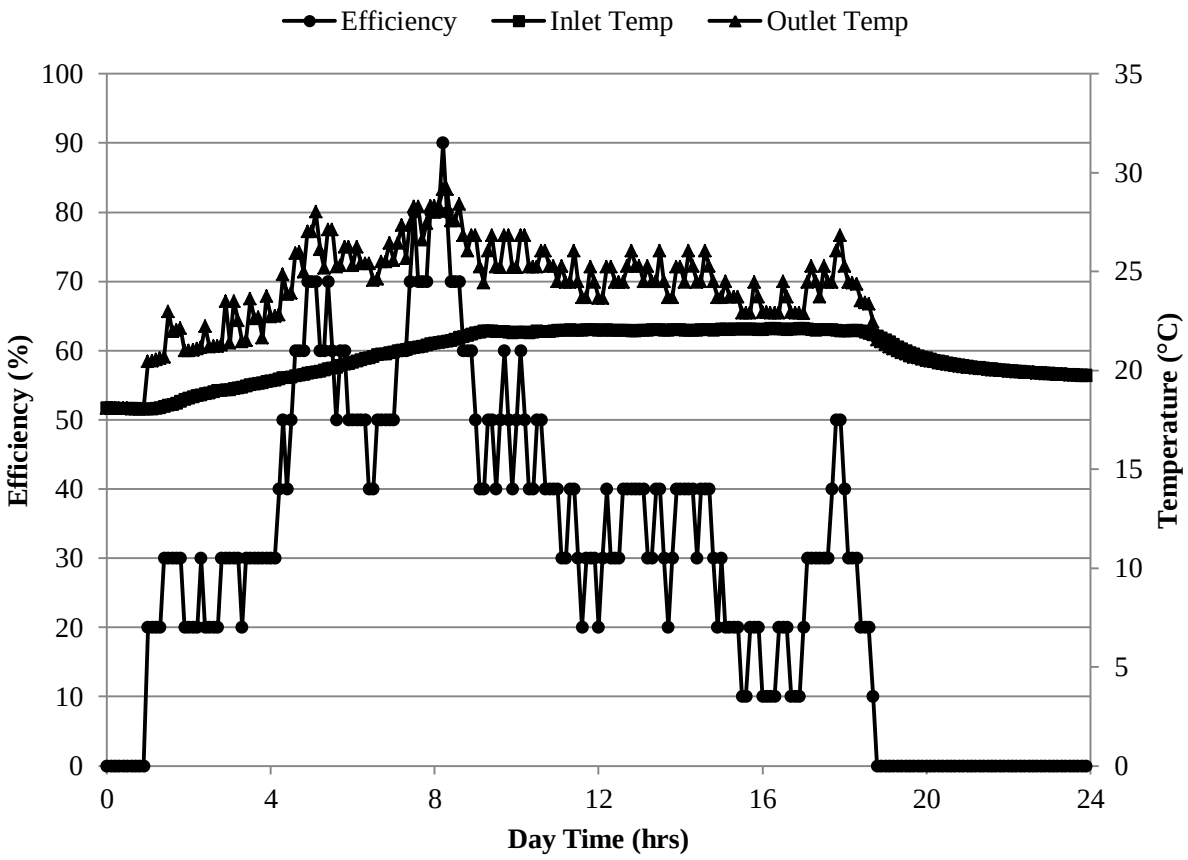

Figure D.2: The unit heater efficiency and the inlet and out air temperature on November 4 in Saskatoon (case A).